CHARACTERISING THE ANTICANCER EFFECTS OF A SMALL MOLECULE WITH POTENTIAL TO INHIBIT NUCLEAR IMPORT VIA KARYOPHERIN BETA1

Nonkululeko Mkwanazi

Dissertation submitted in fulfilment of the requirements for the degree of

MSc Med in Medical Biochemistry

In the

Division of Medical Biochemistry and Structural Biology

Department of

Integrative Biomedical Sciences

UNIVERSITY OF CAPE TOWN

October 2017

DECLARATION

I, **Nonkululeko Mkwanazi**, hereby declare that the work on which this dissertation is based is my original work (except where acknowledgements indicate otherwise) and that neither the whole work nor any part of it has been, is being, or is to be submitted for another degree in this or any other university.

I empower the university to reproduce for the purpose of research either the whole or any portion of the contents in any manner whatsoever.

Signed by candidate

signature removed

Sign:

Date: 2 October 2017

ACKNOWLEDGEMENTS

I would like to express my most sincere gratitude to the following people:

My supervisor, Prof Virna Leaner for her expertise, constant support and encouragement.

Dr Pauline van der Watt, for her patience and excellent advice in lab meetings.

A/Prof Denver Hendricks, for his constant love, support and warm hugs.

Hajira Guzgay, for being an amazing lab manager and always making sure we are taken care of but most of all for spoiling us with all those great treats.

Robert Samuals, for all the friendly conversations, fatherly support and making sure we always had what we needed in the lab.

Members of the cancer lab: Tamara Stelma, Sarah Carden, Andrew Wischart and Ursula Adong, for welcoming me into the lab and lending a helping hand.

I would like to give special thanks to Aderonke Ajayi Smith, for her amazing friendship, endless advice and assistance but most of all for her loving spirt. I will truly miss our laughs and conversations.

To the members of the Zenda Woodman lab: Bahiah Meyer, Bianca Abrahams, Alessandra Unterpertinger and Riley Traviss, for their constant support and friendly chats.

Mr Ronnie Dreyer for assistance with cell cycle analysis.

Mr Rodney Lucas, for his patience during animal training and his continuous assistance during animal work.

Warren Olifant, for his assistance with the ADME pharmacokinetic assays.

Susan Cooper, for her assistance in fluorescent microscopy.

National Research Foundation (NRF) and Ernst & Ethel Ericksen scholarship, for their financial assistance.

I would like to give special thanks to my family. To my parents, Sipho & Khosi Mkwanazi, words cannot express my gratitude and appreciation. Thank you for the unconditional love, constant support and most of all believing in me. To my amazing siblings, Africa & Busi Mkwanazi, for standing by my side always.

Most importantly I would like to give thanks to God. "The LORD is the one who goes ahead of you; He will be with you He will not fail you or forsake you. Do not fear or be dismayed." Deuteronomy 31: 8.

TABLE OF CONTENT

ABBREVIATIONS

~	Approximately
˚C	Degrees Celsius
%	Percentage
ABL	Abelson Murine Leukaemia
ADME	Absorption, Distribution, Metabolism and Excretion
APC	Adenomatous polyposis coli
BCA	Bicinchonic Acid
BCl-2	B-cell lymphoma-2
BSL	Biosafety Level
CAM	Calcineurin
cNLS	classical Nuclear Localization Signal
Compound 53	C53
Compound 60	C60
CRM1	Chromosomal maintenance 1
DMEM	Dulbecco's Modified Eagles Medium
ER	Estrogen Receptor
EGFR	Epidermal Growth Factor Receptor
EC50	Half maximal effective concentration
FBS	Fetal Bovine Serum
FDT	Free Drug Theory
Fu	Free fraction

GI	Gastrointestinal
HCL	Hydrochloric Acid
HER2	Human Epidermal Growth Factor Receptor
HIF-α	Hypoxia-inducible factor alpha
HPLC	High Pressure Liquid Chromatography
IFγ	Interferon gamma
IGF	Insulin Growth Factor
IL-2	Interleukin 2
IL-10	Interleukin 10
INI-43	Inhibitor of Nuclear Import 43
i.p	Intraperitoneal injection
KPNB1	Karyopherin Beta 1
KPNα	Karyopherin Alpha
LC-MS/MS	Liquid Chromatography mass spectrometry
LogD	Partition coefficient
LogP	Apparent permeability
MEK	MAPK/ERK Kinase
MetID	Metabolite Identification
MTT	3-[4,5-dimethylthiaol-2-yl]-2,5-diphenyltertazolium bromide
NFAT	Nuclear Factor of activated T cells
NF-κB	Nuclear factor kappa-light-chain-enhancer of activated B cells
NLS	Nuclear Localization Signal
NPC	Nuclear Pore Complex

Nup	Nucleoporin
PAMPA	Parallel Artificial Permeability Assay
PARP	Poly ADP-ribose Polymerase
PI3K	Phosphoinositide 3-Kinase
PI	Propidium Iodide
PIK1	Polo-like Kinase 1
PMA	Phorbol Myristate Acetate
PS	Penicillin Streptomycin
PTHrp	Parathyroid Hormone related Protein
RIPA	Radioimmunoprecipitation assay buffer
RNase	Ribonuclease
SBDD	Structure Based Drug Design
SDS	Sodium Dodecyl Sulphate
SDS-PAGE	SDS polyacrylamide gel electrophoresis
SEM	Standard Error of Mean
SINE	Selective Inhibitors of Nuclear Export
SLS	Sodium Lauryl Sulphate
SPR	Surface Plasmon Resonance
TBST	Tris Buffered Saline Tween-20
$t_{1/2}$	Half life
VEGF	Vascular Endothelial Growth Factor

Units

ng	nanograms
µg	microgram
mg	milligram
g	gram
µM	micromolar
mM	millimolar
M	molar
µl	microliter
ml	millilitre
L	litre
µm	micrometre
mm	millimetre
V	Volt
rpm	revolutions per minute

ABSTRACT

The Karyopherin superfamily is a group of soluble transport proteins which are involved in nuclear-cytoplasmic trafficking. Studies have shown the involvement of Karyopherin proteins in nuclear pore assembly, nuclear membrane assembly and DNA replication. Since all these cell regulatory functions are critical for normal cell function, dysregulation of Karyopherin proteins may have an impact on cancer cell survival. Previous research in our laboratory and in that of others has shown that Karyopherin Beta 1 (KPNB1) is elevated in and necessary for the survival of cervical cancer cells as inhibiting its expression with siRNAs interfered with the proliferation of cancer cells. KPNB1 has thus been proposed as an anticancer target. In addition to inhibition by siRNA, an *in silico* screen for small molecules with potential to bind KPNB1 identified a number of compounds that are currently under investigation for their cancer cell killing effects. In this study, we investigated the ability of a novel small molecule 1-benzyl-4[(4-methoxy-1-naphyl) methylamino]-N-methyl pyrrolidine-2-carboxamide (Compound 53) to kill cancer cells and inhibit the activity of KPNB1 cargo proteins. In addition, the *in vitro* pharmacokinetic properties and *in vivo* toxicology of Compound 53 (C53) were investigated.

Cervical (HeLa and CaSki) and oesophageal (WHCO6 and Kyse30) cancer cell lines were found to be more sensitive to C53 treatment compared to non-cancer cells (FG_0), with EC_{50} values of ~ 20 μM for the cancer cell lines and ~ 30-40 μM for the non-cancer cells. C53 treatment significantly inhibited proliferation in cancer cell lines. The reduction in proliferation in cancer cells was associated with a block in the G1 phase of the cell cycle and a change in the expression of cell cycle related proteins such as CyclinD1 and CDK4. C53 treatment resulted in cell death via apoptosis as observed using Annexin V staining and PARP cleavage.

To assess whether C53 interferes with KPNB1 associated nuclear import, we investigated the effect of C53 on the activity of KPNB1 cargo proteins, NFAT and NF-κB as well as investigate its effect on KPNB1 localisation. The results show that C53 has no effect on the localisation of KPNB1 but it does however block the nuclear activity of the KPNB1 cargoes, NFAT and NF-κB. In order to predict the behaviour of C53 in a living system, *in vitro* ADME pharmacokinetic studies showed that C53 has moderate solubility, permeability and protein binding however, rapid clearance was shown by liver microsome assay. *In vivo* repeated dose toxicology studies showed that C53 is tolerable in nude mice.

Taken together, the data presented in this study shows that a novel small molecule, C53 has a negative effect on the proliferation of cancer cells, inhibits the nuclear import of KPNB1 cargoes, displays tolerable *in vitro* ADME pharmacokinetic properties and showed no toxic side effects *in vivo*. These results suggest that C53 targets KPNB1 and shows potential as an anticancer molecule.

Surgery and radiation are still the most common methods used to remove cancer cells from the body. These methods are specifically used for localised tumours which have not metastasised, and therefore can be removed surgically or directly killed by high radiation e.g. localised breast cancer and prostate cancer tumours [5,6]. Chemotherapy is also a common method used to treat cancer and involves administering drugs which target rapidly dividing cells. Chemotherapy not only kills rapidly dividing cancer cells but also kills rapidly dividing normal cells which leads to side effects such as vomiting, hair loss and mouth sores [4]. The side effects associated with chemotherapies are largely thought to be due to the off-target effects of chemotherapy. To try and minimize off target effects, recent research strategies include investigations focussed on targeted therapies.

1.3 Targeted therapy as an anticancer approach

Targeted therapy is a class of cancer therapy designed to specifically interfere with molecular targets which have been shown to be essential for tumour growth. With the increasing knowledge of molecular events underlying human cancer, the ability to target specific genes or proteins which are essential for cancer cell survival has become possible [7]. Unlike conventional chemotherapeutic approaches which mainly target rapidly dividing cells, targeted therapy homes in on characteristics that are essential for cancer progression [4]. An example of a drug with a specific target is Tamoxifen which was approved in the 1970s. Tamoxifen is a therapy used for the treatment of breast cancer and functions by binding to the Estrogen Receptor (ER) which in turn inhibits estrogen from binding the ER. By interfering with the binding of estrogen, Tamoxifen can modulate the ER activity in patients with ER-positive breast cancer [7].

CHAPTER 1:

LITERATURE REVIEW

1.1 Cancer

Cancer is a group of diseases characterised by the abnormal growth of cells which have the potential to invade and spread to other parts of the body. Worldwide cancer is one of the leading causes of mortality with approximately 14 million new cases recorded in 2012. In 2012, approximately 8.8 million deaths in low and middle-income countries was attributed to cancer [1]. Even though there has been substantial progress regarding cancer prevention and treatment, the global cancer burden continues to rise due to a growing and aging population as well as increasing risk factors such as smoking, unhealthy food choices and obesity [2]. These statistics highlight the necessity for early detection methods and developing better treatments for cancer.

1.2 Current cancer treatments

Cancer development is a multistep process generally involving genetic mutations which in turn drive the transformation of normal cells. Recent advances in genomic, proteomic and bioinformatic technologies are revealing the complexity of the genetic interplay involved in cancer progression which has made treatment of cancer very difficult [3]. Clinicians have access to a number of approaches to treat cancer including surgery, chemotherapy, immunotherapy, radiation, target therapy and hormone therapy. Based on the type of cancer, one or a combination of these treatment methods can be used [4].

The discovery of tumour suppressor genes and oncogenes has resulted in improving the understanding of cancer development, which has allowed the introduction of more cancer target therapies [7]. Examples of these include a series of receptor proteins and protein kinases that have been shown to be mutated or overexpressed in human cancer. These include the Epidermal Growth Factor Receptor (EGFR), Insulin Growth Factor (IGF) receptors, Human Epidermal growth factor Receptor 2 (HER2), Abelson Murine Leukemia (ABL) and MAPK/ ERK Kinase (MEK) [7]. The inactivation of several of these kinases with target specific inhibitors have shown positive clinical results in patients with cancer and have been FDA approved to treat various cancers [7,8]. Examples of FDA approved tyrosine kinase inhibitors include Lapatinib a HER2 inhibitor used to treat breast cancer, Nilotinib an ABL inhibitor used to treat chronic myelogenous leukemia, Gefitinib an EGRF inhibitors used to treat non-small cell lung cancer. The successes of some of these target therapy drugs illustrates the power of this approach and shows the need for further investigation into the molecular studies of human cancers [8].

1.3.1 Types of target therapies

The aim of target therapy is to reduce or block the growth and spread of cancer cells by interfering with a specific target that cancer cells are highly reliant on [9]. Target therapies include small molecule inhibitors and monoclonal antibodies. Small molecule inhibitors are low molecular weight chemical agents that are designed to target specific cellular proteins. Monoclonal antibodies, which are large, generally do not enter the cell therefore target proteins on the cell surface or outside of the cells [10].

Many different target therapies have been used for cancer treatment. Some of the types of target therapy include signal transduction inhibitors, gene expression modulators, apoptosis inducers and angiogenesis inhibitors. Signal transduction refers to the process of communication used by regulatory molecules to control essential cell processes such as differentiation, growth and survival. Alteration in signal transduction components may lead to increased proliferation, sustained angiogenesis and tissue invasion which is the case in most human cancers [11]. Some commercially available compounds which target altered signal transduction elements such as tyrosine kinases include Gefitinib, an inhibitor of the ErbB-1 receptor kinase used to treat non-small cell lung cancer and Trastuzumab, an antibody used to target the HER- 2 receptor to treat HER- 2 positive breast cancer [11].

Gene expression modulators are target therapy agents that modify the function of proteins which are involved in controlling gene expression. In cancer, this is specifically important as cancer is associated with abnormal gene mutations and gene expression patterns [12]. Many gene expression modulators trigger cell death by apoptosis. Apoptosis is a tightly regulated form of cell death which maintains the healthy survival of cells. Defects in apoptosis has been shown to lead to cancer and autoimmunity [13]. Cancer cells can use mechanisms to suppress apoptosis and in turn become resistant to apoptotic agents. Therefore, the development of apoptotic inducers for cancer cells is an approach to target the antiapoptotic mechanisms in cancer [13]. Examples of drugs which induce apoptosis include AT-101 and ABT-263 which are currently undergoing clinical trials. These drugs target the antiapoptotic B-cell lymphoma-2 (BCl-2) family of proteins which in turn leads to the induction of apoptosis [14].

Angiogenesis refers to the production of blood vessels. This process is essential to provide tumours with oxygen and nutrients which allows for their growth. Angiogenesis may be an

important contributor to tumour progression, invasion and metastasis. An example of a growth factor secreted by tumour cells is the Vascular Endothelial Growth Factor (VEGF) which is a pro-angiogenic factor mediates blood vessel formation [15]. Targeting angiogenesis has led to the development of several commercially available compounds such as neutralizing antibodies Bevacizumab and Ramucirumab as well as some tyrosine kinase inhibitors which also target angiogenesis (Sunitinib and Sorafenib) [15].

Different target therapies thus target different molecules with the aim to reduce the spread of cancer. The above examples are commercially available compounds that target a variety of cancer dependent targets. The success of these compounds provides a platform for further development of new target therapy compounds with the hope of targeting cancer specific characteristics with reduced off-target effects.

1.3.2 Identification of cancer targets

The advancement of genomics, sequencing and high throughput technology has made it possible to understand diseases better but also identify potential gene targets which could be used in targeted therapy [16]. Previous work done in our laboratory used cDNA microarray analysis to profile the gene expression patterns of normal and cervical cancer tissue to identify specific genes that associate with cervical cancer [17]. Numerous genes with differential expression in cervical cancer tissue were identified and amongst these, multiple members of the nuclear transport family of proteins were shown to be overexpressed in cervical cancer tissues in comparison to normal tissues. These proteins belong to the Karyopherin super family which function in the shuttling of macromolecules between the nucleus and cytoplasm [17].

1.4 Nuclear cytoplasmic transport is an essential cellular function

In eukaryotic cells, a double membrane known as the nuclear envelope separates the nucleus from the cytoplasm. Due to this spatial segregation, efficient mechanisms of transport are required to transport macromolecules across the nuclear envelope which allows for a level of regulation which does not exist in prokaryotic cells [18]. Processes such as DNA and RNA synthesis occur in the nucleus while protein synthesis occurs in the cytoplasm. For these cellular processes to work together selective transport of proteins and ribonucleoproteins between the nucleus and cytoplasm is required. This process is known as the nuclear cytoplasmic transport. Large macromolecules are transported through large protein complexes, which cross the nuclear envelope, known as Nuclear Pore Complexes (NPCs) [18]. The NPC is a highly selective 'channel' which allows entry into and out of the nucleus and regulates the transport of macromolecules [19]. The function of the NPC is to prevent the transport of nonspecific macromolecules, yet allow the diffusion of water, sugars and ions. In addition to its role in nuclear transport research has shown that the NPC play a role in gene expression regulation. It has been shown that the regulation in gene expression can be achieved by modulating the transcription factors involved in nuclear cytoplasmic transport or by regulating epigenetic enzymes [20,21]. The NPC is also able to regulate gene expression by controlling the proportion of transcription factors in the nucleus and cytoplasm, for example NF-κB accumulation in the nucleus is determined, in part, by Nucleoporin 88 (Nup88) [22]. Defects in the NPC have been implicated in different human pathologies such as cancer, viral infections and cardiovascular pathologies [23].

Other cellular components critical for nuclear transport include the nucleo/cytoplasmic machinery e.g Karyopherin proteins and Ran. See section 1.5 for discussion of these.

1.4.1 Nuclear cytoplasmic transport is altered in cancer

Nuclear cytoplasmic transport is a tightly regulated process which involves the import or export of cargo between the nucleus and cytoplasm. There is evidence in the literature that nuclear cytoplasmic transport pathways are altered in cancer cells. Defects in the nuclear cytoplasmic transport process have been detected in several human cancers including breast, cervical, colorectal and ovarian cancers [24]. These defects have been shown to occur in the general nuclear cytoplasmic transport machinery or in signal transduction pathways via the mislocalisation of transcription factors [24]. Since the cellular localisation of protein is crucial for normal cell function, cancer cells are thought to utilize this process of nuclear cytoplasmic transport via the NPC to evade anticancer mechanisms [25]. It is no surprise that disruption of nuclear cytoplasmic transport associates with oncogenesis since subcellular localisation of proteins is of such importance for cellular function [26]. Regulated transportation of protein ensures that the correct amount of protein is present at the right place at the right time. Therefore, mislocalisation of protein or transcription factors can lead to loss of function or harmful toxic activity at the wrong place. The transcription factor forkhead box O3a (FOXO3a) is an example of a tumour suppressor whose function is dependent on localisation. Cytoplasmic localisation of this transcription factor has been correlated with poor survival in breast cancer while nuclear localisation correlates with increased sensitivity to radiation [27]. Several oncogenes and tumour suppressors are often mislocalised in cancer e.g. p53, β-Catenin, Nuclear factor kappa-light-chain-enhancer of activated B cells (NF-κB), Nuclear Factor of activated T cells (NFAT) and Hypoxia-inducible factor alpha (HIF-α) (Table 1). Other proteins such as p27, Adenomatous polyposis coli (APC) and Rb, which play an important role in preventing cancer initiation and progression, have also been reported to be mislocalised in cancer [26].

Table 1: Proteins which have been shown to be mislocalised in different human cancers [26].

Protein	**Function**	**Cancer**	**Normal Localisation**	**Mislocalisation**
FOXO	Transcriptional factor	Various cancers	Nucleus	Cytoplasm
B-Catenin	Win signalling	Colorectal cancer	Cytoplasm	Nucleus
p53	Transcriptional factor	Various cancers	Nucleus	Cytoplasm
Galectin-3	Beta-galactoside-BP	Various cancers	Nucleus	Cytoplasm
BARD1	BRAC1 interacting protein	Breast cancer	Cytoplasm	Nucleus
BRAC1	DNA repair	Breast cancer	Cytoplasm	Nucleus
NF-κB	Transcription factor	Various cancers	Cytoplasm	Nucleus
NPM1	Ribonucleoprotein	AML	Nucleus	Cytoplasm
p21WAF1	Cell cycle inhibitor	CML, ovarian, breast	Nucleus	Cytoplasm
p27KIP	Cell cycle inhibitor	AML, breast	Nucleus	Cytoplasm
RUNX3	Transcription factor	Gastric cancer	Nucleus	Cytoplasm
INI1	Tumour suppressor	Rhabdoid tumours	Nucleus	Cytoplasm
RB	E2F BP	Various cancers	Nucleus	Cytoplasm
HIF-1α	Transcription factor	Breast, prostate cancer	Cytoplasm	Nucleus
NFAT	Transcription factor	Various cancers	Nuc/Cyt	Nucleus
PTEN	Phosphatase	Various cancers	Nuc/Cyt	Cytoplasm
Bcr-Abl	Kinase	CML	Nuc/Cyt	Cytoplasm
Fbw7γ	Ubiquitin ligase	Various cancers	Nucleus	Not nuclear

Some of the proteins that have been shown to be mislocalised are also implicated in different human cancers. For example, the NF-κB signalling pathway has been shown to play a role in cancer initiation and progression while p53 has been reported to be mutated in several human cancers [28,29].

Other than the mislocalisation of proteins, defects in the general machinery of the nuclear cytoplasmic transport process have also been observed in human cancers. These defects include the overexpression of certain transport machinery e.g. CRM1, Cas and KPNα as well as KPNB1 [17,30]. A research focus in our laboratory has an interest on KPNB1 expression and activity in cancer cells.

1.5 Karyopherin B1 (KPNB1) mediated nuclear-cytoplasmic transport

1.5.1 Nuclear-cytoplasmic transport

The trafficking of cargo between nuclear and cytoplasmic compartments is essential for proper cellular function [31]. There are two main mechanisms of translocation across the nuclear envelope, (i) passive and (ii) active transport. Passive transport refers to a diffusion-based process which is dependent on Brownian motion via the central pore. This process is limited to molecules that fall below the size range of 40 to 60 KDa [31]. Active transport, also known as facilitated transport, is dependent on proteins which facilitate transport such as Karyopherin proteins. The transport of cargoes occurs via the nuclear pore complex which acts as a passage for translocation into and out of the nucleus [32]. This form of transport is specific to larger molecules such as transcription factors, enzymes, nuclear receptors, RNA and proteins [32]. Active transport requires the presence of translocation signals known as the nuclear localisation or nuclear export signals which are found on the proteins that require

translocation across the nuclear envelope. The Nuclear Localisation Signal (NLS) acts as recognition signals which can be recognized by a special family of transport receptors such as the Karyopherins [32].

1.5.2 Karyopherin proteins as nuclear transport proteins

The Karyopherin super family consists of a series of transport receptors which play a role in transporting proteins in and out of the nucleus via the nuclear pore complex. The nuclear transport protein responsible for shuttling protein and RNA into the nucleus are known as Importins while the nuclear receptors that shuttle protein and RNA out of the nucleus are known as Exportins [32]. Although there are a variety of NLSs and Karyopherins with different cargo preferences, the classical nuclear import pathway recognizes a specific lysine-rich classical Nuclear Localisation Signal (cNLS) which initiates the pathway (Figure 1.1). The lysine-rich cNLS is recognized by Karyopherin-α (KPNα) which is an adaptor importin specialised in cNLS recognition [31]. Once KPNα binds the cargo via the cNLS, Karyopherin-B1 (KPNB1) import protein, binds KPNα forming a trimeric complex. A Ras-relate small guanosine diphosphatase known as RanGDP binds the importin and provides energy for nuclear import allowing the trimeric complex to enter the nucleus. In the nucleus the RanGDP bound to KPNB1-Kpnα-cargo complex gets converted to RanGTP by a GTPase enzyme known as RanGAP which causes the dissociation of the cargo [33]. The RanGTP bound KPNB1-KPNα complex then translocates back into the cytoplasm where RanGTP is hydrolysed into RanGDP in the cytoplasm for another round of nuclear import [34]. The non-classical import pathway is another KPNB1 dependent import pathway. In the non-classical nuclear import pathway, the NLS of certain cargoes e.g. Histones and Ribosomal proteins are directly recognized by KPNB1 which then binds the cargo. The KPNB1-cargo complex then translocates into the nucleus via the NPC and upon binding to the RanGTP the cargo is released [35].

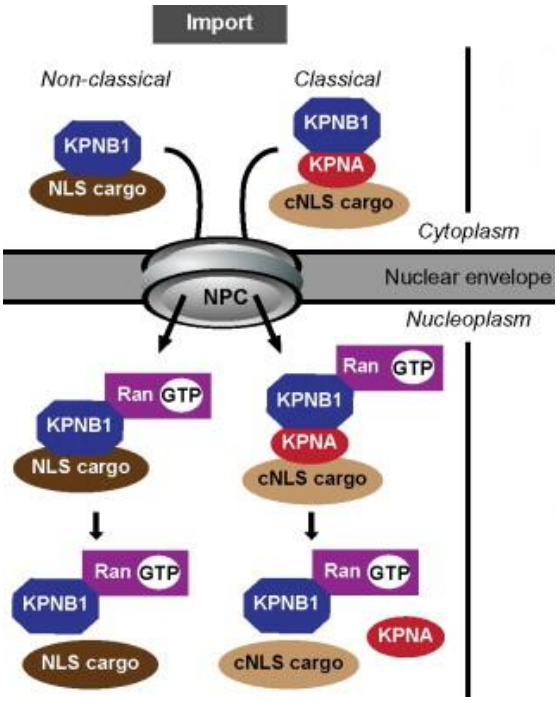

Figure 1.1. A representative image of the KPNB1 dependent nuclear import pathway. In the Non-classical import pathway (Left), KPNB1 binds the cargo and transports it into the nucleus via the NPC. In the nucleus Ran-GTP binds to KPNB1 which causes the cargo to dissociate. In the Classical import pathway (Right), an adaptor protein (KPNα) binds the cargo which then causes the binding of KPNB1 forming a trimeric complex (Right). The trimeric complex then enters the nucleus and associates with Ran-GTP to dissociate the cargo [35].

Although Karyopherin B1 mediates the nuclear import of a large amount of proteins, several Karyopherin B-like importins namely, Importin 2,3,4,5,7,8,9,11,12 and 13 have been identified all of which play a role in importing various proteins into the nucleus. These Karyopherin B-like proteins have similar molecular weights (95-145 KDa) and contain helical HEAT repeats [36]. Table 1 lists the different human importins and their respective cargoes. Interestingly, Importin 7 has the highest identified cargoes and in some cases Importin 7 has been shown to act in complex with Importin-B. Like KPNB1, these importins also recognize specific NLS on proteins. For example, Importin-B2 recognizes diverse sequences called PY-

NLS. There are over 100 human proteins with the PY-NLS which are recognized by Importin-B2 [37]

Table 1: List of Karyopherin B-like importins and their respective cargoes [37].

Importins	**Examples of cargoes transported**
Importin 2	c-Jun, ribosomal protein, c-Fos
Importin 3	HuR, hnRNP A1
Importin 4	HIF1-α, Vitamin D receptor
Importin 5	c-Jun, ribosomal protein
Importin 7	ERK1/2, MEK1, SMAD3/4, c-Jun, HIF1-α, GR, Sox-2
Importin 8	SMAD1/3/4, glucocorticoid receptor
Importin 9	Sox-2, c-Jun, ARX
Importin 11	UbcH6, UB2E2
Importin 12	MLF2, RBM4
Importin 13	c-Jun, ARX, GR

Some of the transport receptors in the nuclear cytoplasmic transport pathway have been implicated in different human cancers. For example, CRM1 which is an export protein has been shown to be over expressed in cervical, ovarian, pancreatic cancer [17,39,40] and implicated in poor patient survival while the adaptor protein KPNα is overexpressed in ovarian, breast, cervical cancer and linked to short disease- free survival [17,41,42]. Unlike CRM1 and KPNα, there are limited studies of the link of KPNB1 and human cancers. Research in our laboratory has shown elevated expression of KPNB1 in cervical cancer cell lines and patient tissues in comparison to non-cancer cells [43]. Research by Kuuisto *et al*. has shown elevated expression of KPNB1 in breast cancer cell lines [44]. Research has also shown elevated expression of KPNB1 in bladder and gastric cancer [45,46]. The increasing evidence of KPNB1 being overexpressed in various cancer suggests its potential as a target for target therapy.

1.5.3 KPNB1 as a target for cancer therapy

KPNB1 has been shown to have function in nuclear transport as well as regulate mitosis and other cell regulatory functions such as nuclear pore assembly, nuclear membrane assembly and DNA replication in the S phase [47]. Since KPNB1 is involved in nuclear import as well as different non-transport cellular processes it is essential that its expression is tightly regulated to maintain cellular homeostasis.

Studies have shown that elevated expression of KPNB1 may correlate to increased nuclear import and export efficiency [48]. This increased transport efficiency has been suggested as a possible mechanism for cancer cells to cope with increased proliferative and metabolic demands. Using bioinformatic and molecular biology approaches research in our laboratory showed that the overexpression of KPNB1 observed was due to the dysregulation of E2F/Rb

activity in cervical cancer cells [17]. When KPNB1 expression was inhibited using siRNA, cell death in cervical cancer cells was observed with minimal effects on non-cancer cells [48]. Elevated expression of KPNB1 has also been shown in breast cancer cells where suppression of KPNB1 by siRNA resulted in reduced proliferation of breast cancer cells [49]. Recent research has identified KPNB1 as a possible target for lung adenocarcinoma treatment. This research showed that Polo like Kinase 1 (PLK1) inhibition lead to reduced expression of KPNB1 where reduced expression lead to a reduction in cancer cell proliferation via apoptosis [50]. The increased expression and reliance of cancer cells on KPNB1 in comparison to non-cancer cells suggests it has potential as an anticancer target.

1.5.4 KPNB1 Structure

The KPNB proteins have been reported to vary in size between 90 KDa and 130 KDa. KPNB1 is composed of 19 helical motifs commonly known as HEAT repeats. The HEAT repeats are each approximately 40 residues long. The main repeat unit consists of a hairpin made up of 2 B- helices known as helix A and helix B which are separated by a sharp turn (Figure 1.2). One turn forms a long acidic loop at HEAT 8 which is critical for the regulation of substrate binding and release during translocation [51].

Figure 1.2. KPNB1 containing 19 HEAT repeats. Helix A and B are connected by a sharp acidic loop at HEAT 8 which essential for substrate binding and release. HEAT repeat 1-8 are required for RanGTP binding while HEAT 7-19 are required for KPNα binding. HEAT repeat 4-8 are required for binding nucleoporins during nuclear import [51].

Since KPNB1 plays a role in classical nuclear import via the interaction of KPNα and RanGTP, these proteins should have specific binding regions on KPNB1. Crystal structure analysis revealed that RanGTP binds KPNB1 via the amino-terminal domain while cargo binds via the carboxyl domain. The full length KPNB1 complexed with the binding domain of KPNα was shown to form a snail-like super helix in which the C- and N-terminal HEAT repeats were near [52]. The RanGTP bound form of KPNB related protein KPNB2 forms an S-like twisted right handed helix [53]. Knowing the regions of KPNB1 required for its function e.g the KPNα and Ran binding domain, allows for the investigation into molecules that may target these regions. In identifying targeted therapies, structure-based approaches can be used.

1.6. Identification of small molecule inhibitors in drug discovery

The main aim of targeted therapy is to identify small molecule inhibitors or antibodies which selectively bind a target which cancer cells are highly dependent on [9]. While previous studies have shown that cancer cells are dependent on KPNB1 for their survival, few inhibitors that target KPNB1 as an anticancer approach have been identified. Research aimed at identifying small molecule inhibitors against KPNB1 presents a novel anticancer approach.

The process of drug discovery utilizes different modelling methods to study chemical and biological systems [54]. The use of computational and experimental methods has been of value in the identification of novel therapeutic compounds. Structure based drug design methods is a prominent method in drug discovery which uses the 3-D structural information gathered from the protein [54].

1.6.1 Structure based drug design (SBDD) and molecular docking of chemical compounds

In the process of drug discovery and design, understanding the fundamentals of how small molecule ligands recognize and interact with macromolecules is crucial in identifying novel compounds. Structure based drug design (SBDD) refers to the use of structural data, usually obtained experimentally or through computational modelling, to design/identify chemical compounds which bind a specific target [55]. The purpose of SBDD is to identify ligands with specific stereochemical and electrostatic attributes allowing for strong binding to the receptor of interest. The process of SBDD is a cyclic process which starts with a known target structure which is identified through *in silico* studies. After molecular modelling of the target and potential compounds, synthesis of the most promising compounds takes place. Next the compounds are tested for their biological activities to obtain relevant biological information (potency, activity, efficacy). Once biological information is collected the SBDD process starts again with new steps to incorporate molecular modifications to improve binding affinity of chosen compound [56].

Molecular docking is a common method used in SBDD due to its ability to predict the conformation of small-molecule ligands within the appropriate binding site of the receptor of interest. The first molecular docking algorithm was developed in the 1980s and since then, molecular modelling has become an essential tool in drug discovery [56].

The docking process requires a 3-D structure of the ligand and the receptor. The ligand/compound is docked into the binding site and different conformations are explored until the most likely binding conformation is identified. The process is carried out until convergence to the conformation with minimum energy [56].

1.6.2 Pharmacology in drug design

Rational drug design assumes a simple relationship between exposure of a drug and its therapeutic effect. However, since living system are far more complex the relationship is not that straight forward. Many failures of drug candidates in drug development is due to undesirable pharmacokinetic properties such as short half-life ($t_{1/2}$), poor absorption or excessive metabolism. The failure rate of many drug candidates illustrates the importance of incorporating pharmacokinetics in drug discovery and development [57].

Pharmacokinetics can be defined as the study of a drug's movement in the body. This can be investigated through Absorption, Distribution, Metabolism and Excretion (ADME). Research has shown that the initiation of early pharmacokinetic screening in the form of ADME *in vitro* and *in vivo* screening has decreased the proportion of compounds failing in clinical trials. The aim of ADME screening is to eliminate or improve drug candidates in the early stages of drug development [57]. *In vitro* ADME screening uses different assays to investigate specific characteristics of a compound which will affect the absorption, distribution, metabolism and excretion in a living system. Absorption refers to how a drug will be taken up into the blood which is usually affected by the permeability and lipophilicity of a compound. Distribution refers to how a drug will be transported which usually is via the blood hence the solubility of a drug is important. Metabolism refers to how a compound is broken down by metabolising enzymes to form metabolites. This has important implications for the clearance of a drug but also allows for the identification of specific metabolites which could be more active then the parent drug [57,58]. Lastly, Excretion refers to how the compound will by excreted from the system. Investigating properties such as solubility, plasma protein binding, lipophilicity, permeability and metabolic stability is important in providing crucial pharmacokinetic data which can guide future animal and clinical studies [58]. Therefore, the incorporation of

pharmacokinetics in drug discovery of small molecule inhibitors in the early stages of drug development will allow for better understanding of how these compounds may act in a living system.

1.7 Inhibitors of nuclear transport

KPNB1 plays an important role in nuclear cytoplasmic transport by acting as a transport protein which imports various cargo selectively. The elevated expression of KPNB1 has been implicated in various human cancers which has made it a target of interest for cancer therapy. Since normal cells seem to be less reliant on KPNB1 for their survival as opposed to cancer cells this makes KPNB1 a potential for target therapy [17].

Drugs which target KPNB1 are still limited. The first KPNB1 targeting small molecule inhibitor to be identified was Karyostatin 1A. Karyostatin 1A was shown to bind KPNB1 with high affinity and specifically targeted the classical import pathway *in vitro* and *in vivo.* Although Karyostatin 1A showed anticancer activity, its off-target effects have not been investigated [59]. Other inhibitors such as peptide inhibitors and small molecule peptidomimetic inhibitors of the classical import pathway have been used to study nuclear import *in vivo* however, these inhibitors were not successful as they are not cell permeable [60].

Importazole, a 2,4-diaminoquinazoline is currently the only commercially available small molecule inhibitor of KPNB1 which has been reported [60]. Therefore, future investigation and identification of additional small molecule inhibitors of KPNB1 could provide novel therapeutics for cancer treatment.

1.7.1 Identification of small molecules with inhibitory activity against KPNB1 function

Previous work in our laboratory aimed at identifying potential KPNB1 inhibitors. A structure-based computational screen was performed in collaboration with the Molecular Modelling Facility of the James Graham Brown Centre at the University of Louisville, Kentucky, USA. An *in silico* screen for small molecules with potential to bind KPNB1 was performed using the known crystal structure of KPNB1. The region of KPNB1 targeted included the overlapping RanGTP and KPNα binding sites of KPNB1. This RanGTP and KPNα overlapping region has been shown to be essential for KPNB1 mediated nuclear transport [51]. A library of drug-like compounds was screened against the target site and ranked according to their potential KPNB1-binding affinity. Forty-seven of the highest ranked compounds were then screened in cell culture studies for their ability to block nuclear import and their effect on cancer cell viability. Several compounds were identified of which Inhibitor of Nuclear Import 43 (INI-43), Compound 53 (C53) and Compound 60 (C60) were selected from 16 compounds which had cell killing activity at ≤ 50 μM, a concentration in the range of that of current chemotherapeutics tested on cervical cancer cell lines in culture [62]. Our lab has done extensive studies on INI-43 which showed anticancer activity as well as inhibition of KPNB1 [62]. The focus of this MSc study is to investigate C53 as a novel compound with anticancer activity and its potential to inhibit KPNB1 associated nuclear import.

1.7.2 C53 as a potential KPNB1 small molecule inhibitor

C53, chemically known as 1-benzyl-4[(4-methoxy-1-naphyl) methylamino]-N-methyl-pyrrolidine-2-carboxamide is a pyrrolidine derivative (Figure 1.3). Interestingly, studies have shown that pyrrolidine has anticancer activities and acts as an inhibitor of Matrix metalloproteinases 2 and 9 which have been reported to have a key role in tumour growth,

invasion and metastasis in cancer tissues [63]. Our study aims to further investigate and characterise C53 as a small molecule with anticancer activity.

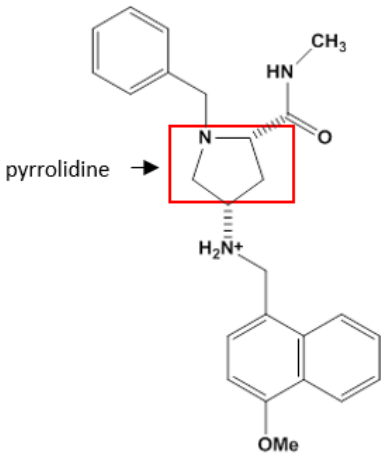

C53

Figure 1.3 Chemical structure of C53 (1-benzyl-4[(4-methoxy-1-naphyl) methylamino]-N-methyl-pyrrolidine-2-carboxamide)

1.8 Significance of the study

Recent work suggests that KPNB1 is overexpressed in cervical cancer tissues and necessary for the proliferation of cancer cells, while non-cancer cells are minimally affected. This suggests that KPNB1 mediated nuclear import is a possible target for anticancer therapeutics. This study investigates a novel small molecule inhibitor, as an experimental compound for nuclear import inhibition with anticancer properties. In addition, *in vitro* characterisation of the pharmacokinetics properties as well as the investigation of the *in vivo* toxicology of C53 will be explored.

1.9. Project Aims

This project aims to:

1) investigate the anticancer properties of a novel small molecule, C53 by monitoring its effects on cell proliferation, cell cycle and apoptosis using cervical cancer cell lines.
2) investigate the effects of C53 on the activity of known KPNB1 target proteins.
3) investigate the *in vitro* ADME pharmacokinetic properties of C53 to determine the solubility, lipophilicity, permeability, plasma protein binding and metabolic stability of C53.
4) investigate the *in vivo* toxicology of C53 in a nude mouse model

CHAPTER 2:

MATERIALS AND METHODS

2.1 MATERIALS

2.1.1 Cell lines

Human cervical carcinoma cell lines, CaSki and HeLa, normal lung fibroblasts, WI38 as well as its transformed counterpart SVIWI38, were all obtained from American Type Culture Collection (ATCC, Rockville, MD, USA). The oesophageal carcinoma cell line WHCO6 was established originally from a South African patient with oesophageal squamous cell carcinoma, and was kindly provided by Prof R. Veale from the University of Witwatersrand, South Africa. KYSE30 was originally established by Shimada et al. and was purchased from the German Resource Centre for Biological Materials (Braunschweig, Germany) [64]. The normal skin fibroblasts FG_0 and DMB were obtained from the Department of Medicine at the University of Cape Town.

2.1.2 Chemical Compounds

Compound 53, C53 (2S,4S)-1-benzyl-4-[(4-methoxy-1-naphthyl) methylamino]-N-methyl-pyrrolidine-2-carboxamide was obtained from Syngene (ZINC identification no. 20598662) in a yellow/brown gum form at a 95% purity. C53 was dissolved in DMSO to a stock concentration of 100 mM and kept in the dark at room temperature. Inhibitor of nuclear import Importazole was purchased from Sigma-Aldrich (St Louis, MO, USA) and dissolved in DMSO to a stock concentration of 50 mM and stored at 4˚C.

2.1.3 Animals

Animal ethics approval was obtained from the Faculty of Health Sciences Animal Ethics Committee, University of Cape Town (protocol number 016/ 014) for *in vivo* studies. Male and female athymic mice (UCT 21) of the age of 4-6 weeks were obtained from the Faculty of Health Science Animal breeding unit (University of Cape Town). Athymic mice were used because these mice are immunocompromised therefore they do not reject tumour cells from other species. The mice were housed 6 per cage in autoclaved polysufane cages with sterile wood shavings as bedding in a room kept at constant temperature and humidity in the BSL2 unit (University of Cape Town). Mice were fed a regular autoclaved chow diet and water containing antibiotics and multi-vitamin. Mice were housed under 12-hour light and darkness cycles. Handling of mice was performed in strict accordance with the BSL2 guidelines of the Animal Ethics Committee.

2.2. METHODS

2.2.1 Tissue cell culture

All cells, except for the normal skin fibroblasts, were cultured in Dulbecco's Modified Eagles Medium (DMEM) (Invitrogen, USA) containing 10% Fetal Bovine Serum (Gibico, Paisley, Scotland) and penicillin streptomycin (PS) (100 µg/mL). Normal skin fibroblasts were cultured in DMEM containing 20% Fetal Bovine Serum (FBS) supplemented with penicillin streptomycin (PS) (100 µg/mL). All cells were grown in 100 mm tissue culture dishes and incubated in a humidified incubator at 37°C containing 95% air and 5% CO_2. Media was changed every 2 days and cells were plated once ±70 % confluency was reached.

2.2.1.3 Mycoplasma testing

To ensure that cells were not contaminated with Mycoplasma, Mycoplasma tests were performed on all cell lines used. Cells were cultured as described in section 2.1.2, until they reached ± 70% confluency. Cells were then trypsinized then neutralized with media before centrifugation for 3 minutes. The pelleted cells were resuspended in PS-free media, plated on a cover slip and incubated for 24 hours. Cells were washed twice with 1 X PBS (pH 7.1) and fixed for 10 minutes. Cells were then stained with DAPI before being mount using mowiol and left overnight in the dark. The following day cells were visualized on the Zeiss Anxiovert 200 inverted fluorescent microscope (Carl Zeiss, Jena, Germany). The presence of blue small speckles in the cytoplasm and cell membrane indicated mycoplasma contamination.

2.2.2 MTT EC_{50} determination

Cells were plated at 5000 cells/well in a 96-well plate and left to adhere overnight. Cells were treated with different concentrations of C53 for 48 hours. Following 48 hours of C53 treatment, MTT (3-(4,5-dimethylthiazol-2-yl)-2,5-diphenyltetrazolium bromide) reagent was

added (5 mg/ml) to the cells for 4 hours after which Solubilization reagent (10% SLS in 0.01 M HCl) was added to each well to solubilize the crystals. Following 24 hours of incubation absorbance was read at 595nm. Absorbance readings were used to plot a dose response curve and determine the EC_{50} (concentration of drug for half-maximal response) using the Graph pad prism software.

2.2.3 Cell proliferation assay

To measure the proliferation of cells, cells were plated at a density of 1000 cells/ well in a 96 well plate. The following day cells were treated with varying concentrations of C53 (0-40 µM) and viable cells were examined every 24 hours for 4 days using the MTT reduction assay method as previously described (section 2.3).

2.2.4 Annexin V/PI Staining assay

Apoptosis was examined by flowcytometry after staining with Propidium Iodide (PI) (100 µg/ml) and Alexa Fluor 488 annexin V (cell apoptotic marker). Briefly, cells were plated in 60 mm plates at a density of 1,5 x 10^5 cells/ plate and treated with either DMSO (control) or 20 and 40 µM C53 for 48 hours. Following treatment, cells were harvested, and staining method was carried out according to the manufacturer's instructions (Alexa Fluor 488 Annexin V/Dead Cell Apoptosis Kit, Introgen, OR, USA). After staining with Alex Fluor 488 annexin v and PI binding buffer was added to the samples, mixed gently and analysed by flow cytometry. PI cannot penetrate live cells and apoptotic cells but penetrates dead cells, dying them with red fluorescence. The population of cells are distinguished based on the various fluorescence colours where live cells show little to no fluorescence, apoptotic cells show green fluorescence and dead cells show red and green fluorescence. The percentage

population of apoptotic cells is determined by flow cytometry, measuring the fluorescence using 488 nm excitation and 530 nm emission.

2.2.5 Western blot analysis

2.2.5.1 Protein extraction and protein quantification

2.2.5.1.1 Whole cell protein extraction

Cells were grown to 70% confluency in a 60 mm cell culture dish and treated with appropriate concentration of C53 for a designated period. Media from each plate was collected in 12 mL tubes. Cells were washed twice with ice cold 1 X PBS and the PBS wash was added to the appropriate 12 mL tubes. A fixed volume (60 µl) of a cocktail (Active RIPA) containing radioimmunoprecipitation assay buffer (RIPA), 1 X complete protease inhibitor (Sigma, USA) and 1 mM Na_3VO_4 phosphatase inhibitor was added to each plate before cells were scraped using a cell scraper. Cell lysates were collected in eppendorf tubes and kept on ice. Cells collected in media (12 ml tubes) were centrifuged for 3 minutes at 10000 rpm. Pellets were resuspended in 40 µl Active RIPA and added to the cell lysates collected. Lysates were sonicated for 8 seconds then centrifuged at 4˚C for 10 minutes at 10000 rpm. The supernatant was transferred to new eppendorf tubes and protein was quantified using BCA (Bicinchoninic Acid) Assay (Pierce ThermoScientific, USA). The BCA assay is based on the reduction of Cu^{+2} to Cu^{+1} under alkaline conditions (Biuret reaction). The reduction of Cu^{+2} by the protein is a function of protein concentration which was determined spectrophometrically by a colour change from green to purple measured at an absorbance of 595nm. Bovine serum albumin (BSA) standard curve was done using concentrations ranging from 50 µg/ml to 2000 µg/ml by adding 100 µl of the BCA working solution to 10 µl of each concentration in a 96-well plate. This was followed by a 30 minutes incubation at 37 ˚C, and absorbance values read at 595nm.

To determine protein concentration, 5 µl of protein extract was diluted with 15 µl of dH_20 and the same procedure followed for BSA standard curve to obtain absorbance readings. Using the BSA standard curve protein concentrations were calculated.

2.2.5.1.2 Nuclear Cytoplasmic fractionation

To examine the change in localisation of a protein of interest (KPNB1) post treatment with C53, the nuclear proteins were harvested separately from the cytoplasmic proteins. Cells were plated and treated with varying concentrations of C53 for a designated period. After treatment, media from cells was removed and cells were washed twice with ice cold 1 X PBS followed by the addition of trypsin (600 µl) to dissociate cells. Complete media (600 µl) was added and cells were collected in eppendorfs on ice. Cells were centrifuged at 4˚C at 3000 rpm for 5 minutes after which supernatant was discarded and pellet was resuspended in harvest buffer (150 µl) on ice for 5 minutes (recipes in appendix). After 5 minutes, cells were centrifuged at 5000 rpm for 10 minutes after which the supernatant (cytoplasmic fraction) was collected in new eppendorfs tubes and stored at -80˚C. The nuclear pellet was resuspended in Buffer A (500 µl) and centrifuged at 5000 rpm for 5 minutes. The pellet was then slightly resuspended in Buffer C (150 µl) and vortexed for 15 minutes at 4˚C followed by centrifugation at 14000 rpm at 4˚C for 10 minutes. The supernatant which contained the nuclear proteins was collected in new eppendorf tubes and stored at -80˚C (recipes for buffers provided in appendix). Nuclear and cytoplasmic protein fractions were quantified using BCA as described in section 2.6.1.1.

2.2.5.1.3 SDS-PAGE Gel Electrophoresis

Fixed concentrations were loaded onto SDS-PAGE gel. 5X loading dye was added to the protein and total volume (30 µl) was made up using RIPA. Protein was denatured by heating

of the samples at 90˚C for 5 minutes using a heating block. Equal amounts of protein samples were loaded onto 10 -15% polyacrylamide gels and electrophoresis performed at 180 V for approximately 1 hour in 1X running buffer (recipe in appendix). After electrophoresis, the proteins were transferred onto a nitrocellulose membrane at 100 V for 70 minutes on ice using 1X transfer buffer (recipe in appendix). After transfer, the membrane was blocked in 5% Milk powder in TBST (TBS Tween) for 2 hours with gentle shaking.

2.2.5.1.4 Antibody incubation

After blocking, the membrane was washed three times with TBST for 5 minutes each. The membrane was probed with primary antibodies over night at 4˚C, gently shaking. (see Table 2.6 for conditions). The following day the membrane was washed three times, 5 minutes each, with TBST to remove unbound antibody before probing with secondary antibody for 1 hour at room temperature with gentle shaking. Following incubation with secondary antibody, the membrane was washed a further three times with TBST for 5 minutes each.

2.2.5.1.5 Immunodetection

The protein bands of interest were detected using a chemiluminescent substrate system, LumiGlo (KPL, Gaithersburg, USA), according to manufacturer's instructions. The membrane was incubated with equal volumes of each substrate for 1 minute. The protein bands were visualised by exposing the nitrocellulose membrane to X-ray films for a duration of time, followed by immersing film in developer (AGFA G128), water then fixative (AGFA G33C) followed by rinsing the membrane with water. The amount of GAPDH (whole cell and cytoplasmic protein) or Histone H3 (nuclear protein) was measure as an internal control.

2.2.5.1.6 Re-probing of membrane

In order to investigate more than one protein on the same membrane re-probing was done. Membranes were stripped using 10% Acetic acid for 10 minutes gently shaking. Stripping is done to remove the primary and secondary antibodies of previous protein of interest to allow for re-probing of another protein. The membrane was washed with TBST to remove the acetic acid. The membrane was then blocked using 5% Milk in TBST for 2 hours while gently shaking after which membrane was probed with antibodies as previously described (section 2.6.3).

Table 2.1: Antibodies and incubation conditions

Primary antibody	Primary antibody conditions	Secondary antibody	Secondary antibody conditions	Substrates
Parp-1 (H250) [sc-7150, Santa Cruz Biotechnology]	1: 1000 TBST	Goat anti Rabbit [Bio-Rad]	1: 5000 TBST	LumiGlo® chemiluminescent substrate (KPL, USA)
cyclin D1 (HD11) [Santa Cruz Biotechnology]	1: 250 TBST	Goat anti Mouse [Bio-Rad]	1:2000 TBST	LumiGlo® chemiluminescent substrate (KPL, USA)
CDK4 (H-22) [Santa Cruz Biotechnology]	1:500 TBST	Goat anti Rabbit [Bio-Rad]	1:2000 5% Milk-TBST	LumiGlo® chemiluminescent substrate (KPL, USA)
KPNB1 (ab45938) [Abcam]	1:5000 TBST	Goat anti Rabbit [Bio-Rad]	1: 5000 TBST	LumiGlo® chemiluminescent substrate (KPL, USA)
GAPDH (0411) [sc-47724, Santa Cruz Biotechnology]	1: 5000 5% Milk-TBST	Goat anti Mouse [Bio-Rad]	1: 5000 5% Milk-TBST	LumiGlo® chemiluminescent substrate (KPL, USA)
Histone H3 (D1H2) cell signalling	1:5000 TBST	Goat anti Rabbit [Bio-Rad]	1:5000 TBST	LumiGlo® chemiluminescent substrate (KPL, USA)

2.2.6 Cell cycle analysis

The cell cycle profile of cells treated with C53 was determine by DNA staining with PI. Briefly, 2 x 10^5 cells were plated in a 60 mm dish and treated with various concentrations of C53 (0-40 μM) for 48 hours. Post treatment, the media was collected in 12 ml tubes on ice. The cells were washed twice with ice cold PBS before being trypsinized. Cells were collected in the same 12 ml tubes and pelleted at 10000 rpm for 2 minutes. The cells were then fixed with ice cold 100% ethanol and store at -20˚C for 3 days. Following fixation, cells were centrifuged and ethanol was removed. The cells were washed twice with ice cold PBS before the pellet was resuspended in ribonuclease (RNase)-PBS solution (50 μg/ml) and incubated for 30 minutes to remove the RNA. Following incubation cells were stained with staining solution containing PI (1 mg/ml) and incubated for a further 20 minutes. After staining, cells were analysed on a BD Accuri™ C6 flow cytometer (BD Biosciences, USA) and the cell cycle profile with the percentage of cells in each cell cycle phase was analysed using the ModFit LT™ software.

2.2.7 Luciferase assays

The luciferase assays were used to monitor the activity of NFAT or NF-κβ regulated transcription. The rationale behind this assay is that the cargoes (NFAT or NF-κβ) need to be transported into the nucleus for transcription to take place, where transcription leads to fluorescence emission. Therefore, we used the luciferase assays to investigate whether C53 treatment affects luciferase activity.

To assay for NFAT luciferase activity, 30000 cells/well were plated in a 24-well plate and allowed to adhere overnight. The following day cells were transfected with 50 ng GFP-NFAT plasmid (Addgene plasmid #24219, [65]), 50 ng NFAT-Luciferase (Addgene plasmid #10959, [66]) and 5 ng Renilla with the addition of 0.4 μL of the transfection reagent Genecellin™

(Celtric Molecular Diagnostic, South Africa). The following day transfection media was removed before treating cells with varying concentrations of C53 (0-40 µM) in fresh media for 24 hours. Cells were stimulated with 0.5 µM Phorbol Myristate Acetate (PMA) (Sigma) and 1.3 µM Ionomycin (Santa Cruz Biotechnology, Ca, USA) 3 hours before the end of treatment. Ionomycin is added to increase Ca^{+2} flux which is required for NFAT activity while PMA is added to ensure full NFAT induction [67]. After treatment incubation, cells were washed twice with ice cold PBS then lysed using 1 X passive lysis buffer for 15 minutes. After lysis luciferase activity was assayed using the Dual-Luciferase® Reporter assay system (Promega) according to manufacturer's instruction and activity was measured using the Veritas™ microplate luminometer (Promega).

To assay for NF-κB/ p65 luciferase activity, 30000 cells/well were plated in a 24-well plate and allowed to adhere overnight. The following day cells were transfected with 50 ng NF-κB/p65 luciferase reporter plasmid (Promega) and 5 ng Renilla using 0.4 µL GeneCellin™ transfection reagent. The following day cells were treated with varying concentrations of C53 (0, 20 µM and 40 µM) for 24 hours and stimulated with 500 nM PMA for 3 hours before the end of the treatment incubation. Cells were then lysed using 1 X passive lysis buffer for 15 minutes gently shaking after which luciferase activity was assayed using the Dual-Luciferase® Reporter assay system (Promega) according to manufacturer's instruction and activity measured using Veritas™ microplate luminometer (Promega).

2.2.8 Immunofluorescence microscopy

To analyse cellular localisation of KPNB1, cells were plated on ethanol flamed glass coverslips at 120 000 cells/ well in a 6-well plate. The following day cells were treated with the

appropriate treatment. Cells were then washed twice with ice cold PBS before being fixed using 4% paraformaldehyde in PBS for 15 minutes at room temperature. After fixing, fixing solution was removed and cells were washed twice with PBS. Cells were then permeabilized with 1 mL 0.25% Triton X-100 in PBS and incubated for 10 minutes at room temperature. Following permeabilization, cells were washed thrice with PBS before 1 ml blocking buffer (1% BSA in PBST + 0.3 M Glycine) was added to each well and incubated for 30 minutes. After incubation cells were probed with primary antibody in blocking buffer for 1 hour followed by three 5 minutes washes with PBS. Then secondary antibody (Cy3 Goat anti Rabbit) in blocking buffer was then added to the cells and incubated at room temperature 1 hour in the dark. After the secondary antibody incubation, cells were washed with PBS then stained with DAPI (200 µg/mL) diluted in PBS (1:400) for 5 minutes. Cells were washed once with PBS before being mounted on the slide using mowiol. Slide was left to dry in the dark overnight. The following day images were visualised and captured using a Zeiss Anxiovert 200 inverted fluorescent microscope (Carl Zeiss, Jena, Germany). The primary antibody used was rabbit anti-KPNB1 (Santa Cruz Biotechnology) diluted at 1: 100. Secondary antibody used was Cy3 Goat anti Rabbit (Jackson ImmunoResearch, USA) diluted at 1: 300.

2.2.9 ADME Pharmacokinetic assays

In vitro ADME assays were performed with assistance from H3D Africa based at the University of Cape Town.

2.2.9.1. Plasma protein binding assay

The plasma protein binding assay was used to investigate the percentage of drug (C53) bound to plasma protein found in human blood plasma. The plasma protein binding of a drug has an impact on the drugs distribution in the body.

The plasma protein binding assay was performed in a 96-well micro titre plate with pooled human blood plasma (blood bank K3 EDTA). The blood plasma, which was thawed at 37˚C, was spiked with 10 mM stock of C53 (1 µM). The total concentration sample was prepared by immediately removing an aliquot of the human blood plasma spiked with C53 and quenching it with ice cold acetonitrile containing carbamazepine (0.0236 µg/ml, internal standard) then placed in the freezer. Duplicate aliquots of spiked plasma were transferred to a 96-well microtiter plate and incubated on a shaker at 37˚C for 30 minutes to allow for protein binding. After shaking, duplicate samples were then transferred to ultra-centrifuge tubes and ultracentrifuged (Beckman Optima L-80XP) at 37˚C for 4 hours. This allowed the separation of free drug from protein bound drug. Control samples Warfarin, MMV390048 and Caffeine were diluted in duplicates in blood plasma protein in a 96-well plate and incubated on the shaker for 4 hours at 37˚C. After 4 hours, aliquots (40 µl) of both samples and controls were transferred to a 96-well deep well plate and quenched with ice cold acetonitrile with carbamazepine (0.1 µM, internal standard). All samples were then centrifuged at 3000 rpm for 10 minutes and resulting supernatant was filtered. Analyte concentration of compound samples (containing C53) as well as controls were determined by LC-MS/MS (Agilent Rapid Resolution HPLC, AB SCIEX 4000 QTRAP MS).

2.2.9.2 Kinetic solubility

The Kinetic solubility assay was performed to investigate the solubility of C53 in an aqueous medium. The kinetic solubility assay was performed using a miniaturised shake flask method. Briefly, C53 was dissolved in DMSO to a stock concentration of 10 mM. The 10 mM stock solution was used to prepare calibration standards (10-220 µM) in DMSO and added to phosphate buffer (PBS, pH 7.4) to a final DMSO concentration of 2%. Solutions were shaken for 2 hours at

25˚C to allow solubilisation of test compound (C53). Solutions were filtered and analysed by HPLC-DAD (Agilent 1200 Rapid Resolution HPLC with diode array detector). The aqueous solubility of samples was determined using a best fit calibration curve constructed from the calibration standards [68].

2.2.9.3 Parallel Artificial Permeability Assay (PAMPA)

PAMPA is an *in vitro* assay used to investigate the passive transcellular permeability of a drug. For a drug to enter the circulatory system it needs to pass through membranes, hence PAMPA assay mimics these membranes to monitor permeability of a compound.

The PAMPA assay was performed in 96-well MultiScreen Filter plates (Millipore, 0.4 µM PCTE Membrane), in triplicates. The membrane filters were pre-coated with 5% hexadecane in hexane and allowed to dry before the start of the assay. The wells of the 96-well donor plate were filled with buffer (pH 6.5), spiked with C53 (1 µg/mL). Membrane integrity marker, Lucifer yellow, was added to the wells of the MultiScreen donor plate. Phosphate buffer (pH 7.4) was added to the 96-well acceptor plate. The donor plate was then slotted into the acceptor plate forming a sandwich assembly then incubated for 4 hours at room temperature, gently shaking (50 rpm) to allow passive diffusion of compound. Following incubation, samples from acceptor wells were transferred to the analysis plate and acetonitrile containing carbamazepine (0.0236 µg/mL) was added to the samples before analysis by LC-MS/MS (Agilent Rapid Resolution HPLC, AB SCIEX 4500 MS). Membrane integrity was analysed by calculating the apparent permeability (P_{app})of Lucifer yellow using Modulus microplate reader [69]. The normalised peak areas were used to calculate the P_{app} for the samples.

2.2.9.4 Lipophilicity

The lipophilicity assay was used to investigate the lipophilicity of C53 which refers to how well a compound dissolves in fats/oils. The lipophilicity of a drug is important as it affects the solubility and metabolism of a drug.

The lipophilicity assay makes use of the shake flask method. Experiments were done in triplicate. Briefly, 10 µL of C53 (10 mM) was added to a 1:1 mixture of phosphate buffer (pH 7.4) and n-octanol in a microtiter plate. The solutions were shaken (1500 rpm) for 2 hours at room temperature. Following shaking, samples were centrifuged to fully separate the octanol/ PBS layers. The samples were analysed by HPLC-DAD (Agilent 1200 Rapid Resolution HPLC with diode array detector) to determine the partition coefficient ($LogD_{7.4}$) [70]. This was done by determining the amount of compound in each layer (PBS and n-octanol).

2.2.9.5 Microsomal Stability

The metabolic assay was performed to investigate how quickly C53 is broken down by metabolic enzymes to determine the half-life and clearance of the compound.

The metabolic assay was performed in a 96-well microtiter plate, in duplicates. 1 µM of C53 was incubated individually in mice, rat and pooled human liver microsomes (0.4 mg/mL) at 37˚C at varying time points. Incubation was done in the absence and presence of the cofactor NADPH (1 mM). Reactions were quenched at the various time points by adding 300 µL acetonitrile containing the internal standard, carbamazepine (0.0236 µg/mL). The amount of C53 in the supernatant was then analysed by LC-MS/MS (Agilent Rapid Resolution HPLC, AB SCIEX 4000 QTRAP MS) to determine the disappearance of the parent compound which is used to determine the half-life and clearance of the compound. Metabolite searches were not conducted within this assay [71].

2.2.10 C53 Toxicology studies *in vivo*

In order to investigate whether C53 is tolerable in nude mice a toxicology pilot study was performed. A total of 24 nude mice were randomized into four groups of six mice each. The three test groups received 10 μg/g, 30 μg/g and 50 μg/g of C53 in 7.5% DMSO in PBS while the control group received 7.5% DMSO in PBS only. Mice were injected interperitoneally (i.p) twice per week for 28 days. The mice were weighed four times a week and their well-being was monitored daily for the entire experimental period. At the end of 28 days, mice were euthanized by halothane over dose. Autopsies of each mouse was performed by an animal technician from the animal unit at UCT to analyse if drug caused any toxic effects internally. Signs of toxicity include inflammation of organs mainly the liver, discolouration of organs or unusual deposits at sight of injection. The liver of each mouse was then removed and weighed.

2.2.11 Statistical analysis

All experiments were performed at least two independent times. Experiments were performed in duplicates, triplicates or quadruplicates and expressed as mean ± standard error of mean (SEM), unless stated otherwise. The statistical significance was determined using the two-tailed student t-test (paired) using Microsoft Excel where a p-value of < 0.05 was considered as statistically significant.

CHAPTER 3:

INVESTIGATING THE EFFECT OF C53 ON CANCER CELL BIOLOGY

3.1 INTRODUCTION

Targeted therapies are a form of cancer treatment that target key characteristics in malignant cells responsible for driving tumorigenesis. The advantage of this form of therapy is its specificity for targeting pathways on which cancer cells are dependent on [72]. The identification of the altered expression of KPNB1 in cervical cancer patient tissue and cell lines in comparison to normal cell lines as well as the induction of apoptosis in cancer cells lines after inhibition of KPNB1 expression suggests a dependency of cervical cancer cell lines on KPNB1 function [17,44]. These studies suggest that KPNB1 has potential as an anticancer therapeutic target.

There are multiple ways in which a protein target can be inhibited. One manner is the use of a small molecule inhibitor that targets the protein of interest. An investigation of possible inhibitors of KPNB1 through structure based *in silico* screening and cell based assays performed by our laboratory in collaboration with researchers at the University of Louisville identified a number of potential small molecule inhibitors of KPNB1, including compounds named C43 (INI43) and Compound 53 (C53). Extensive research has been done on INI43, which revealed that it has anticancer properties as well as nuclear import inhibition properties [62]. The aim of this study is to investigate the anticancer properties of the previously undescribed compound, C53 on cancer cell biology. Different aspects of cancer cell biology

were investigated including cell survival, proliferation, cell cycle progression and cell death inducing mechanism.

To investigate the potency of a drug-like compound the half maximal effective concentration (EC_{50}) is measured. The EC_{50} is defined as the concentration of a drug required to induce a 50% response after a specified exposure time [73]. Therefore, to investigate the cell survival of cancer cells we determined the EC_{50} of C53 in a panel of cell lines. For the assessment of the effect of C53 on proliferation, cancer cells were treated with C53 and proliferation was monitored over a specified period. Since cancer cells are characterised by uncontrolled proliferation an anticancer agent should ideally reduce the proliferation of cancer cells. Research has shown that the aberrant cell proliferation that characterises cancer associates with alterations in cell cycle progression [74]. To investigate the effect of C53 on cell cycle progression we monitored the cell cycle profile of cells treated with C53 by flow cytometry.

In order to investigate whether C53 induces cell death, we analysed the morphology of cells post treatment with C53. Cells undergoing cell death are characterised by specific morphological features e.g apoptotic cells have blebbed membranes; autophagic cells are characterised by vacuoles (autophagosomes) while necrotic cells are usually burst open. The mode of cell death was further investigated by Annexin V/PI staining which distinguishes the percentage of cells undergoing cell death and determines whether the cell death is apoptotic. In viable cells, phosphatidylserine (PS) is located on the inner membrane of the cell membrane. However, in apoptotic cells PS is translocated to the outer leaflet of the membrane. Annexin V/PI staining is useful in detecting apoptotic cells because the Annexin V binds to the translocated PS on apoptotic cells.

3.2 RESULTS

3.2.1 EC_{50} determination for C53 in non-cancer cells, cervical and oesophageal cancer cell lines.

The EC_{50} (concentration of drug required to produce a half maximal response) of C53 was determined in a panel of cancer (CaSki, HeLa, Kyse30, WHCO6, transformed (SVIWI38)) and non-cancer (FG_0, WI38, DMB) cells. Cells were plated in a 96-well plate and treated with varying concentrations of C53 for 48 hours after which MTT reagent was added to quantify the number of viable cells. Absorbance readings of viable cells were analysed using Hill plots and EC_{50} values determined (Figure 3.1). The EC_{50} results with 95% confidence intervals are tabulated in Table 3.1 and show that CaSki and HeLa cervical cancer cells as well as Kyse30 and WHCO6 oesophageal cancer cells had EC_{50} values of approximately 20 μM. The transformed fibroblast cell line SVIWI38, had an EC_{50} value of 27 μM while the non-cancer fibroblasts had EC_{50} values of between 30 and 40 μM. These results show that C53 has a cell killing effect of ~20 μM in cancer cells which is 1.5-2 fold lower than that of non-cancer fibroblasts suggesting that the cancer cell lines are more sensitive to C53 (Figure 3.2).

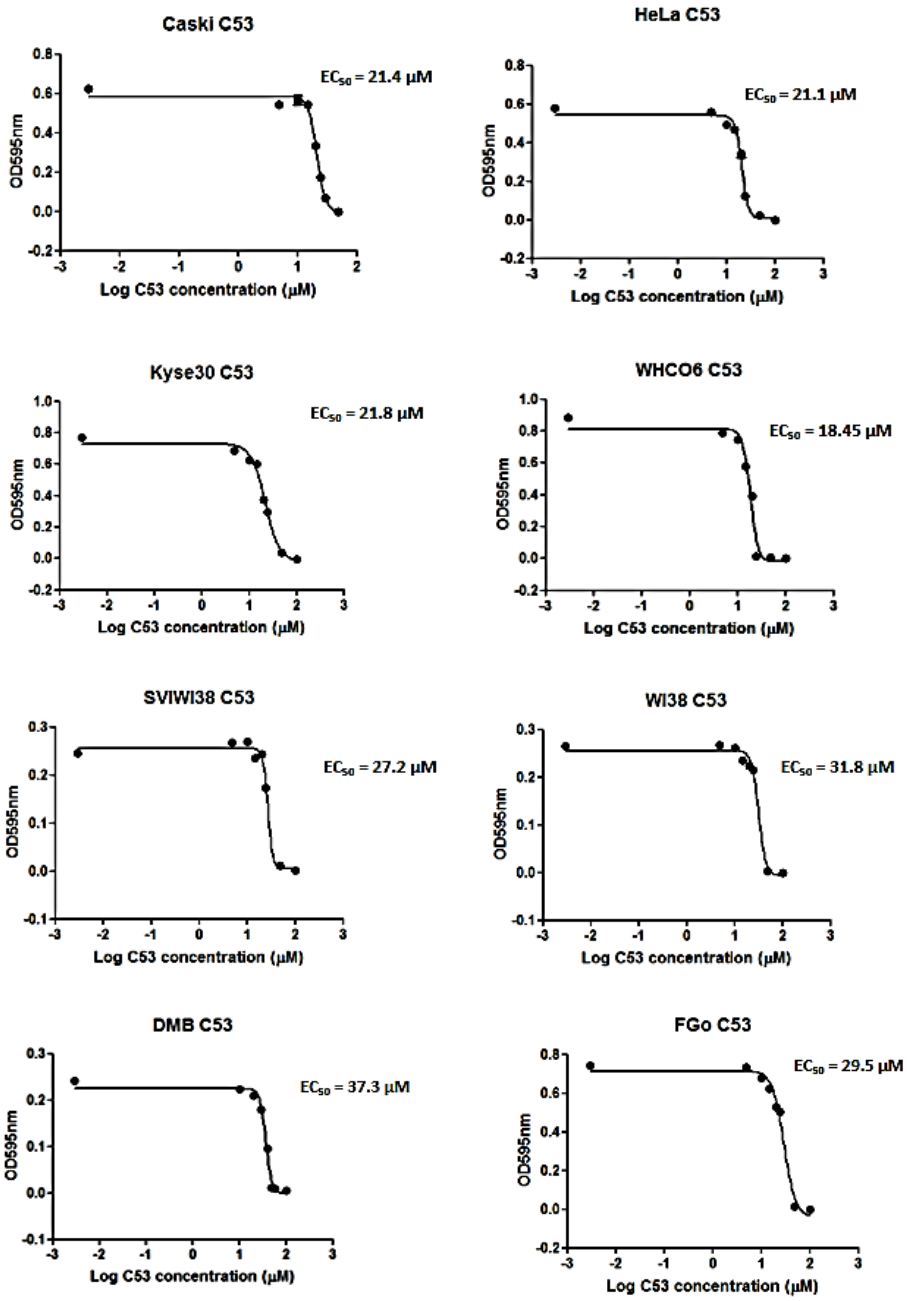

Figure 3.1 EC_{50} determination in cervical cancer, oesophageal cancer and non-cancer cells. Cervical cancer (HeLa and CaSki) cells, Oesophageal cancer (Kyse30 and WHCO6), transformed fibroblast cell line, SVIWI38 and non-cancer fibroblast (WI38, FG_0 and DMB) cells were treated with increasing concentration of C53 for 48 hours after which viable cells were examined by an MTT assay. Hill plots and EC_{50} values were quantified using Graph Pad Prism software. Experiments were performed in triplicate and repeated at least two independent times. Representative hill plots are shown.

Table 3.1: Average EC_{50} values of C53 in cervical and oesophageal cancer cell lines as well as non-cancer cells

	Cell line	EC_{50} value (µM)	95 % Confidence Interval
Cervical cancer	CaSki	20.8	19.3 – 22.3
Cervical cancer	HeLa	20.2	16.4 – 25.1
Oesophageal cancer	Kyse30	20.1	16.4 – 24.6
Oesophageal cancer	WHCO6	20.5	16.2 – 26.2
Transformed	SVWI38	27.1	20.8 – 35.6
Fibroblast	WI38	31.8	24.2 - 41.8
Fibroblast	FG_0	30.6	28.2 – 38.7
Fibroblast	DMB	39.9	35.0 – 45.5

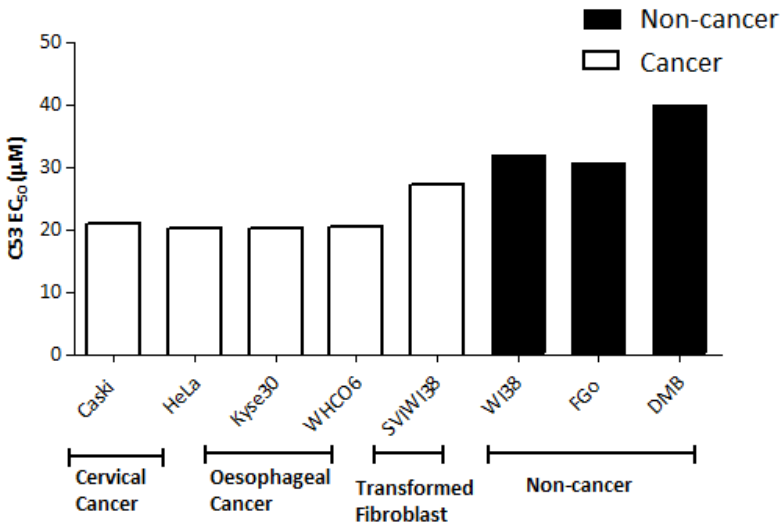

Figure 3.2. A summarised graph of the average C53 EC_{50} values in cervical, oesophageal and non-cancer cells. MTT assay was used to determine EC_{50} values in cancer and non-cancer cell lines. The non-cancer (black) cells show higher EC_{50} values than the cancer cell lines (clear bars). Experiments were performed in triplicate and repeated at least two independent times.

3.2.2 Effect of C53 on cell proliferation of cervical cancer cells and normal fibroblast.

Having established that C53 has enhanced cytotoxic effects on cervical and oesophageal cancer cell lines which have shown elevated expression of KPNB1 in comparison to normal fibroblasts, we next investigated the effect of C53 on cell proliferation of cervical cancer cell lines which was the focus of this MSc thesis. For this assay, cervical cancer cell lines HeLa and CaSki as well as normal fibroblast FG_0 were treated with the vehicle control, DMSO or 10 µM, 20 µM (EC_{50}) and 40 µM C53 and cell proliferation was evaluated over four days using the MTT assay. Cell proliferation was quantified and the results show that 20 µM and 40 µM C53 treatment significantly reduced the cell proliferation of HeLa and CaSki cell lines while 10 µM C53 only showed inhibitory effects at day 4 of C53 treatment (Figure 3.3 A and B). C53 treatment at 10 µM and 20 µM concentrations had little effect on the proliferation of non-cancer FG_0 cells however, 40 µM C53 treatment inhibited the proliferation of FG_0 (Figure 3.3 C). These results show that C53 selectively reduces the proliferation of cancer cell lines at doses of 10 µM and 20 µM, while non-cancer FG_0 cells remained unaffected at these concentrations.

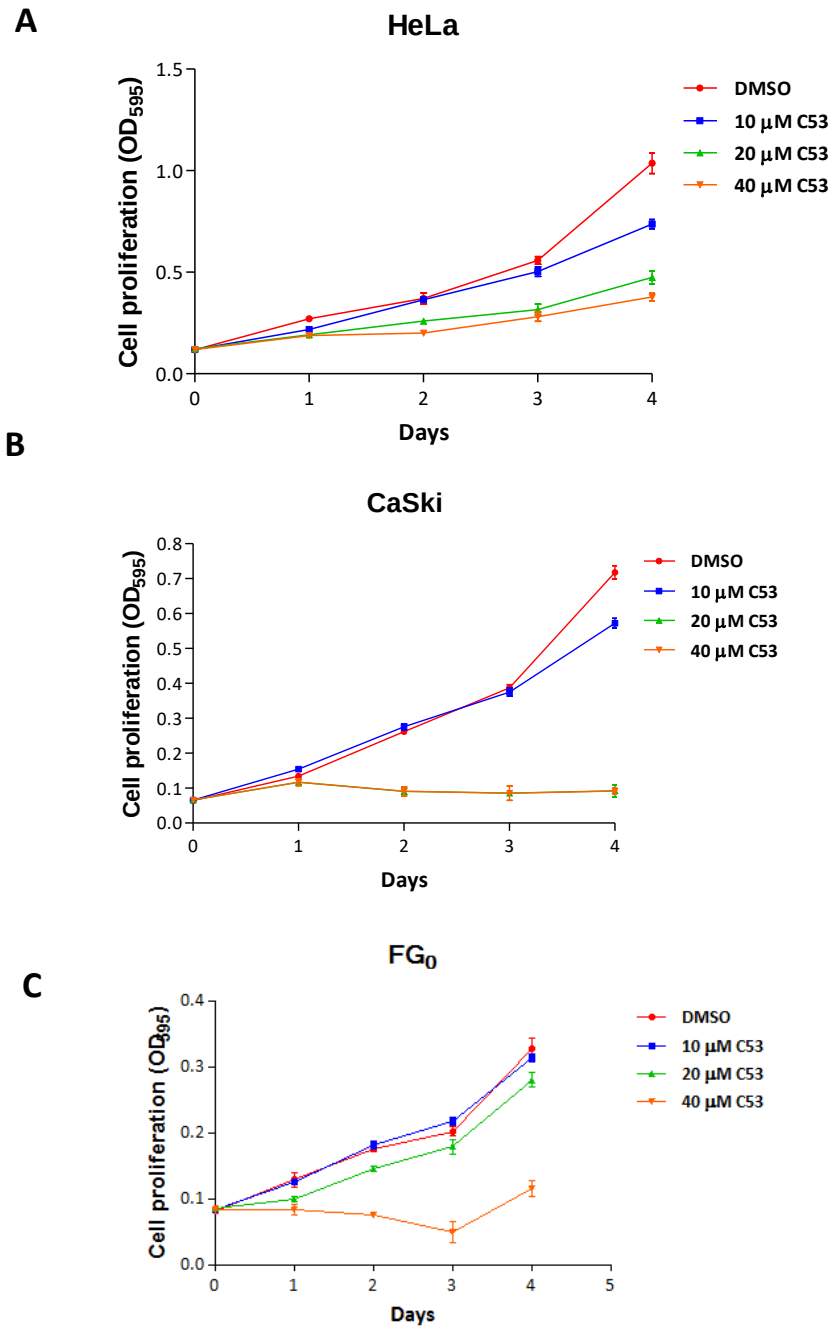

Figure 3.3 Effect of C53 on the cell proliferation of HeLa, CaSki and FG_0 cells. Cells were plated and treated with increasing concentrations of C53 or DMSO (control) and cell proliferation was measured by MTT assay over 4 days. (A) HeLa and (B) CaSki cells showed a reduction in cell proliferation for 20 µM and 40 µM while proliferation reduction was seen at day 4 for 10 µM C53. (C) FG_0 proliferation was unaffected for 10 µM and 20 µM C53 treatment however 40 µM C53 has an effect. Experiments were performed in triplicate and repeated two independent times. Results shown are the mean ±SEM.

3.2.3 Effect of C53 on cell cycle progression of cervical cancer cells lines.

Since C53 had inhibitory effects on the cell proliferation of both HeLa and CaSki cell lines, cell cycle analysis was performed to determine if the inhibitory effects were associated with alterations in cell cycle progression. Cell cycle analysis was performed on both HeLa and CaSki cell lines treated with either DMSO (control) or 20 µM and 40 µM C53 for various time points. For CaSki cells treated with C53, an increase in the G1 phase with a decrease in the S and G2/M phase was observed (Figure 3.4 A). Quantification of the data shows a significant increase in the percentage of cells in the G1 phase and a significant decrease in the percentage of cells in the S and G2/M phase of the cell cycle (Figure 3.4 B). A significant increase in cells in the SubG1 phase was observed at 40 µM C53. For HeLa cells, cell cycle analysis similarly showed an increase in G1 phase with a decrease in the S phase for both the 20 and 40 µM C53 treatment (Figure 3.5 A). Quantification of the results showed a slight but significant increase in G1 phase with a decrease in S phase (Figure 3.5 B). Together, these results suggest that C53 treatment results in a delayed G1/S progression. These effects seemed more prominent in CaSki cervical cancer cells.

A

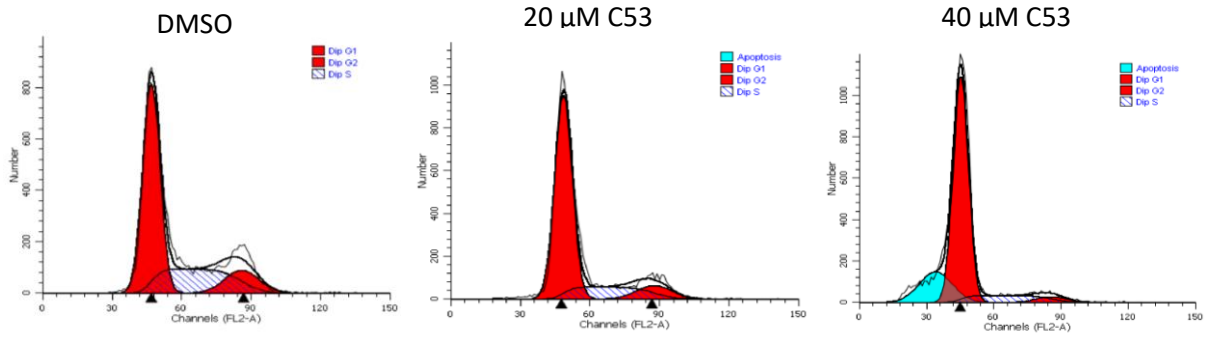

B

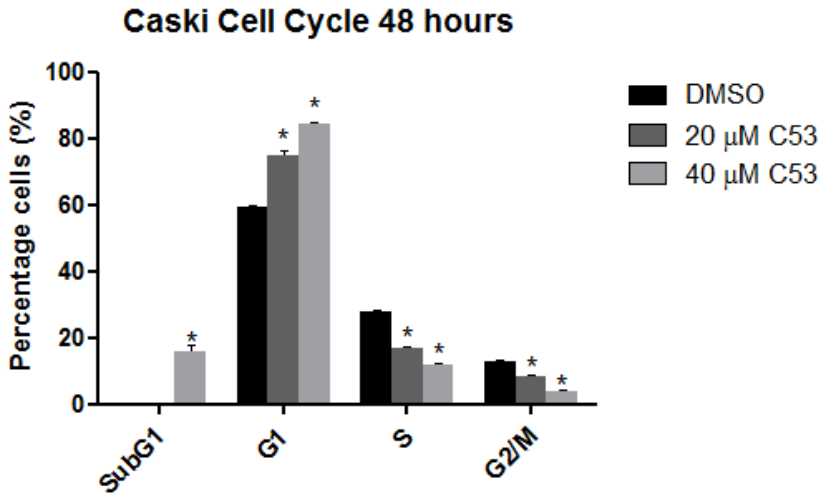

Figure 3.4 C53 induces a G1-phase cell cycle arrest in CaSki cell line. Cells were plated and treated with either DMSO (control) or 20 and 40 µM C53 for 48 hours after which cell cycle analysis was done using a flow cytometer. **(A)** CaSki cell cycle profiles show a decrease in S and G2/M phase for 20 and 40 µM C53 treatment. Cell cycle profiles also show an increase in the SubG1 phase for 40 µM C53 treatment **(B)** Quantified cell cycle analysis 48 hours post treatment with C53 show a significant increase in G1 with a decrease in S and G2/M phase for 20 and 40 µM C53. Result values indicate the mean $\pm$ SEM of experiments performed in triplicate and repeated at least two independent times (*p< 0.05).

A

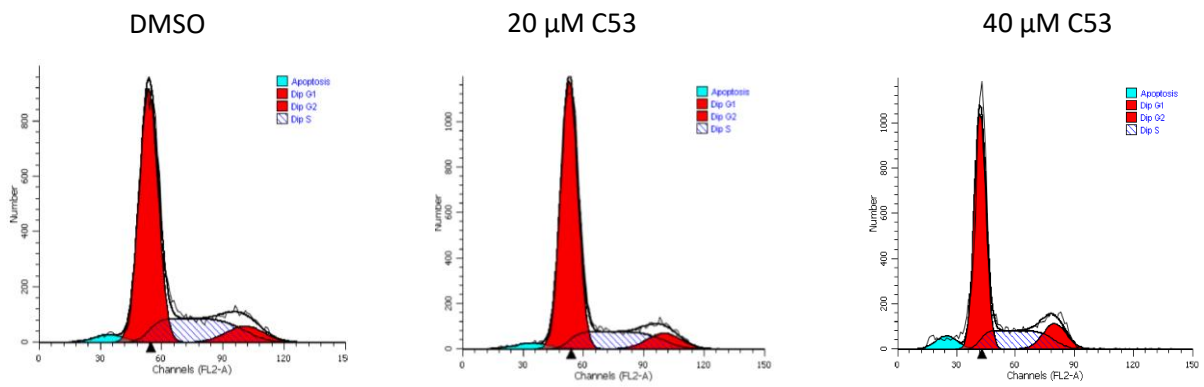

B

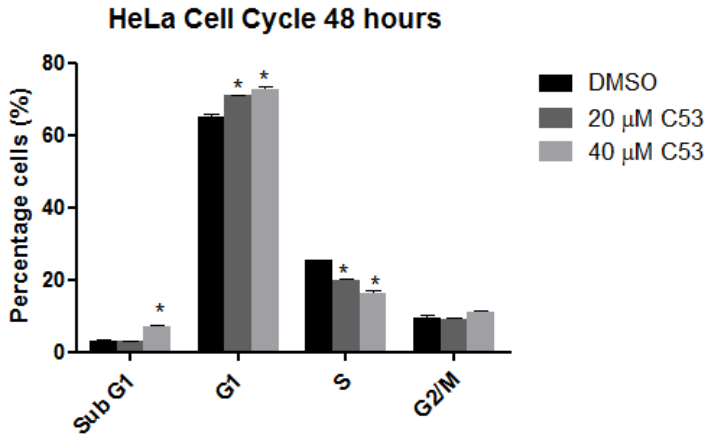

Figure 3.5 C53 induces a G1-phase cell cycle arrest in HeLa cell line. Cell cycle profile of HeLa cells treated with either DMSO or 20 and 40 µM C53 for 48 hours after which cells were analysed using a flow cytometer. **(A)** Cell cycle profiles shows a slight increase of G1 phase for 20 and 40 µM C53 with a decrease in S phase for 20 µM and 40 µM C53 treatment. Profile also shows an increase in Sub G1 for 40 µM C53 treatment **(B)** Quantified cell cycle analysis of HeLa cells 48 hours post treatment with C53. Results show a slight significant increase in G1 with a decrease in S phase for both 20 µM and 40 µM C53 treatment. Results indicate the mean $\pm$ SEM of experiments performed in triplicate and repeated at least two independent times (*p< 0.05).

3.2.4 The effect of C53 on markers associated with cell cycle progression

In the cell cycle of vertebrate cells, preparation for the S phase takes place in the G1 phase which is triggered by regulation of cyclin D1-CDK4/6 complex. The formation of this complex regulates DNA synthesis and promotes the progression of cells through G1-S phase of the cell cycle [75]. To explore the potential mechanism by which C53 causes a delayed G1/S progression, protein expression levels of cell cycle markers were investigated in HeLa and CaSki cell lines in response to 20 µM and 40 µM C53 treatment for 48 and 72 hours. The markers examined included proteins expressed in G1 phase; cyclin D1 and CDK4. Western blot analysis for Cyclin D1 and CDK4 showed that treatment with 20 and 40 µM C53 resulted in a reduction in Cyclin D1 and CDK4 levels at 48 and 72 hours in both HeLa and CaSki cell lines (Figure 3.6 A and B). These results support the cell cycle analysis data showing that C53 treatment results in a G1/S delay.

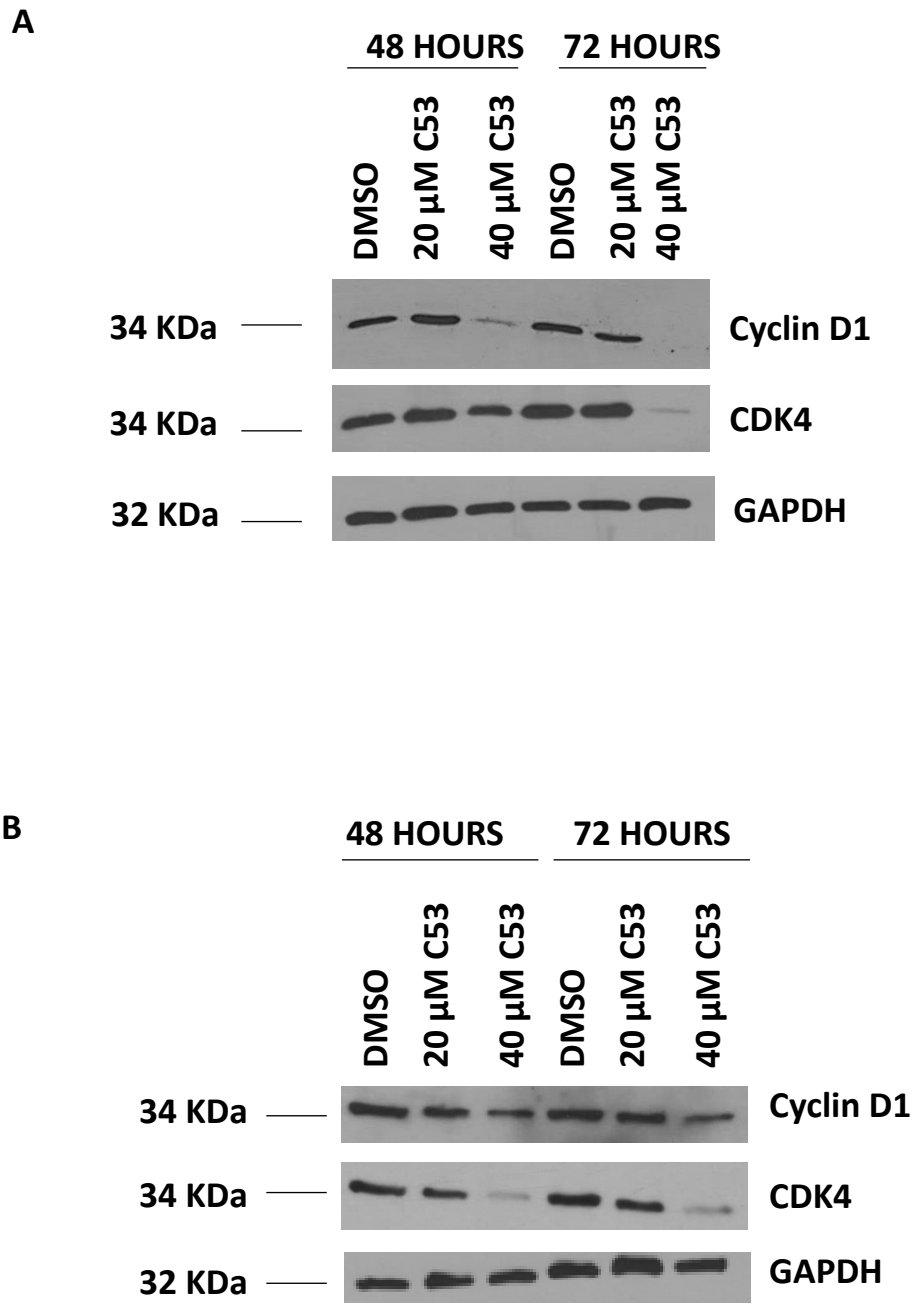

Figure 3.6 Effect of C53 on G1 phase cell cycle markers. **(A)** HeLa and **(B)** CaSki cells were plated and treated with either DMSO or 20 µM and 40 µM C53 for 48 or 72 hours. Cell cycle markers were investigated via western blot, with GAPDH as the loading control. Results show a decrease in the amount of CyclinD1 and CDK4 for both HeLa and CaSki cell lines. Results shown are representative of experiments repeated at least two independent times.

3.2.5 C53 induces cell death via apoptosis.

3.2.5.1 Monitoring morphological changes induced by C53 treatment.

Having established that C53 inhibited cell proliferation and blocked cell cycle progression we next investigated the mechanism of cell death associated with C53. Different forms of cell death can be characterised by morphological criteria and classified as either apoptotic, necrotic or autophagic. Apoptotic cells are morphologically characterised by cell shrinkage, membrane blebbing and condensation of the chromatin while necrosis is characterised cytoplasmic and organelle swelling followed by bursting of the cell releasing cell content into extracellular space. In the case of autophagy (which can be catabolic or pro-survival), autophagic cells can be characterised by the formation of autophagic vacuoles known as autophagasomes [76].

To understand the mode of cell death induced by C53, HeLa and CaSki cells were treated with 20 µM or 40 µM C53 for 48 hours and the morphology of the cells were observed using phase contrast microscopy. Images captured using light microscopy show healthy cells for the control HeLa and CaSki cell lines (Figure 3.7 A). The presence of rounded cells showing signs of membrane blebbing was observed at 20 µM C53 treatment (Figure 3.7 B). Both HeLa and CaSki cell lines treated with 40 µM C53 showed substantially more cell shrinkage (Figure 3.7 C). These morphological changes suggest that C53 may be inducing cell death through apoptosis.

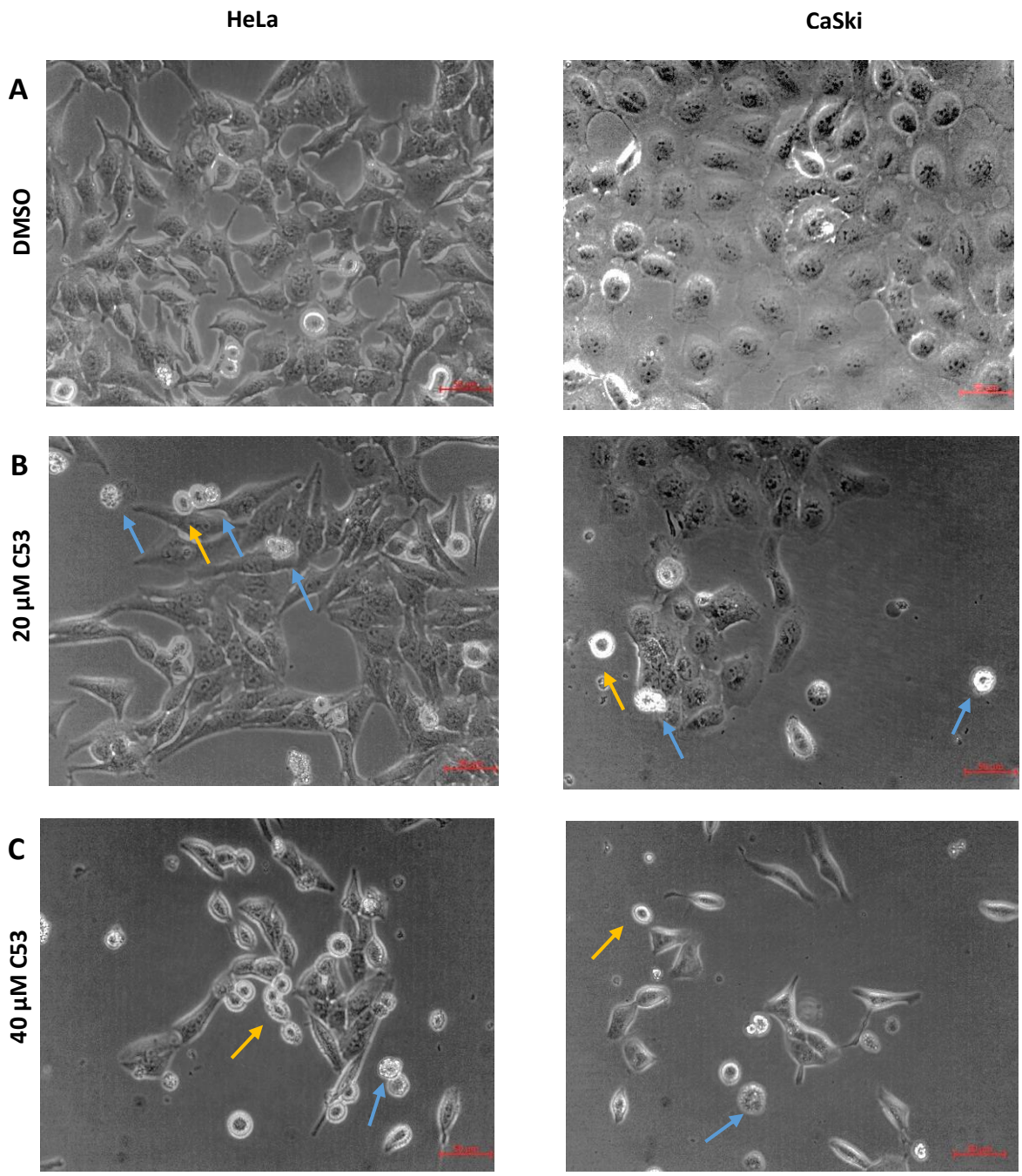

Figure 3.7. The morphological effect of C53 treatment. HeLa and CaSki cells were treated with either **(A)** DMSO or **(B)** 20 and **(C)** 40 µM C53 for 48 hours. Images show an increase in shrank rounded cells for 20 and 40 µM C53 for both HeLa and CaSki cell lines. Images were captured with a Primovert inverted light microscopy at 20X magnification. Yellow arrows indicative of rounded and lifting cells. Blue arrows show signs of membrane blebbing indicative of apoptosis.

3.2.5.2 Annexin V/PI staining shows C53 treatment causes cell death by apoptosis.

Results from morphological analysis of HeLa and CaSki cells post C53 treatment suggested that the cells were undergoing apoptosis. To confirm this, Annexin V/PI assays were performed using HeLa and CaSki cells that were treated with either DMSO (control) or 20 µM and 40 µM for 48 and 72 hours. The Annexin V/PI staining assays distinguished cells as live, early apoptotic, late apoptotic and dead. This assay can distinguish early apoptotic cells from late apoptotic cells because late apoptotic cells are Annexin V positive and PI positive because the membrane of late apoptotic cells are disintegrated therefore allowing PI staining to enter the cells and bind the DNA while the membrane of early apoptotic cells are still intact therefore not allowing PI staining but allowing for binding of Annexin V on PS. Therefore, late apoptotic cells and early apoptotic cells can be distinguished in the Annexin V/PI staining assay. The results showed a small but significant decrease in live cells and an increase in early and late apoptotic cells for both HeLa and CaSki cell lines treated with C53 for 48 hours (Figure 3.8 A). At 72 hours treatment, a substantial and significant decrease in the percentage of live cells for both HeLa and CaSki cell lines was observed and an associated increase in early and late apoptotic cells was observed in both 20 µM and 40 µM C53 treatment (Figure 3.8 B). These results confirm that C53 treatment triggers apoptosis of cervical cancer cell lines. The results also show that CaSki appears more sensitive to C53 treatment in comparison to HeLa cells.

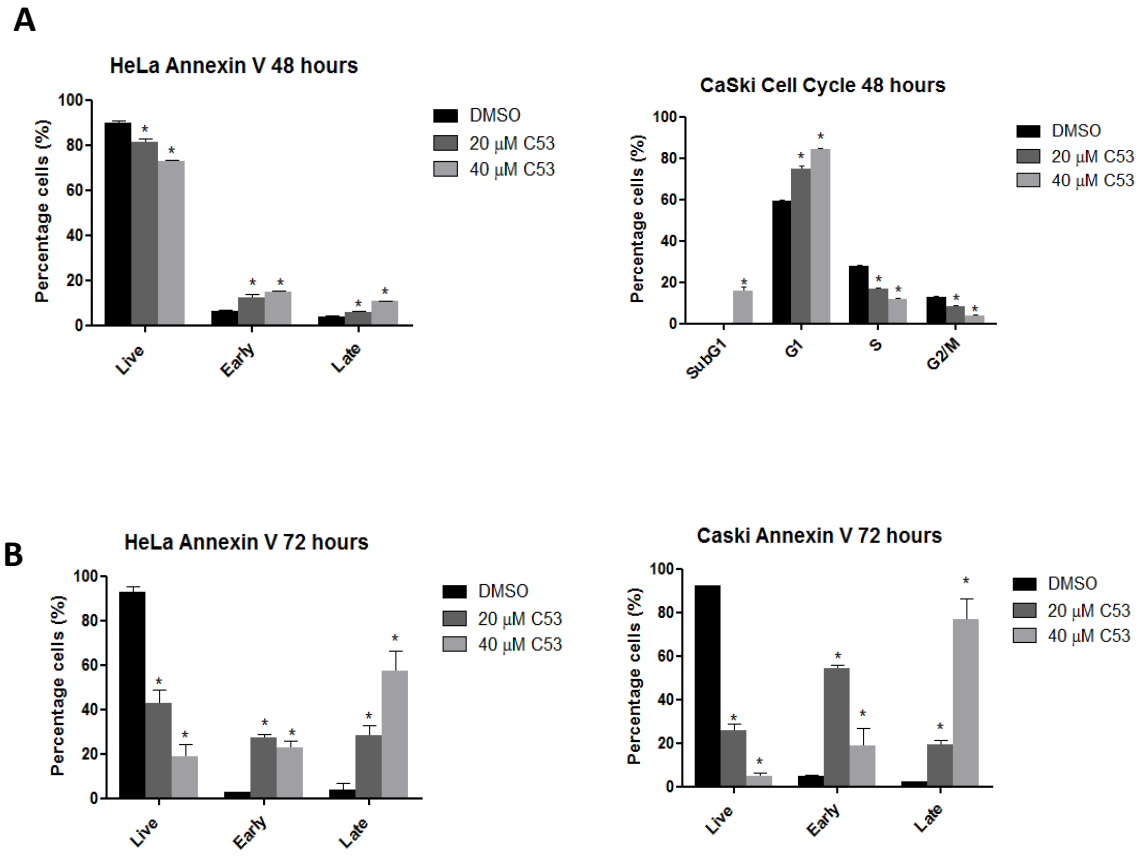

Figure 3.8. C53 induces apoptosis. CaSki and HeLa cells were plated and treated with either DMSO (control) or 20 µM and 40 µM C53 for 48 hours or 72 hours after which cells were stained using the Alexa Fluor 488 Annexin V/Dead Cell Apoptosis Kit and analysed by flow cytometry. **(A)** Results show a small but significant decrease in percentage of live cells at 48 hours C53 treatment with an increase in apoptotic cells. **(B)** At 72 hours there is a substantial decrease in the percentage of live cells and an increase in the percentage of apoptotic cells in both HeLa and CaSki cell lines. Results shown are the mean ±SEM of experiments performed in triplicate and repeated at least two independent times (*p< 0.05).

3.2.5.3 C53 induces PARP cleavage

Results from the morphological images and Annexin V/PI assay showed that C53 induces apoptosis in a time dependent manner. To further validate these results, the protein level of Poly (ADP-ribose) Polymerase (PARP) was investigated in HeLa and CaSki cell lines in response to C53. PARP is a known substrate of Caspase 3 and is cleaved from 116 KDa to an 89 KDa fragment during early apoptosis [77]. The presence of cleaved PARP was evaluated by western blot analysis after C53 treatment at 48 and 72 hours for HeLa and CaSki cells. The results showed a dose dependent increase in cleaved PARP at 48 and 72 hours treatment for HeLa cells (Figure 3.9 A). CaSki cells similarly showed the presence of cleaved PARP after C53 treatment (Figure 3.9 B). The presence of cleaved PARP is an independent confirmation that C53 induces cell death via apoptosis.

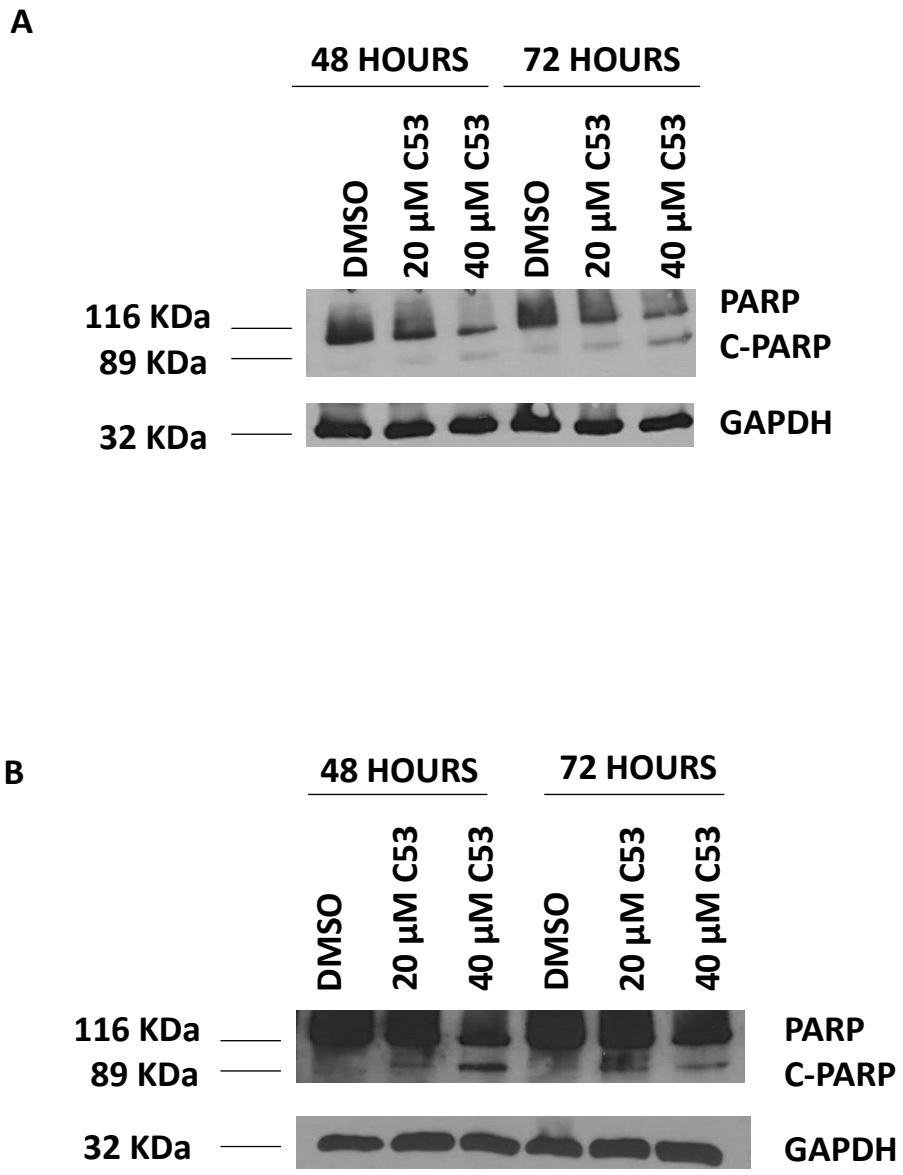

Figure 3.9 C53 Induces PARP cleavage. HeLa and CaSki cells were both treated with DMSO or 20 µM and 40 µM C53 for 48 or 72 hours. PARP cleavage was investigated via western blot, with GAPDH as a loading control. **(A)** HeLa and **(B)** CaSki cells showed an increase in cleaved PARP in a time and concentration dependent manner. Results shown are representative of experiments performed two independent times.

3.3 DISCUSSION

This chapter focused on testing the anticancer properties of a novel pyrrolidine derivative, C53. We report that C53 inhibits the proliferation of cervical cancer cells and induces a delay in G1/S cell cycle progression as well as cell death via apoptosis.

C53 (1-benzyl-4[(4-methoxy-1-naphyl) methylamino]-N-methyl-pyrrolidine-2-carboxamide) a potential small molecule inhibitor of KPNB1 is a pyrrolidine derivative. There are reports in literature that show pyrrolidine derivatives having anticancer activity. A study done by Wana *et al.* showed the development and synthesis of a series of pyrrolidine derivatives that showed anticancer activity through the inhibition of Mcl-1 in MDA-MB-231 (breast cancer), PC-3 (prostate cancer) and K562 (chronic myelogenous Leukemia cell) cell lines [78]. Another study done on pyrrolidine derivatives showed that a caffeoyl pyrrolidine derivative inhibits tumour invasion and metastasis through the suppression of matrix metalloproteinase activity [79]. The use of pyrrolidine derivatives for targeted cancer therapies shows their potential as anticancer compounds.

Previous work in our lab extensively investigated a small molecule inhibitor of KPNB1, INI43. Like C53, INI43 was selected from an *in silico* study investigating several compounds with potential to bind KPNB1 and inhibit its nuclear import function. INI43 showed anticancer activity in cervical cancer cells lines as well as inhibitory effects on KPNB1 mediated transport [64]. To date small molecule inhibitors which target nuclear import are limited. Most research has focused on Selective Inhibitors of Nuclear Export (SINEs). The first identified SINE was Leptomycin B, which was an inhibitor of the nuclear export protein CRM1. However, due to toxic side effects in clinical trials, Leptomycin B was discontinued [80]. The discovery of Leptomycin B led to the development of other SINE which include Atjadone C,

Anguinomycin, Aoniothalamin, as well as the small molecule inhibitors, N-azolylacrylates and CBS9106 [81]. These compounds were shown to bind CRM1 and stop cell proliferation in cancer cells. In recent years, more small molecules SINE of CRM1 have been developed e.g KPT-185 and Selinexor. KPT-185 was investigated extensively *in vitro* and showed promise however, *in vivo* study of the compound was unsuccessful due to poor pharmacokinetics [82]. This led to the development of Selinexor, the first small molecule SINE to reach clinical trials. SINEs are now being explored in many clinical trials as anticancer agents. This evidence highlights the potential in the inhibition of nuclear transport in cancer cells.

With Importazole being one of the few commercially available inhibitors of nuclear import further extensive research and development, like that of SINEs, is required for nuclear import inhibition [60]. Like CRM1, KPNB1 was also shown to be overexpressed in various malignancies thus shows potential as an anticancer target. The results in this chapter provides preliminary evidence of the anticancer effects of the novel small molecule inhibitor of nuclear import, C53 that warrants further investigation.

CHAPTER 4

INVESTIGATING THE EFFECT OF C53 ON KPNB1 CARGO PROTEINS

4.1 INTRODUCTION

KPNB1 has been shown to play a key role in importing cargoes into the nucleus through two major pathways known as the non-classical and classical pathways [32,34]. Cargoes imported by KPNB1 in the classical import pathway include Stat3, NF-κB and NFAT which are only activated once in the nucleus [44]. Examples of cargoes imported in the non-classical import pathway include Snail [83] and Parathyroid Hormone-related Protein (PTHrP) [78]. There are some cargoes imported by KPNB1 which have been implicated in cancer such as Snail, NF-κB, Stat3 and NFAT [85]. Inhibition of KPNB1 therefore has an advantage of inhibiting the import of cargoes which have been associated with tumorigenesis.

KPNB1 has been shown to be overexpressed in cancer cells and appears to be more reliant on KPNB1 function than non-cancer cells [17,44]. This led to the proposal that KPNB1 has potential as a druggable target [17]. The first small molecule inhibitor of KPNB1 identified is Karyostatin A1. Karyostatin A1 was shown to bind KPNB1 with high affinity and specifically targeted the classical import pathway *in vivo* and *in vitro* [59]. A commercially available KPNB1 inhibitor, Importazole has been shown, through FRET-based studies, to interfere with the interaction of KPNB1 and RanGTP therefore blocking KPNB1 mediated nuclear import however, no anticancer properties were investigated in this study [60]. Therefore, there is a search for novel KPNB1 inhibitors with anticancer properties.

Using a structure based *in silico* approach our study identified C53 as a potential small molecule inhibitor of KPNB1. In the previous chapter, we reported that C53 has anticancer properties using cervical and oesophageal cancer cell lines. In this chapter, we investigated the effect of C53 treatment on the nuclear activity of KPNB1 cargo proteins; NFAT and NF-κB transcription factors. The activity of these transcription factors was monitored using the NFAT or NF-κB/p65 dual reporter assays as a measure of nuclear presence and activity. The effect of C53 on the localisation of KPNB1 was also investigated using immunofluorescence and nuclear cytoplasmic fractionation.

4.2 RESULTS

4.2.1 Investigating the effect of C53 on KPNB1 mediated cargo import

For cargoes to be imported by KPNB1 through the non-classical or classical import pathway they must be recognized through specific NLSs. Previous studies have shown a number of the cargoes imported by KPNB1 e.g. NF-κB and nuclear factor of activated T cells (NFAT) are implicated in cancer [85,86]. Therefore, the inhibition of the nuclear import of these cargoes may have implications for cancer cells.

In this section, we investigated the effect of C53 treatment on the activity of NFAT and NF-κB/p65 using the dual reporter luciferase activity assay. Transcriptional activity was used as a measure of functional activity of NFAT and NF-κB in the nucleus.

4.2.1.1 C53 treatment inhibits NFAT nuclear activity

For the NFAT pathway to be activated there needs to be a calcium flux which drives the dephosphorylation of NFAT by the protease, Calcineurin (Cn). This dephosphorylation exposes the NLS found on NFAT which is recognized by KPNα. After recognition, a trimeric complex (KPNα, NFAT and KPNB1) is formed which translocate from the cytoplasm into the nucleus. In the nucleus, NFAT dissociates from the Karyopherins and initiates the transcription of downstream targets such as Interleukin-2 (IL-2), Interleukin-10 (IL-10) and Interferon gamma (IFNγ) [87].

As previously mentioned there are several karyopherin B-like receptors which import different protein into the nucleus through specific NLS recognition [37]. In the case of the NFAT transcription factor, research has shown that it is shuttled between the nucleus and cytoplasm in a KPNB1- dependent manner through the classical import pathway [88]. Since NFAT contains an NLS which is recognized by KPNα/KPNB1, we anticipated that C53 would

influence the transcriptional activity of NFAT on the basis that C53 was selected as a potential small molecule inhibitor of KPNB1 and NFAT is dependent on KPNB1 for nuclear import. The presence and transcriptional activity of NFAT was measured through a NFAT reporter luciferase assay (Figure 4.1).

For this assay, HeLa cells were transfected with GFP-NFAT and NFAT Reporter (Luc) plasmids. Control and C53 treated cells were stimulated with PMA and Ionomycin for 3 hours and cell lysates were harvested for luciferase assays. As described by Northrop *et al.* PMA is added to activate NFAT import while Ionomycin is added to induce the calcium flux [89]. Our results show a significant increase in NFAT activity in cells co-stimulated with PMA and Ionomycin indicative of NFAT nuclear import and activation. C53 treatment at 20 μM and 40 μM resulted in a slight but significant decrease in NFAT activity (Figure 4.1 B). Since only live cells were harvested reduction in transcriptional activity is not due to apoptosis. Decrease in NFAT transcriptional activity is ~ 1.3 fold. The physiological relevance of this is not yet clear at present. There are examples in literature that have shown slight but significant decreases in NFAT transcriptional activity such as Importazole which showed a ~1.4-1.6 fold decrease as well as Ivermectin which showed a ~1.4 fold decrease in NFAT transcriptional activity [62]. These results suggest that C53 treatment reduces the transcriptional activity of NFAT.

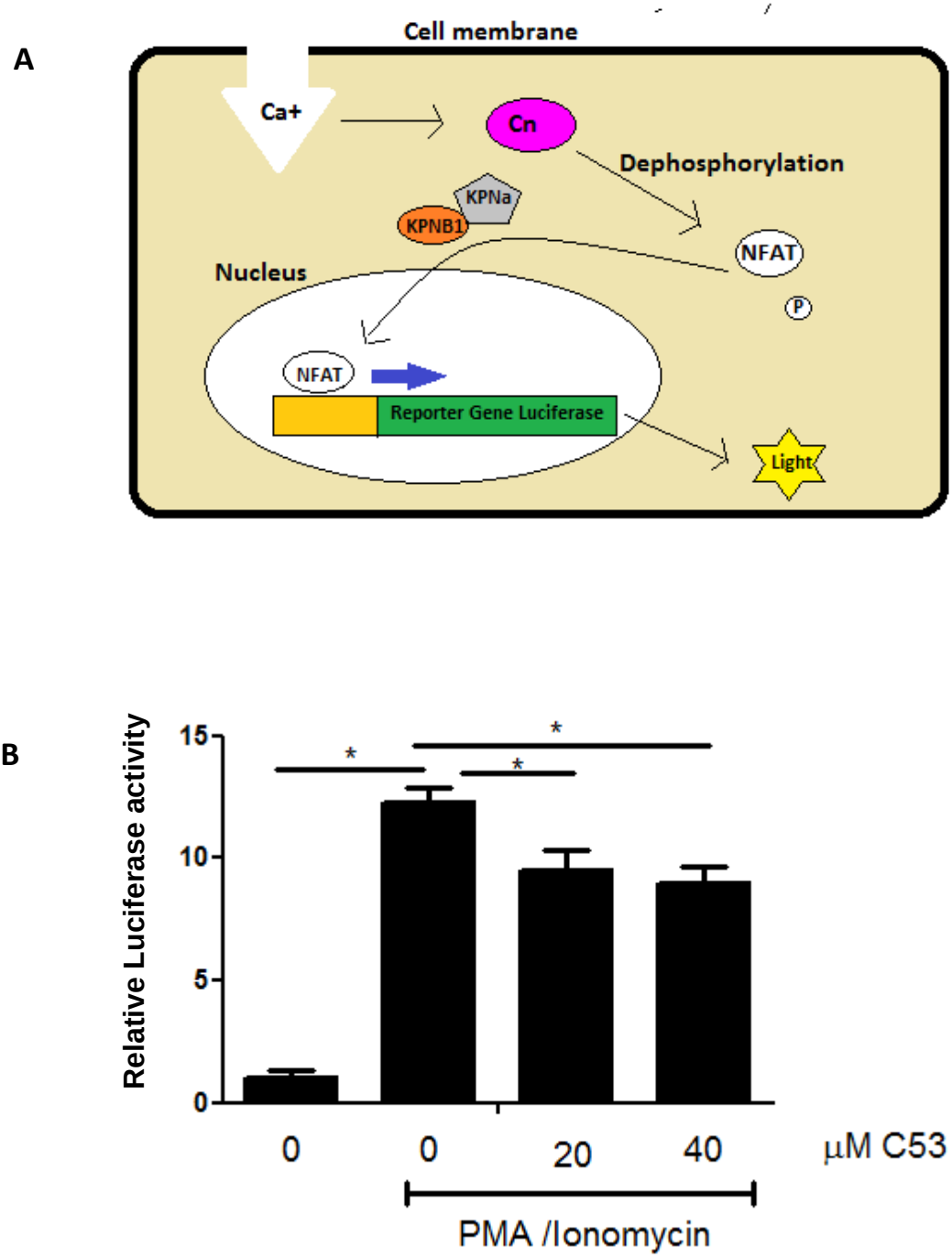

Figure 4.1. Treatment with C53 results in a downregulation of NFAT transcription activity. **(A)** Diagrammatic representation of the NFAT assay. **(B)** HeLa cells were transfected with GFP-NFAT plasmid (50 ng) and treated with DMSO (control) or 20 µM and 40 µM C53 for 24 hours. Three hours before the termination of treatment cells were stimulated with 0.5 µM PMA and 1.3 µM Ionomycin. Cells were harvested for analysis by luciferase assay. Promoter activity was normalized to Renilla. Results show a significant decrease of NFAT activity after C53 treatment. Experiments were performed in quadruplicate and repeated at least two independent times (*$p<0.05$).

4.2.1.2 C53 treatment reduces NF-κB/p65 transcriptional activity

NF-κB is a transcription factor which plays a role in inflammation, proliferation and apoptosis. A well-defined subunit of NF-κB is the p50/p65 dimer. This dimer, in its inactive form, is bound to IκB which is usually localized in the cytoplasm. Upon stimulation by cytokines or stressors, the classical NF-κB pathway is activated. A IKK complex which compromises of catalytic units phosphorylates IκB which triggers its degradation. This then frees the NF-κB (p50/p65) subunit exposing its NLS to be recognized by the nuclear transport proteins for import into the nucleus where it activates gene expression [90]. The NF-κB transcription factor contains classical NLS motifs which when recognized initiates nuclear import via the KPNB1-dependent classical nuclear import pathway. Studies have shown that TNFα-activated NF-κB heterodimers are transported into the nucleus after recognition by importin α3 or importin α4 both of which interact with KPNB1 [91]. We therefore investigated the effects of C53 on NF-κB activity as it is a known KPNB1 cargo.

For this assay, HeLa cells were transfected with promoter reporter plasmid containing an NF-κB consensus binding site included in a minimal promoter. Renilla-Luciferase was used as a control for transcription efficiency. The cells were treated with either DMSO (vehicle) or 20 μM and 40 μM C53 for 24 hours followed by stimulation with PMA 3 hours prior to termination of C53 treatment. Cell lysates were harvested, and luciferase activity monitored as a measure of NF-κB activity. Results showed a significant decrease of NF-κB/p65 dependent transcription activity with 20 μM and 40 μM C53 treatment compared to that of the PMA stimulated control cells (Figure 4.2). These results suggest that C53 treatment significantly inhibits NF-κB/p65 dependent transcription activity in a dose dependent manner.

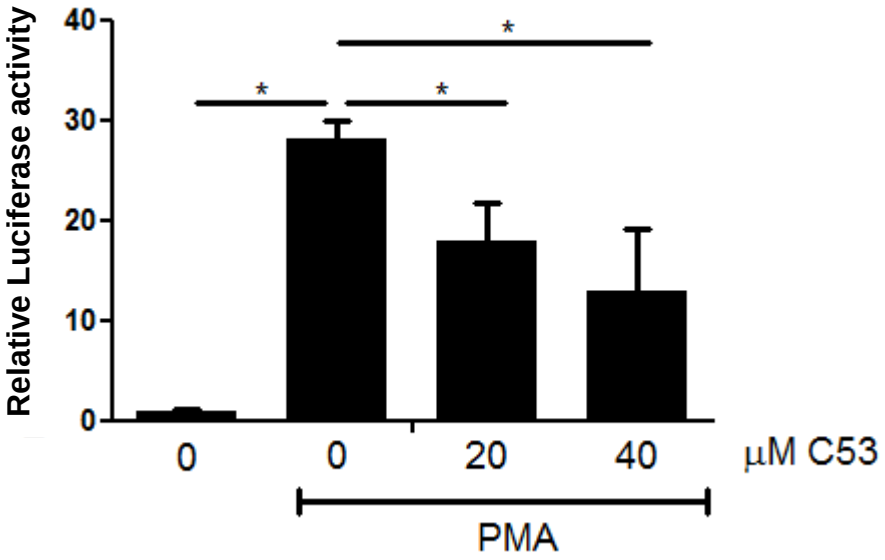

Figure 4.2. C53 treatment reduces the luciferase transcriptional activity of NF-κB p65. NF-κB/p65 luciferase reporter assay revealed a significant decrease in p65 activity for cells treated with 20 μM or 40 μM C53 for 24 hours. Results were normalized to Renilla-Luciferase as a control for transcription efficiency. Experiments were performed in quadruplicate and repeated at least two independent times (*$p<0.05$).

4.2.3. Comparison of the effects of C53 to that of commercially available KPNB1 inhibitor, Importazole on NFAT activity.

Having shown that C53 significantly reduces NFAT and NF-κB import activity we were interested in comparing its effects with that of commercially available KPNB1 inhibitor, Importazole. Importazole has been shown to interfere with KPNB1 mediated import [60].

Experiments were set up as described previously. Results showed an increase in NFAT activity in HeLa cells with PMA and Ionomycin which correlates with NFAT nuclear import. Treatment with 20 µM and 40 µM C53 resulted in a significant decrease in NFAT activity, as previously observed (Figure 4.3 A). The results of C53 or Importazole treatment similarly inhibited NFAT activity at both 20 µM and 40 µM (Figure 4.3 B). These results show that C53 has similar effects on NFAT nuclear import as that of the commercially available KPNB1 small molecule inhibitor, Importazole.

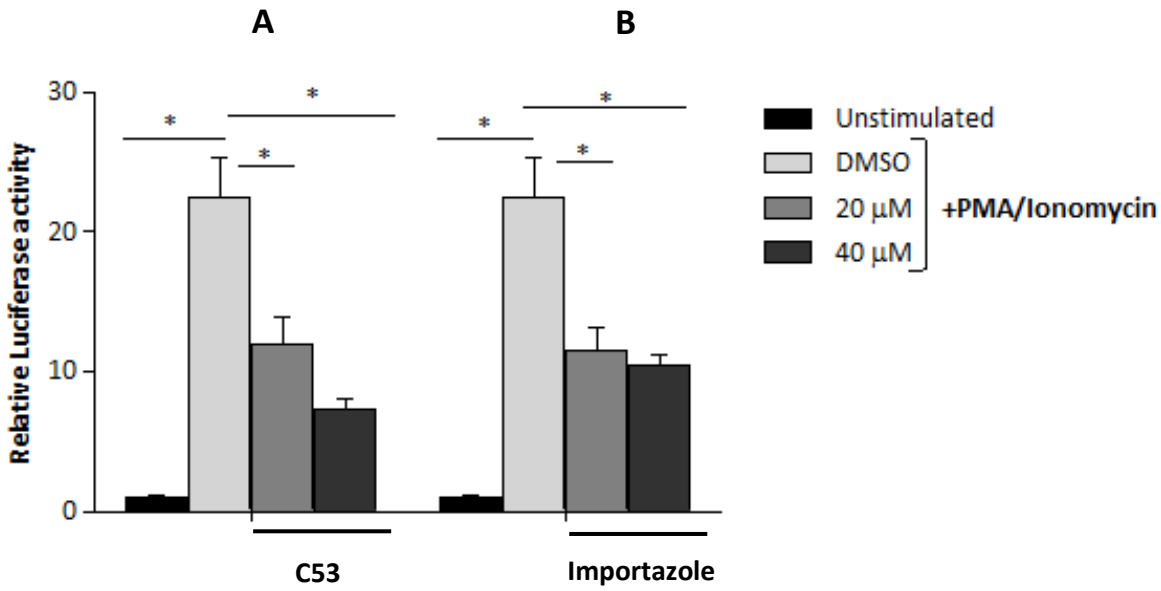

Figure 4.3. Comparison of the effects of C53 or Importazole on NFAT activity. Results of the NFAT luciferase activity assay revealed that **(A)** C53 inhibits NFAT activity in a similar manner to that of **(B)** Importazole after 24 hours of treatment. Promoter activity was normalised to Renilla. Experiments were done in triplicate and repeated at least two independent times (*$p<0.05$).

4.2.4. The effect of C53 on KPNB1 localisation

Having established that C53 inhibits the nuclear import and activity of NFAT and NF-κB we next investigated the effect of C53 on KPNB1 localisation. The localisation of KPNB1 was investigated by immunofluorescence assays.

Briefly, HeLa cells were plated on cover slips and treated with either DMSO (vehicle) or 20 µM and 40 µM C53 for 24 hours after which cover slips were probed with a KPNB1 antibody. Inverted Fluorescent Microscope was used to monitor KPNB1 fluorescence in the Cy3 fluorescent channel and DAPI used for nuclear fluorescence. The results showed that without treatment, KPNB1 was present mostly in the nucleus for majority of the cells (Figure 4.4 A). In 20 µM C53 treated cells the localisation remained largely in the nuclear compartment (Figure 4.4 B). A notable increase in overall KPNB1 fluorescence was observed after 40 µM C53 treatment in comparison to the control cells.

Quantification of the fluorescence across a cell using a representative immunofluorescent image of a single cell was performed with DAPI fluorescence indicating the nucleus. The fluorescence across the cell was quantified using the ImageJ software. The DAPI and Cy3 (KPNB1) fluorescence intensity was then plotted and compared. Results show very similar fluorescent intensities and localisation patterns when comparing untreated (DMSO) to 20 µM C53 treatment (Figure 4.5 A and B). For cells treated with 40 µM C53, an increase in KPNB1 fluorescence across both the cytoplasmic and nuclear compartments (overall) was observed (Figure 4.5 C). These results suggest that 40 µM C53 treatment may cause an elevation in KPNB1 expression. However, the results are not sufficiently conclusive evidence that C53 affects the localisation of KPNB1. These experiments were also performed in CaSki cells, but the data was difficult to interpret likely due to the epithelial-like morphology which resulted

in cells being more compact and overlapping one another making it difficult to distinguish the nuclear compartment from the cytoplasm and one cell to another.

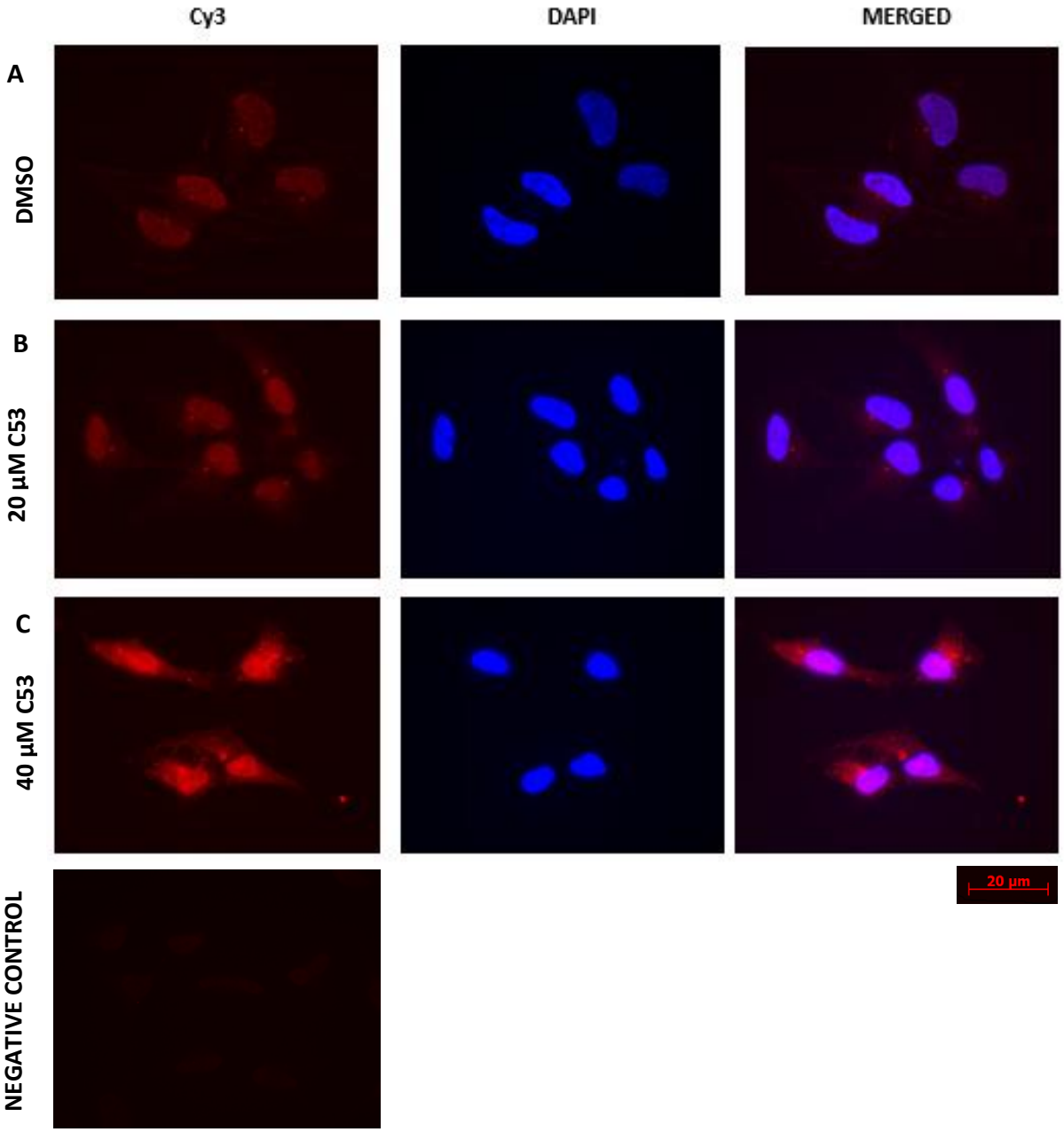

Figure 4.4 C53 had no effect on the localisation of KPNB1. HeLa cells were plated on cover slips flamed and treated with either DMSO or 20 µM and 40 µM C53 for 24 hours. Cells were probed with KPNB1 antibody and visualized by fluorescent microscopy to analyse localization of KPNB1 in the cell. **(A)** Localisation of KPNB1 is nuclear in control cells. (**B)** 20 µM C53 treated cells showed a nuclear localisation for KPNB1 while **(C)** 40 µM C53 showed an increase in KPNB1 fluorescence in both nuclear and cytoplasmic compartments. Experiments were performed two independent times.

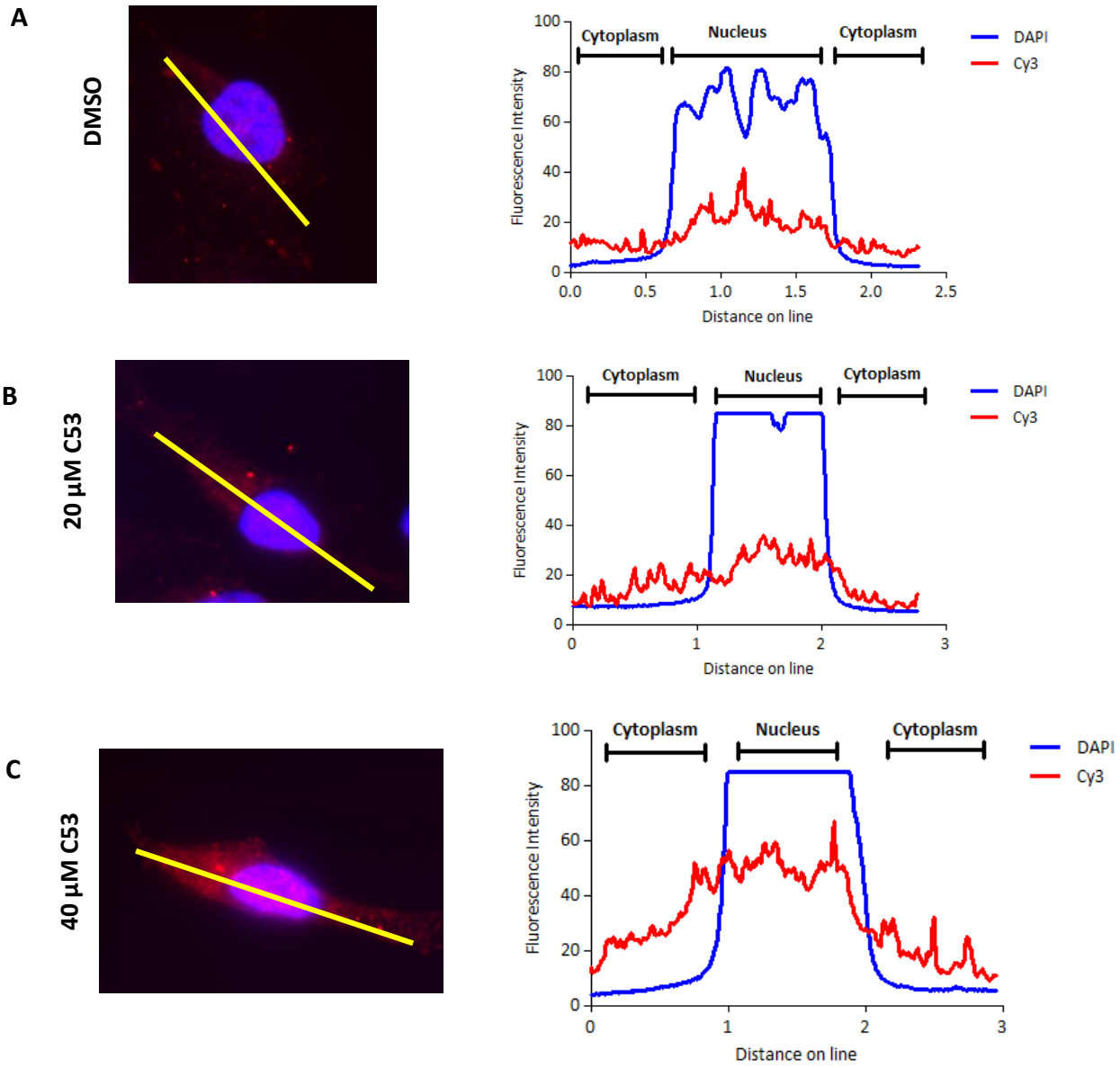

Figure 4.5. C53 caused an increase in fluorescent intensity at highest dose. Cells were treated with C53 for 24 hours and probed with KPNB1 (Cy3) antibody and DAPI (nuclear stain). Images were captured using fluorescent microscopy and a representative image was used to quantify the KPNB1 (Cy3) and DAPI fluorescence intensity using ImageJ. DAPI fluorescence indicative of nuclear localisation. **(A)** Quantification of fluorescence for control cells shows an increase of KPNB1 in the nuclear compartment which is seen for **(B)** 20 µM C53 treatment too. **(C)** For 40 µM C53 treatment a substantial proportional increase in KPNB1 fluorescence is observed in both nuclear and cytoplasmic compartments. Experiments were performed two independent times and representative images are shown.

4.2.5 Investigating the nuclear localisation of KPNB1 using nuclear/cytoplasmic fractionation.

Immunofluorescent analysis of KPNB1 in response to C53 treatment suggested an increase in KPNB1 expression for 40 µM C53 but effects on nuclear localisation were not apparent. We therefore investigated the localisation of KPNB1 using nuclear cytoplasmic fractionation. Nuclear and cytoplasmic proteins were harvested from DMSO, 20 µM and 40 µM C53 treated cells for 48 hours. This time point coincided with changes in cell proliferation.

The levels of KPNB1 in the nuclear and cytoplasmic fractions was analysed by western blot. Little to no change in KPNB1 levels in the nuclear or cytoplasmic KPNB1 was detected for both 20 µM and 40 µM treatment (Figure 4.6). Together these results suggest that C53 affects the nuclear presence of KPNB1 cargo proteins but has little/no effect on the subcellular localization of KPNB1 itself.

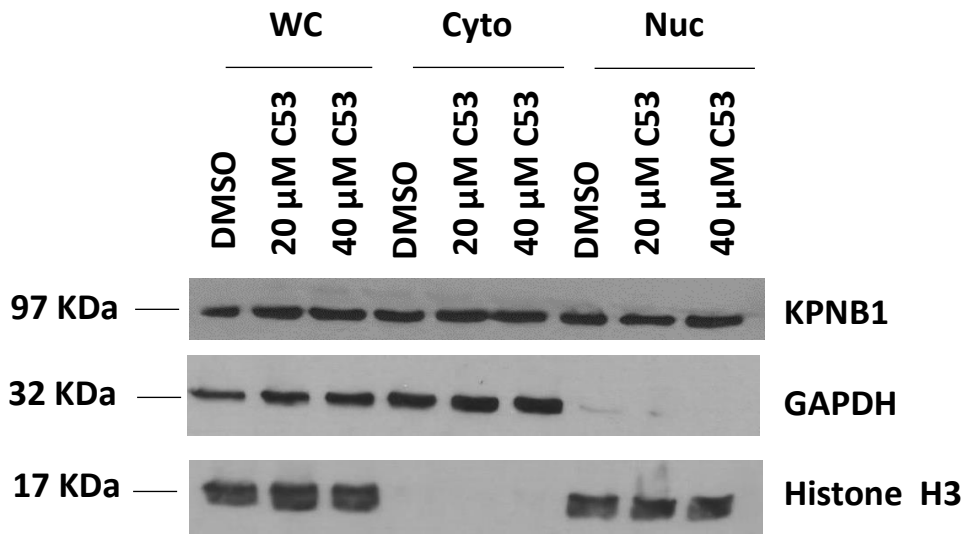

Figure 4.6. C53 lead to no change in localization in KPNB1. Western blot analysis of nuclear and cytoplasmic proteins from HeLa cells treated with C53 for 48 hours. Whole cell proteins (WC) served as a control of KPNB1 expression. GAPDH and Histone H3 were used as cytoplasmic and nuclear loading controls, respectively. Results showed no change in localisation or expression of KPNB1 after 48 hours of C53 treatment. Experiments were performed two independent times.

4.3 DISCUSSION

The small molecule, C53 was identified for its potential to bind and inhibit KPNB1 function. Previously we investigated the effect of C53 on cancer cell biology. The effect of C53 treatment on KPNB1 mediated nuclear import has not yet been investigated. Therefore, in this chapter we performed a preliminary investigation of the effect of C53 treatment on the import of known KPNB1 cargo proteins as well as the effect on KPNB1 localisation.

We firstly investigated the effect of C53 on KPNB1 cargo protein import. Like INI43, a previously described KPNB1 inhibitor, C53 was shown to inhibit the import and activity of KPNB1 cargoes, NFAT and NF-κB [92]. As previously mentioned, NFAT and NF-κB were selected on the premises of being cargoes that are shuttled between the nucleus and cytoplasm in a KPNB1-dependent manner. Next, we investigated the effect of C53 on KPNB1, its potential target. Our results showed that C53 had no effect on the subcellular localisation of KPNB1. Together these results show that C53 significantly inhibits the nuclear import of KPNB1 cargo proteins, however it does not affect the localisation of KPNB1. We speculate that C53 could interfere with the binding of cargoes however, it may not block the shuttling of KPNB1 between the nuclear and cytoplasmic compartments. Due to limited time, we were unable to test this hypothesis. Ideally, biophysical assays such as crystal structures of KPNB1 bound to the small molecule is required. This forms part of future research in our laboratory which includes protein purification and crystallography. Crystal structures of KPNB1 protein in combination with KPNα and Ran have been solved. The unliganded crystal structure of human KPNB1 has not been solved yet. Therefore, compound binding studies are limited to computational docking [93].

There are very few small molecules identified to date that target KPNB1.The first small molecule inhibitor of KPNB1 identified was Karyostatin 1A. This compound was shown to inhibit KPNB1 mediated import. Through cargo studies, two cargos namely FITC-BSA-NLS as well as GFP-NFAT were shown to accumulate in the cytoplasm after treatment with Karyostatin 1A at concentrations of 10 µM and 25 µM respectively. Using docking studies as well as Surface Plasmon Resonance (SPR), to measure the interaction of the compound with KPNB1, Karyostatin 1A was shown to interfere with the Ran-GTP and KPNB1 interaction which in turn affected nuclear import. These results provided the first evidence of a potential small molecule inhibitor of nuclear import [59]. Karyostatin 1A off-target effects have however not yet been investigated. One of the commercially available inhibitors of KPNB1, Importazole has also been shown to bind KPNB1 through FRET-based studies. Like Karyostatin A1, Importazole was also shown to interfere with the RanGTP and KPNB1 interaction [60].

More recently, research by Kim *et al* discovered an Aminothiazole derivative ((E)-N-(5-benzylthiazol-2-yl)-3-(furan-2-yl) acrylamide) with anticancer properties. Through proteomic studies this aminothiazole derivative was shown to target KPNB1. The competitive binding assay further showed that the compound binds KPNB1 with a strong binding affinity (Kd = 20 nM) [94]. Further work by Siyoung *et al.* showed that the aminothiazole derivative binds on the concave surface of KPNB1 [95]. Crystal structures of KPNB1 with any of these compounds however are not available yet.

Future work in our laboratory aims to purify KPNB1 and perform biophysical assays to investigate the binding of INI43 and C53 to KPNB1. The results in this chapter however provides evidence that small molecules like C53 affect the nuclear import of KPNB1 cargo proteins.

CHAPTER 5

CHARACTERISATION OF THE *IN VITRO* ADME PHARAMACOKINETICS AND *IN VIVO* TOXICOLOGY OF C53

5.1 INTRODUCTION

The drug discovery and development process involves the use of *in vivo* and *in vitro* experimental models. The different models ranging from cell culture to animal work, healthy humans and patients involved in clinical trials are used at different stages of drug discovery and development to determine the efficacy and safety of candidate drug-like compounds [88]. We have preliminary evidence that C53 has cancer cell killing effects using cell culture models. To add to the biological data generated for C53, we performed *in vitro* pharmacokinetic studies on C53.

Pharmacokinetics refers to the study of the movement of a drug in the body which can be investigated through Absorption, Distribution, Metabolism and Excretion (ADME) studies. The ADME parameters can be tested in both *in vivo* and *in vitro* models. These parameters are extremely important in the prediction of drug behaviour in animal models or patients. *In vitro* ADME models involve the use of assays that give pharmacokinetic parameters such as plasma protein binding, solubility, permeability and metabolic stability. *In vivo* ADME models involve the use of animals or human subjects to provide information such as clearance, oral bioavailability, distribution and exposure of drugs [96]. These findings are critical to the future success of a compound as a treatment agent.

Research has shown that many of the failures of drug candidates occurred due to poor pharmacokinetic properties e.g. poor absorption or excessive metabolism [57]. The early

screening of pharmacokinetic properties in the form of *in vitro* and *in vivo* ADME screens has significantly decreased the portion of failing drug candidates in clinical trials [36]. Therefore, this evidence shows the need of early pharmacokinetic screening of drug like compounds to improve the success of compounds that are tested further in living systems and clinical trials.

This chapter is aimed at the early characterisation of the *in vitro* ADME pharmacokinetic properties of C53. *In vitro* assays included plasma protein binding, lipophilicity, kinetic solubility, permeability and metabolic stability which were done with assistance from H3D Africa, based at the University of Cape Town. In this chapter we also investigated the *in vivo* toxicology of C53 in a nude mouse model.

5.1.1 Plasma protein binding

Plasma protein binding refers to the extent which a drug binds to plasma protein. The increased importance of plasma protein binding lies in the fact that there is a high concentration of proteins in plasma of which numerous drugs bind. The percentage of drug binding can have implications on distribution which can be explained through the Free Drug Theory (FDT). The FDT states that in the absence of energy-dependent processes (pH gradient, uptake transporters) when steady state equilibrium is reached the percentage of free drug in the plasma is equal to the free drug in the tissue. The free drug is the unbound drug which is available to elicit the pharmacological activity (Figure 5.1). Hence, it is important to measure the extent of plasma protein binding which will also give information on the amount of free drug available to elicit the relevant pharmacological activity [97].

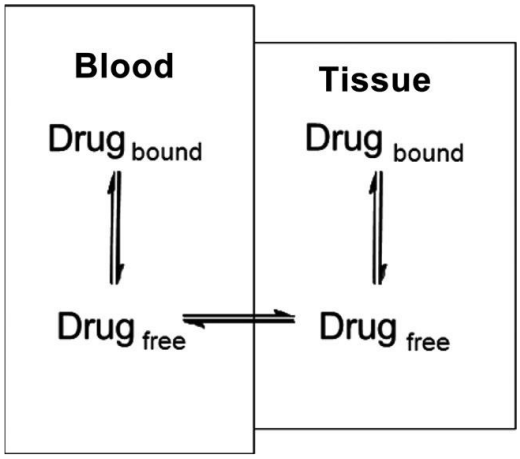

Figure 5.1: The free drug distribution, at equilibrium, between the blood plasma and tissue according to the Free Drug state theory. The amount of free drug in the blood plasma is equivalent to the free drug in the tissue [97].

Plasma protein binding influences the rate of diffusion between plasma and tissue therefore influencing the volume of drug distribution and the drug clearance. It is usually desirable to avoid highly bound drugs as small changes in the plasma protein binding can lead to significant fluctuations in the free drug fraction. The reason the free drug fraction should not fluctuate dramatically is because fluctuation in the free drug may lead to toxic side effects which is more apparent in highly bound drugs in comparison to moderately bound drugs. However, there are commercially available effective anticancer drugs that have high protein binding e.g. Multi Kinase Inhibitor, Sorafenib has a protein binding of 97%; the EGFR-inhibitor, Gefinib has >97% binding and the tyrosine kinase inhibitor, Imatinib has a protein binding of >99%. This evidence shows that every drug acts uniquely and may still have good pharmacological activity despite high plasma protein binding [97]

5.1.2 Lipophilicity

Lipophilicity refers to the ability of a compound to dissolve in fats, lipids or non-polar solvents such as hexane. In ADME studies, a calculated partition coefficient (LogD) is routinely used to analyse lipophilicity *in vitro* which is representative of the molecular desolvation of a compound from aqueous phase to cell membranes and protein binding sites. Lipophilicity is an important ADME parameter as it contributes to a compounds solubility, permeability, potency and metabolism in a living system. Highly lipophilic compounds frequently lead to rapid metabolism, low solubility and poor absorption. Similarly, low lipophilicity leads to poor ADME properties [98]. The optimum range of lipophilicity has been reported to be within a LogD range of 1 and 3 which ensures optimal physiochemical properties [99]

5.1.3 Solubility

Solubility is defined as the concentration of the compound before the appearance of a precipitate. This parameter is important for drugs that are administered orally. It has been established that the solubility, dissolution and gastrointestinal (GI) permeability are fundamental properties which control the extent of drug absorptions and bioavailability [100]. In drug discovery, the amount of insoluble drug candidates has increased over the years with almost 70% of new drug candidates being water insoluble. Therefore, there is a growing need for identifying drug candidates that are water soluble to avoid drug like compounds from precipitating out and causing toxic side effects [100].

5.1.4 Permeability

Due to the ease of this route of administration, the major goal of drug development currently is to develop drugs which can be administered orally. For a drug to reach the systematic circulation it must first pass through the intestinal membranes via passive diffusion, assisted

transport or active transport. A correlation between the intestinal absorption and the intestinal permeability for a drug has been reported [101]. Therefore, the permeability value of a compound is an important index of its human intestinal absorption. There are several *in vitro* models used to measure passive permeability such as Parallel Artificial Membrane Permeability Assay (PAMPA), the human colon adenocarcinoma (Caco-2) cell lines and the Madin-Darby canine Kidney (MDCK) cells. The aim of these *in vitro* assays is to predict the apparent permeability ($LogP_{app}$) of a drug-like compound where a $LogP_{app}$ >-5 is characterised as high permeability while a $LogP_{app}$ <-5 is characterised as low permeability [101].

5.1.5 Metabolic stability

Metabolic stability refers to the biotransformation of a compound over time. Metabolic stability studies represent some of the earliest studies used by pharmaceutical companies to predict *in vivo* pharmacokinetics. The importance of *in vitro* metabolic stability studies is the relation to the metabolic clearance *in vivo*. The metabolic stability *in vivo* has a relationship to the half-life and bioavailability of a compound. Therefore, *in vitro* metabolic stability studies are an important indicator of clearance in a living system. The *in vitro* metabolic liver systems are believed to reflect the hepatic clearance *in vivo* [102]. The hepatic clearance is the

first-pass elimination of a drug where a compound is metabolized by enzymes found in the liver. Subcellular fractions known as liver microsomes or S9 fractions are used to measure the rate of disappearance of a drug within a period which would be representative of the half-life and clearance of the drug. Metabolic stability is thus of importance to predict how quickly a drug is cleared in the system, which would have implications on the dosage and bioavailability of a drug [102].

In this chapter, the above ADME assays will be used to evaluate the *in vitro* pharmacokinetic properties of C53. The results of these assays serve as indicators of how well the compound (C53) will be absorbed, distributed, metabolized and excreted in a living system.

5.1.6 *In vivo* toxicology study of novel compound

Toxicity refers to any adverse effects shown by a substance after administration. Toxicity testing of new compounds is essential in drug discovery and development. The toxicity of a substance can be tested *in vitro* and *in vivo*. Repeated dose toxicity testing refers to a test carried out for a minimum duration of 28 days with the substance being administered repeatedly. Usually in *in vivo* animal models, rodents of any gender and age 5-6 weeks are used. At the end of the study, tissue from various organs are removed and tested by weight or histology changes [103]. Since C53 is a novel compound that has not been previously tested, in this chapter we also tested the repeated dose toxicity of C53 in nude mice for a duration of 28 days. The toxicity will be investigated at three different concentrations of C53 to identify whether C53 is tolerable in a mouse model and if so which concentration is the most tolerable. These results will provide important information of the toxicity of C53 and the concentration of C53 that can be tolerated. This tolerable C53 concentration will be used in future mouse xenograft studies.

5.2 RESULTS

PART I: INVESTIGATING THE *IN VITRO* ADME PHARAMACOKINETICS OF C53

5.2.1 Investigating the plasma protein binding of C53 using human plasma

To evaluate the protein binding of C53, a plasma protein binding assay was performed using human blood plasma. The protein binding assay is used to evaluate how much of the drug is bound to the proteins found in blood plasma. The binding potential of a compound has major implications on its distribution, toxicity and pharmacological activity. For most drugs, the clinical response is dependent on the free (unbound) drug concentration [105].

In this assay, C53 was incubated in 1 µM human plasma for 30 minutes at 37˚C to allow plasma protein binding before ultracentrifugation for 4 hours to allow for the separation of the bound drug from the free drug. All samples including controls were then filtered and supernatant submitted for LC-MS/MS analysis. The results of the protein binding of C53 shows that C53 has a protein binding of 90.3% with the fraction of free drug being 0.09 (Table 5.2). These results suggest that C53 has moderate protein binding.

Table 5.2. Plasma protein binding results for C53 incubated in human plasma. Fu (free fraction) shows free drug. Controls used were Warfarin (high binding) and Caffeine (low binding). Experiment performed in duplicates.

Compound	% Protein Binding	Fu	% Degradation
C53	90.3	0.09	Negligible

5.2.2 Investigating the Kinetic solubility of C53 in PBS (pH 7.4)

Kinetic solubility refers to the concentration of the compound in solution before some precipitate forms. The ability for a compound to be highly soluble in an aqueous media is important for oral absorption. [100].

The Kinetic solubility of C53 was measured using a shake flask method where a 10 mM stock of C53 in DMSO was used to prepare calibration standards (10-220 µM) and spike (1:50) aqueous samples of PBS with a final DMSO concentration of 2%. After shaking, samples were filtered and analysed by High Pressure Liquid Chromatography (HPLC). The calibration standards were used to construct a best fit calibration curve which was used to determine the aqueous solubility of C53. The kinetic solubility was ranked based on a 200 µM preparation in 2% DMSO (Table 5.3).

Table 5.3. Solubility ranking based on a 200 µM preparation in 2 % DMSO.

Solubility Class	Concentration (µM)
High	$\geq$ 150
Moderate	50-150
Low	5-49
Very Low	$\leq$ 5

The results for the kinetic solubility of C53 showed that it has moderate kinetic solubility with a kinetic solubility of 100 µM (Table 5.4). This result suggests that C53 is readily soluble and should not precipitate out in the circulatory system.

Table 5.4. The kinetic solubility results of C53 in PBS (pH 7.4).

Compound	**pH 7.4 Solubility (µM)**
C53	100

5.2.3 Investigating the lipophilicity of C53

In order to investigate the lipophilicity of C53 a miniature shake flask method was used. The shake flask method was adapted to a microtiter plate where 495 µl of octanol was added to 10 µl of C53 (10 mM in DMSO) followed by 495 µL phosphate buffer (0.1 M). The microtiter plate was then mixed to allow for distribution of test compound in the various layers. After mixing, the microtiter plate was centrifuged for 2 hours to allow for the complete separation of the two solvent layers. An aliquot of each phase (Octanol/PBS) was analysed by HPLC to determine the concentration of C53 in each phase. The partition coefficient was then calculated using the LogD calculation (Figure 5.2). The optimal LogD value of a compound is between 1 and 3.

$$\mathbf{LogD_{7.4} = Log10}\left[\frac{\textbf{peak area octanol phase / octanol phase inj. volume}}{\textbf{peak area buffer phase/ buffer phase inj. volume}}\right]$$

Figure 5.2. The $LogD_{7.4}$ calculation used to calculate the partition factor for C53.

The results for C53 show that the partition coefficient of C53 is 2 which is within the optimum range of LogD values (Table 5.4). Drug properties are ranked based on the LogD values (Table 5.5). According to the drug properties, C53 has moderate solubility and permeability as well as slow metabolism. This may suggest that C53 is favourable for oral absorption however rapid renal clearance may be experienced *in vivo.*

Table 5.4. Lipophilicity results for C53 assessed by the Log $D_{7.4}$ value

Compound	$LogD_{7.4}$
C53	2.0

Table 5.5. Impact of $LogD_{7.4}$ on the drug like properties and possible *in vivo* impact [104].

Log $D_{7.4}$	Common Impact of Drug-like Properties	Common Impact *in vivo*
< 1	Solubility high Volume of distribution low Permeability low Metabolism slow	Volume of distribution low. Oral absorption blood brain barrier (BBB) penetration unfavourable. Renal clearance may be high
1-3	Solubility moderate Permeability moderate Metabolism slow	Balanced volume of distribution. Oral absorption and BBB penetration favourable. Renal clearance may be high.
3-5	Solubility low Permeability high Metabolism moderate to high	Oral bioavailability moderate to low. Oral absorption variable.
>5	Solubility low Permeability high Metabolism high	High volume of distribution (especially amines). Oral absorption unfavourable and variable.

5.2.4 Investigating the apparent permeability of C53

The main pharmacokinetic parameters for oral absorption of drugs is permeability and solubility. For a drug to enter the circulatory system and get to its target site it needs to pass through several membranes [101]. PAMPA is an *in vitro* assay which mimics the passive, trans-cellular permeability of a drug like compound being screened for their oral absorption potential.

To screen C53 permeability, a 96-well Multiscreen Filter plate was used. The membrane filters were pre-coated with hexadecane and allowed to dry before commencing with the assay. The hexadecane acts as an artificial lipid membrane which the drug would be required to pass through in a similar manner to the passive diffusion *in vivo*. Phosphate buffer was added to the 96 well acceptor plate. Donor buffer was spiked with C53 (1 µg/ml) before the donor plate was slotted into the acceptor plate forming a sandwich like arrangement. The plates were then incubated with gentle shaking to allow diffusion of C53 to take place. Samples from the acceptor plate were then prepped and analysed by LC-MS/MS to determine the apparent permeability ($LogP_{app}$).

Results from the PAMPA assay show that C53 has an apparent permeability of -4.3 which is categorized as a high permeability value (Table 5.6). This result shows that C53 would be readily absorbed in a living system and making it ideal for oral absorption.

Table 5.6. Permeability (PAMPA) results for C53 at pH 6.5

Compound	**$LogP_{app}$ (pH 6.5)**	**Classification**
C53	-4.3	High

5.2.5 Investigating the hepatic metabolic stability of C53 using liver microsomes

To investigate the hepatic metabolic stability of C53, liver microsomes were used. Metabolic stability was investigated by incubating 1 µM C53 in mouse, rat or pooled human liver microsomes (0.4 mg/ml) at 37˚C at specific time points in the presence or absence of NADPH. NADPH is a cofactor which is required for the initiation of the enzymic reaction. At specific time points reactions were quenched before analysing supernatant by LC-MS/MS. Metabolite searches were not conducted during this assay. The microsomal stability results (Table 5.7) for C53 show the half-life to be 7.2, 4.3 and 4.2 minutes in human, rat and mouse microsomes, respectively. The predicted clearance for all the microsomes was > 250 ml/min/kg which suggests that 250 mL of C53 would be cleared per minute based on the mass of the respective animal. Based on these results, it can be predicted that C53 would have a short half-life and rapid clearance *in vivo*.

Table 5.7. Metabolic stability data of C53 in pooled human, rat and mouse liver microsomes. Predicted *in vivo* clearance shown in the last column.

	Liver microsomes	**Half-life (min)**	**Predicted *in vivo* Clearance (mL/min/kg)**
C53	Human	7.2	>250
	Rat	4.3	>250
	Mouse	4.2	>250

PART II: C53 *IN VIVO* TOXIOCOLOGY STUDIES

5.2.6 Investigating the toxicology of C53 *in vivo*

Toxicity testing of a new compound is essential in drug development. Toxic side effects like those seen for Leptomycin B, are a major reason for drugs not being developed further or being discontinued [105]. Having established that C53 has tolerable ADME pharmacokinetic properties we next investigated the toxicity of C53.

Here we examined the possible toxic side effects of C53 by performing a repeated dose toxicity analysis. C53 was administered interperitoneally twice a week for a period of 28 days. The mice body mass was measured 4 times a week and welfare monitoring of each mouse was performed daily. In the experiment, treatment mice were treated with C53 (10 μg/g, 30 μg/g or 50 μg/g) and control mice received 7.5% DMSO in PBS. Throughout the experimental duration no signs of distress or pain were observed with the animals. Results for all the drug concentrations show a body mass fluctuation similar to that of the control (Figure 5.3 A-C). The gain in body mass at the end of the study, which is represented by a box-and-whisker, shows a significant increase in the body mass gain for 10 μg/g and 30 μg/g C53 treatment compared to the control group of mice while the 50 μg/g C53 group showed no significant change compared to the control group (Figure 5.4). Factors that can affect weight gain include food and water consumption. A possible explanation for why the 10 μg/g and 30 μg/g treated mice gained more weight could be due to more consumption compared to control group which is a factor that causes variability in body mass. Hence, body mass was not the only parameter used for assessment of animal welfare and C53 toxicology (liver mass and autopsie). The body mass recordings as well as the body mass gain at the end of the study show that C53 is tolerable in nude mice.

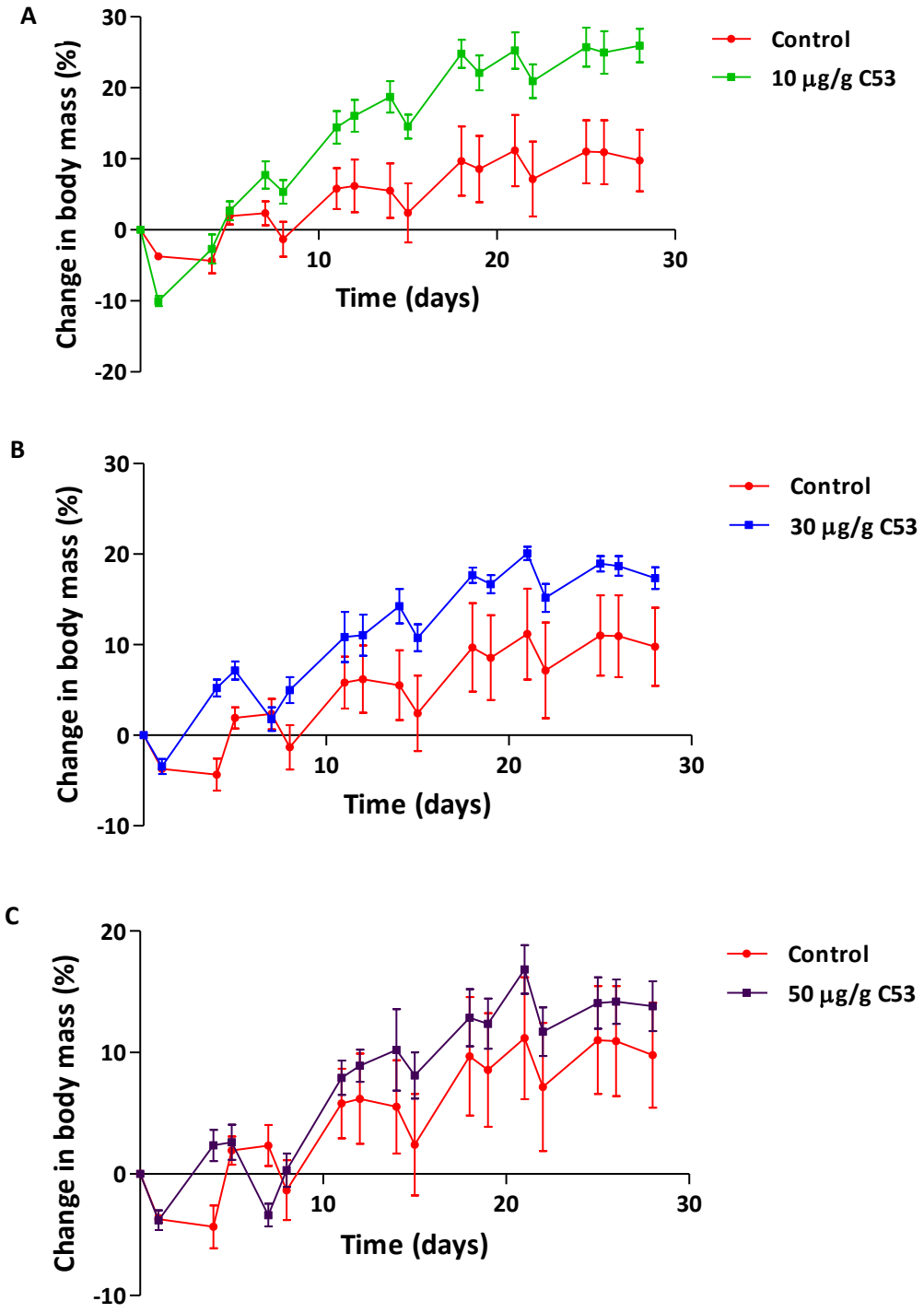

Figure 5.3. Toxicology analysis of C53. The repeated dose toxicology study was carried out using three different concentrations of C53 (10 µg/g, 30 µg/g or 50 µg/g). Body mass was measured the first day of treatment, and 4 times a week thereafter. Body mass was calculated as a percentage increase from the first day measurement for **(A)** 10 µg/g, **(B)** 30 µg/g and **(C)** 50 µg/g. Results shown are the mean ± SEM for each group (n=6).

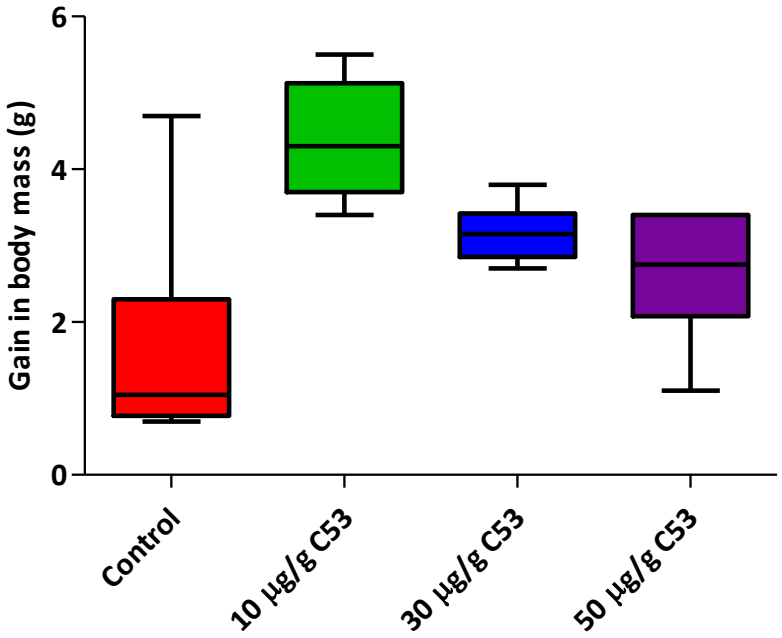

Figure 5.4. Gain in body mass on final day. The repeated dose toxicology study was carried out using three different concentrations of C53 (10 µg/g, 30 µg/g or 50 µg/g). Body mass was measured the first day of treatment, and 4 times a week thereafter. Body mass was calculated as a percentage increase from the first day measurement for 10 µg/g. Box and whisker represents the gain in body mass at the end of the study for each group (n=6). Results shown are the mean $\pm$ SEM.

To further validate that C53 did not cause internal toxic effects, after mice were sacrificed a post-mortem evaluation of each mouse was performed by an animal technician. Post-mortem evaluation of the C53 treated mice versus the control mice concluded no abnormalities e.g discolouration or inflammation, was observed in the spleen, liver, heart, ovaries and kidney. There was no difference in the appearance of the internal organs of the control mice compared to the C53 treated mice (Figure 5.5 A). Since the liver is responsible for the first pass of drug metabolism, research has reported an enlarged liver as a sign of toxicity [106]. We therefore measured the liver mass of the control and C53 treated mice at the end of the study, and normalised it relative to their body mass. Results of the relative liver mass showed no significant difference in the liver masses of the control group versus the C53 treated mice for all C53 concentrations (Figure 5.5 B). Together these results suggest that C53 is tolerable up to, but not restricted to 50 μg/g.

A

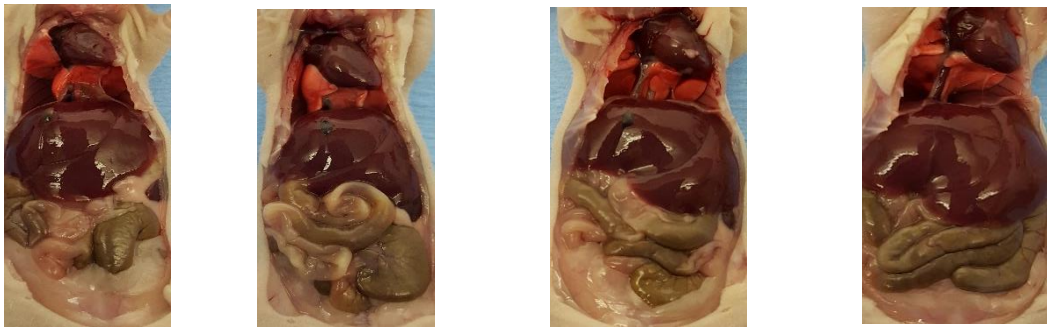

B

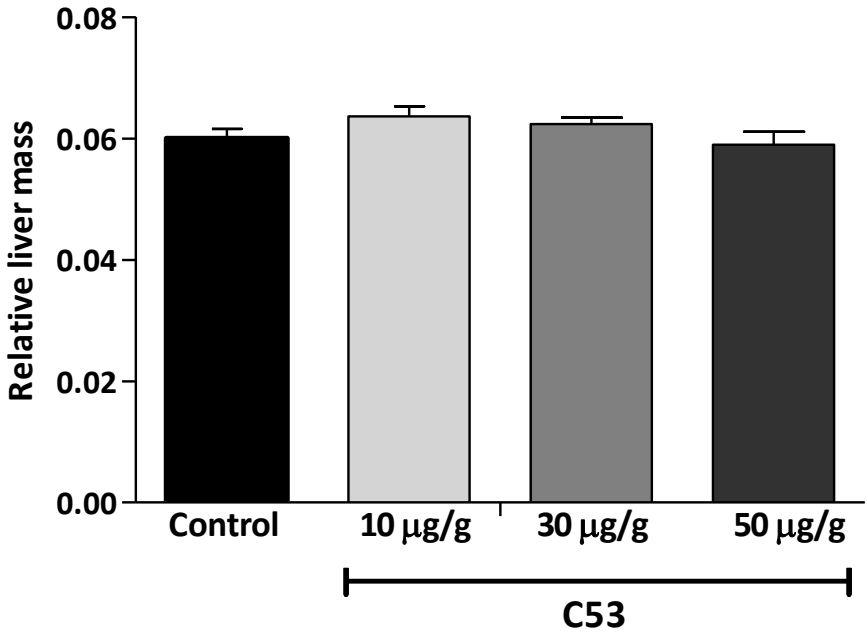

Figure 5.5. Post-mortem evaluation and liver size measurement at the end of toxicology study. (A) Post-mortem evaluation on each mouse for each group of C53 treated and control treated mice were evaluated and showed no toxic side effects in the internal organs. **(B)** At the end of the study mice's liver was removed and measured then normalised to their body mass. Bar graph represents the relative liver mass for each group which showed no significant difference (n=6 per group).

5.3 DISCUSSION

In this chapter, we describe the *in vitro* pharmacokinetic properties and the *in vivo* toxicology study for C53. This is the first study to describe the pharmacokinetic properties of the pyrrolidine derivative, C53 (1-benzyl-4 [(4methoxy-1-naphyl) methylamino]-N-methyl-pyrrolidinecarboxamide). Pharmacokinetic properties of several anticancer drugs have been investigated *in vitro* and *in vivo* for preclinical studies. These drugs include Imatinib, Gefitinib and Sorafenib which are all commercially available small molecule inhibitors used in cancer therapy [105].

The main purpose of pharmacokinetics is to investigate the bodily absorption, distribution, metabolism and excretion of drugs. When a drug is administered orally the first process that takes place is absorption. Drugs administered orally are absorbed by the stomach and small intestine. Next the drug passes through the liver then enters the circulatory system. For the drug to reach its target site it needs to be transported. This occurs through a process known as distribution. Once a drug is distributed throughout the body, it is broken down in a process known as metabolism. This usually occurs in the liver where specific liver enzymes are responsible for the biotransformation of parent drugs into metabolites. The metabolites usually have no effect and are easily excreted however in other drugs the metabolites are pharmacologically active. The final process is excretion. This is when the drug is eliminated from the body primarily through faeces or urine [107].

We investigated the ADME pharmacokinetic properties of C53 using five assays namely plasma protein binding, lipophilicity assay, kinetic solubility, permeability assay and the metabolic stability assay. Results showed that C53 has moderate protein binding and

solubility. Further results showed that C53 has high permeability and optimum lipophilicity while metabolic studies showed that C53 has a short half-life and predicted rapid clearance.

The plasma protein binding of C53 was shown to be 90.3% meaning majority of the compound is bound to the plasma protein. High plasma protein binding is unfavourable however, literature has shown a few commercially available anticancer drugs that have high plasma protein binding. For example, Imatinib (Gleevec) has a plasma protein binding of 95% and is predominantly bound to albumin and α-glycoprotein. While the anticancer drugs Gefinitib and Sorafenib have plasma protein binding of 90% and 99.5%, respectively [108-110]. This evidence shows that a moderate to high plasma protein binding does not necessarily relate to the effectiveness of an agent.

The lipophilicity of C53 was defined as a partition coefficient. Results showed that the partition coefficient (LogD) for C53 was within the optimal range. This result also has specific implications for C53 *in vivo*. According to the drug property rankings by Edward KH *et al.* a LogD value between 1 and 3 would suggest that C53 is favourable for oral absorption and penetration of the blood brain barrier however, rapid clearance *in vivo* may be expected [104]. Positively, C53 showed good solubility and permeability which suggests that the compound has ideal oral absorption properties.

Metabolic studies of C53 using liver microsomes showed that C53 has a short half-life therefore is expected to clear rapidly *in vivo* which is not ideal. Research by Masimirembwa and co-workers previously showed several compounds which where metabolically unstable *in vitro* however, showed low clearance *in vivo* [102]. This was surprising as the metabolic stability *in vitro* usually acts as an indicator for the metabolic clearance *in vivo*. The reason for this observation is that the liver microsomes provide an artificial availability of compound to

the enzymes that, due to protein binding and permeability, does not occur *in vivo*. This would explain the differences in the data obtained in the *in vitro* metabolic studies versus the *in vivo* metabolic studies of the compounds investigated by Masimirembwa and co-workers [102]. Therefore, the liver microsomes may not be a conclusive indication of how a compound will act *in vivo* but merely acts as a possible indicator. This illustrates the importance of evaluating whether the *in vitro* metabolic stability data correlates with the *in vivo* metabolic stability data.

Interestingly, research has shown anticancer compounds where the half-life of the parent compound is shorter than that of the active metabolite. This was the case for Gleevec, a commercially available tyrosine kinase inhibitor. Gleevec showed an elimination half-life of 18 hours but when a metabolic identity (MetID) study was performed a pharmacologically active metabolite of Gleevec (CGP74588) was discovered and this metabolite showed an elimination half-life of 40 hours [108]. Therefore, further studies in the form of MetID may identify possible metabolites of C53 which may be pharmacologically active and have a longer half-life.

Having established the ADME pharmacokinetic properties for C53, next we investigated the toxicology of C53 *in vivo* through a repeated dose toxicology study. Results of the toxicology study showed C53 being tolerable up to but not restricted to 50 µg/g. Post mortem evaluation of mice treated with C53 showed no toxic effects and relative liver mass was not significantly different between control treated and C53 treated mice groups. These results suggest that C53 is tolerable *in vivo*, showing no toxic effects.

In summary, this chapter shows that C53 has moderate solubility and lipophilicity as well as high permeability *in vitro*. C53 also showed moderate plasma protein binding and *in vitro*

metabolic studies showed short half-life in liver microsomes. This data suggests that C53 has ideal characteristics for oral absorption however, further work in the form of metabolite identification (MetID) may be required to identify metabolites with longer half-life and pharmacologically active. *In vivo* toxicology studies showed that C53 is tolerable in nude mice showing no toxic effects externally or internally in all mice groups. This result suggests that C53 is tolerable *in vivo*.

Future work in our lab aims to investigate the *in vivo* ADME pharmacokinetics of C53 and monitor its effect on tumour development using a mouse xenograft model for cervical and oesophageal cancer.

CHAPTER 6

CONCLUSION

Karyopherin proteins are soluble nuclear import or export proteins which are responsible for the shuttling of cargo in and out of the nucleus [31]. The most well characterised Karyopherin is CRM1 which is a nuclear export protein. CRM1 has been shown to be overexpressed in several malignancies and has been shown to be a potential target for anticancer therapeutics [17,35-36]. Many inhibitors of CRM1 e.g. the SINE's have been developed and are being tested in clinical trials [111]. With most research focusing on the nuclear export pathway, very little is known about targeting nuclear import as an anticancer target. Like CRM1, there is growing evidence that the Karyopherin import protein KPNB1 is overexpressed in different cancers [17,44]. The silencing of KPNB1 lead to cell death through apoptosis in cancer cells with little effect on non-cancer cells [17]. This evidence suggests that KPNB1 has potential as a druggable candidate like that of CRM1.

In this study, we investigated a novel small molecule inhibitor, C53 which was selected from *in silico* docking studies as a potential inhibitor of nuclear import that associates with KPNB1. We investigated the effect of C53 on cancer cell biology, the effect of C53 on KPNB1 cargo proteins as well as characterised the *in vitro* ADME pharmacokinetic properties of C53. The *in vivo* toxicology of C53 was also investigated using a nude mouse model in order to investigate whether the compound is tolerable in a living system.

We report that the cancer cell lines tested in our study appeared more sensitive to C53 with EC_{50} values of C53 in cervical and oesophageal cancer cell lines which were 1.5 – 2 fold lower than that of non-cancer cells tested. This sensitivity was validated in cell proliferation studies

where concentrations of 10 µM and 20 µM C53 significantly reduced the cell proliferation of cervical cancer cell lines but had little effect on the non-cancer fibroblast cells, FG_0. The reduction in proliferation was shown to be associated with a G1/S cell cycle delay. The cell cycle delay triggered by C53 treatment also resulted in a decrease in the levels of cell cycle associated proteins, CyclinD1 and CDK4 which are essential proteins for the regulation of the G1 phase of the cell cycle [80]. C53 treatment also induced cell death by apoptosis similar to that described after treatment with another small molecule, INI43 or silencing of KPNB1 with siRNA in cervical cancer cell lines [40,62]. Earlier studies suggest that cancer cells may have increased reliance on KPNB1 hence their increased sensitivity when nuclear import pathways are inhibited.

Crystal structures of KPNB1 have been determined however, the unliganded human KPNB1 crystal structure has not yet solved. Therefore, ligand binding studies with KPNB1 are limited to molecular docking at present [93]. Like INI43, C53 was selected from an *in silico* docking study that identified compounds which potentially bound KPNB1. Other than docking studies, the inhibitory potential of C53 for KPNB1 has not been investigated to date. In the absence of X-ray crystal data of KPNB1:small molecule interaction, we investigated the effect of C53 treatment on the nuclear import of KPNB1 cargo proteins as well as KPNB1 localisation as preliminary evidence that C53 targets the nuclear import pathway. Our study shows that C53 inhibited the nuclear import of KPNB1 cargo proteins slightly however, had no effect on KPNB1 localisation. The inhibition of KPNB1 cargoes by C53 was found to be similar to that described for INI43 and Importazole [62]. This study provides evidence that C53 inhibits KPNB1 cargo proteins however further binding studies in the form of biophysical assays are required to confirm whether C53 binds KPNB1 directly. While molecular docking studies are an indication of possible binding of ligands/compounds to a protein of interest, purified

KPNB1 is required to perform biophysical analysis of KPNB1:C53 interaction. Protein purification and biophysical analysis was outside the scope and timeframe of this MSc project and forms the basis of ongoing research in our laboratory.

With many anticancer agents failing in clinical studies due to unfavourable pharmacokinetics or toxicity, there lies a lot of importance in testing possible drug-like compounds for their pharmacokinetic properties early in the drug development process [60]. A well-known natural compound Leptomycin B, an inhibitor of CRM1 showed great potential as a SINE however due to toxic side effects in clinical trials this compound was discontinued [80]. We therefore, investigated the pharmacokinetic properties of C53 to investigate whether it would be tolerable in a living system.

Our data provided evidence for C53 as a potential anticancer compound using *in vitro* models however, *in vivo* studies provide a realistic model of the tumour microenvironment. Before a compound enters a living system, it is important to have predictive data which could possibly indicate whether it will be tolerable in *in vivo* models. To have a better understanding of how C53 may behave in a living system we performed *in vitro* ADME studies. These studies, included five assays which predicted the solubility, lipophilicity, permeability, plasma protein binding and the metabolic stability of C53. The ADME *in vitro* results revealed that C53 had moderate plasma protein binding and solubility. The lipophilicity was shown to be ideal while the permeability was categorized as high. Metabolic studies revealed that C53 has a low half-life which may suggest rapid intrinsic clearance *in vivo*. These findings suggest that C53 is readily soluble and is ideal for oral absorption however, a short half-life may result in rapid clearance. It should however, be noted that *in vitro* metabolic studies may not necessarily be a conclusive indication of what may occur *in vivo* as several compounds have been shown to

have short half-life *in vitro* but not *in vivo* [102]. The short half- life observed for C53 could be due to a metabolite formation. Since the liver is responsible for the metabolic break down of parent compounds, the products formed (metabolites) after the enzymic reactions may be pharmacologically active and have longer half-lives as observed for Gleevec, a commercial tyrosine inhibitor with anticancer activity [108]. Therefore, the investigation into the metabolites possibly formed by C53 metabolic break down may lead to the discovery of pharmacologically active metabolites of C53 which may potentially have longer half-lives.

With C53 showing promising ADME pharmacokinetic properties we next investigated whether C53 is tolerated in an *in vivo* mouse model. The rationale for this was to determine whether C53 was firstly tolerable in a living system and if so at what concentration. The *in vivo* toxicology study was performed as a pilot for the identification of the drug concentration of C53 to be used in future xenograft studies. The results showed that all the drug concentrations were tolerable as all the mice gained weight in comparison to the control group. Post mortem evaluation showed no toxic effects internally and relative liver masses of C53 treated mice versus control group mice was not significantly different. Together these results show that C53 is tolerable *in vivo*.

In summary, results presented in this dissertation provide evidence that the novel small molecule inhibitor, C53 has anticancer effects *in vitro* and significantly inhibits nuclear import of KPNB1 cargoes. Furthermore, ADME experiments show that C53 has properties ideal for oral absorption but may have rapid clearance *in vivo* as shown by metabolic studies. *In vivo* toxicology studies provide evidence that C53 is tolerable in a nude mouse model. We propose that *in vivo* ADME pharmacokinetics studies on C53 be done to investigate whether *in vitro*

ADME results correlate with *in vivo* ADME results. The *in vivo* efficacy of C53 as a small molecule with anticancer activity also requires further investigation.

6.1 Limitations and future recommendations

1) In this study, we tested the effects of C53 on the proliferation on multiple cancer cell lines, however the effect of C53 on nuclear import of KPNB1 cargo proteins and KPNB1 localization was confirmed using HeLa cells only. Attempts of showing this in CaSki cells had limited success. Despite the optimization of transfection conditions using various transfection agents, CaSki cells showed poor transfection efficiency therefore could not be investigated for the effects of KPNB1 cargo protein import after C53 treatment. Difficulty with CaSki cells was also found in immunofluorescence analysis as the morphology of these is more epithelial-like cells with compact and overlapping packing making quantification of immunofluorescence data difficult. A recommendation for future studies include testing the effects of C53 on nuclear import on other cervical cancer cell lines.
2) While NFAT and NF-κB reporter assay results showed that C53 significantly reduces nuclear import and activity of these KPNB1 cargo transcription factors, this data does not confirm that C53 binds and inhibits KPNB1 directly. Future work will include the use of biophysical assays to confirm direct binding of C53 on KPNB1. This will involve the purification of KPNB1 for its use in protein:drug interaction studies such as circular dichroism, Isothermal Calorimetry and X-ray Crystallography.
3) The ADME *in vitro* results suggest that C53 is ideal for oral absorption but has a short half-life. Future studies could include investigating the metabolites of C53 and determining their half-life. *In vivo* toxicology studies showed that C53 is tolerable in a mouse model therefore *in vivo* ADME will be performed in the future to investigate the behaviour of C53 in a living system to evaluate whether the *in vitro* and *in vivo* ADME results correlate.

REFERENCES

1. Ferlay J, Soerjomataram I, Ervik M, Dikshit R, Eser S, Mathers C et al. GLOBOCAN 2012 v1.0, Cancer Incidence and Mortality Worldwide: IARC Cancer Base No. 11 Lyon, France: International Agency for Research on Cancer; 2013.

2. Global Burden of Cancer collaboration. The Global Burden of Cancer 2013. *JAMA Oncol*. 2015;4:505-527.

3. Chakraborty S, Rahman T. The difficulties in Cancer treatment. *Ecancermedicalscience*. 2012;6:16.

4. Corrie PG. Cytotoxic chemotherapy: clinical aspects. *Medicine*. 2008;36:24-28.

5. Flower Jr FJ, McNaughton CM, Albertsen PC, Zietman A, Elliot DB, Barry MJ. Comparison of recommendations by Urologists and Radiation Oncologists for treatment of clinically localized prostate cancer. *JAMA*. 2000;283:3217-3222.

6. Veronesi U, Luini A, Veichio M, Geco M, Galimeberti V, Merson M. Radiotherapy after breast-preserving surgery in woman with localized cancer of the breast. *N Eng J Med*. 1993;382:1587-1591.

7. Li Yan N, Rosen C, Arteaga. Targeted cancer therapies. *Chin J Cancer*. 2011;30:1-4.

8. Sawyers C. Targeted cancer therapy. *Nature*. 2004;24:294-297.

9. Griffen J. The biology of signal transduction inhibition: basic science to novel therapies. *Semin Oncol*. 2001;28:3-8.

10. Priyanka D. Targeted Therapies and Cancer. *Adv Oncol Res Treat*. 2016;1:1.

11. Rowinsky EK. Signal Events: Cell signal Transduction and Its Inhibition in Cancer. *Oncologist*. 2003;8:5-17.

12. Garnis C, Buys TPH, Lam WL. Genetic alteration and gene expression modulation during cancer progression. *Mol Cancer*. 2004;3:9.

13. Hassan M, Watari H, AbuAlmaaty A, Ohba Y, Sakuragi N. Apoptosis and molecular targeting therapy in cancer. *Biomed Res Int*. 2014;2014:150845.

14. Kang MH, Reynolds CP. Bcl-Petak I, Tillman DM, Houghton A. p53 Dependence of Fas induction and acute apoptosis Inhibitors Targeting Mitochondrial Apoptotic Pathways in Cancer Therapy. *Clin Cancer Res*. 2009;15:1126-1132..

15. El-Kenawi AE, El-Remessy AB. Angiogenesis inhibitors in cancer therapy: mechanistic perspective on classification and treatment rationales. *Br J Pharmacol*. 2013;170:712-729.

16. Chen B, Butte AJ. Leveraging big data to transform target selection and drug discovery. *Clin Pharmacol Ther*. 2017;99:285-97.

17. van der Watt PJ, Maske CP, Hendricks DT, Parker MI, Denny L, Govender D, Birrer M J, Leaner VD. The Karyopherin proteins, Crm1 and Karyopherin B1, are overexpressed in cervical cancer and are critical for cancer cell survival and proliferation. *Int J Cancer*. 2009;124:1829-1840.

18. Nigg EA. Nuclear cytoplasmic transport: signals, mechanism and regulation. *Nature*. 1997;386:779-787.

19. Wente SR, Rout MP. The Nuclear Pore and Nuclear Transport. *Cold Spring Harb Perspect Biol.* 2010;2:a000562.

20. Griffis ER. Distinct functional domains within nucleoporins Nup153 and Nup98 mediate transcription – dependent mobility. *Mol Biol Cell*. 2004;4:1991-2002.

21. Turner JG, Sullivan DM. CRM – 1 mediated nuclear export of proteins and drug resistance in cancer. *Curr Med.* 2008;26:2648-55.

22. Takahashi N. Tumor marker nucleoporin 88 kDa regulates nucleocytoplasmic transport of NfkB. *Biophys Res Commun*. 2008;3:424-30.

23. Denning DP. Disorder in the nuclear pore complex: the FG repeat region of the nucleoporins are natively unfolded. *Proc Natl Acad Sci USA*. 2003;100:2450-2455.

24. Kau TR, Jeffrey C, Silver W, Silver PA. Nuclear transport and cancer: from mechanism to intervention. *Nat Rev Cancer*. 2004;4:106-117.

25. Turner JG, Dawson J, Sullivan DM. Nuclear export of proteins and drug resistance in cancer. *Biochem Pharmacol*. 2012; 8: 1021- 1032.

26. Hill R, Cautain B, de Pedro N, Link W. Targeting nucleocytoplasmic transport in cancer therapy. *Oncotarget*. 2014;1:11-28.

27. Hung MC, Link W. Protein localization in disease and therapy. *J Cell Sci*. 2011;124:3381-3392.

28. Hoesel B, Schmid JA. The complexity of NF-kB signalling in inflammation and cancer. *Mol Cancer*. 2013;12:86.

29. Nigro JM, Baker SJ, Preisinger AC, Jessup JM, Hostetter R, Cleary K, Bigner SH, Davidson N, Baylin S, Devileee P. Muatations in the p53 gene occur in diverse human tumour types. *Nature*. 1989;342:705-708.

30. Behrens P, Brinkmann U, Fogt F, Wernert N, Wellmann A. Implication of the proliferation and apoptosis associated CSE1L/CAS gene for breast cancer development. *Anticancer Res.* 2001;21:2413-7.

31. Faustino RS, Nelson TJ, Terzic A, Perez-Terzic C. Nuclear Transport: Target for therapy. *Nature.* 2007;81:880-886.

32. Tran EJ, Wente SR. Dynamic nuclear pore complexes: life on the edge. *Cell*. 2006;125:1041-1053.

33. Mosammaparast N, Pemberton LF. Karyopherins: from nuclear-transport mediators to nuclear-function regulators. *Cell Biol*. 2004;14:547-556.

34. Melchior F. RanGTPase cycle: One mechanism-two functions. *Curr Biol*. 2001;11:257-260.

35. Muhlhausser P, Muller E.-C, Otto A, Kutay U. Multiple pathways contribute to nuclear import of core histones. *EMBO Reports.* 2001;2:690–696.

36. Chook YM, Suel KE.Nuclear import by karyopherin betas: recognition and inhibition *Biochem Biophys Acta.* 2011; 9:1593-1606

37. Flores K, Seger R. Stimulated nuclear import by β-like importins *F1000Prime Reports* 2013;5:41.

38. Monica N. Regulation of Nucleocytoplasmic Transport in Skeletal Muscle. *Curr Top Dev Biol*. 2011;96:273-302.

39. Noske A, Weichert W, Niesporek S, Roske A, Bulcendahl AC, Koch I. Expression of nuclear export protein chromosomal region maintenance/export 1/XPO1 is a prognostic factor in human ovarian cancer. *Cancer*. 2008;112:1733-1743.

40. Huang WY, Yue L, Qiu WS, Wang LW, Zhou XH, Sun YJ. Prognostic value of CRM1 in pancreas cancer. *Clin Invest Med.* 2009;32:E315.

41. Zheng M, Tang L, Huang L, Ding H, Liao WT, Zeng MS. Overexpression of karyopherin-2 in epithelial ovarian cancer and correlation with poor prognosis. *Obstet Gynecol* 2010;116:884-91.

42. Dahl E, Kristiansen G, Gottlob K, Klaman I, Ebner E, Hinzmann B. Molecular profiling of laser-microdissected matched tumor and normal breast tissue identifies karyopherin alpha2 as a potential novel prognostic marker in breast cancer. *Clin Cancer Res*. 2006;12:3950-3960.

43. Stelma T, Chi A, van der Watt PJ, Verrico A, Lavia P, Leaner VD. Targeting nuclear transporters in cancer: Diagnostic, Prognostic and therapeutic potential. *IUBMB Life*. 2016;68:268-280.

44. Kuusisto HV, Wagstaff KM, Alvisi G, Roth D M, Jans DA, et al. Global enhancement of nuclear localization-dependent nuclear transport in transformed cells. *FASEB J.* 2012;26:1181–1193

45. Dyrskjot L, Kruhoffer M, Thykjaer T, Marcussen N, Jensen JL, Moller K, Orntoft TF. Gene expression in the urinary bladder: a common carcinoma in situ gene expression signature exists disregarding histopathological classification. *Cancer Res*. 2004;64:4040-4048

46. Wu MS, Lin YS, Chang YT, Shun CT, Lin MT, Lin JT. Gene expression profiling of gastric cancer by microarray combined with laser capture microdissection *World J Gastroenterol*. 2005;11:7405-7412.

47. Azmi AS. Unveiling the role of nuclear transport in epithelial-to-mesenchymal transition. *Curr Cancer Drug Targets*. 2013;13:906-14.

48. Angus L, van der Watt P, Leaner VD. Inhibition of the nuclear transporter, Kpnβ1, results in prolonged mitotic arrest and activation of the intrinsic apoptotic pathway in cervical cancer cells. *Carcinogenesis*. 2014;35:1121-1131.

49. Sheng C, Qiu J, He Z, Wang H, Wang Q, Guo Z, Zhu L, Ni Q. Suppression of Kpnβ1 expression inhibits human breast cancer cell proliferation by abrogating nuclear transport of Her2. *Oncol Rep*. 2018;39:554-564

50. Sekimoto N, Suzuki Y, Sugano S. Decreased KPNB1 Expression is Induced by PLK1 Inhibition and Leads to Apoptosis in Lung Adenocarcinoma. *Journal of Cancer*. 2017;8:4125-414.

51. Strom A, Weis K. Importin-b-like nuclear transport receptors. *Genome Biol*. 2001;2:3008.

52. Kutay U, Izaurralde E, Bischoff FR, Mattaj IW, Gorlich D. Dominant-negative mutants of Importin B block multiple pathways of import and export through the nuclear pore complex. *EMBO J*. 1997;16:1153-1163.

53. Chook YM, Blobel G. Structure of the nuclear transport complex karyopherin-b2–Ran.GppNHp. *Nature*. 1999;399:230-237.

54. Mandal S, Moudgil MN, Mandal SK. Rational drug design. *Eur J Pharmacol.* 2009;625:90–100.

55. Wilson GL, Lill MA. Integrating structure-based and ligand-based approaches for computational drug design. *Future Med Chem*. 2011;3:735–750.

56. Huang SY, Zou X. Advances and challenges in protein-ligand docking. *Int J Mol Sci*. 2010;11:3016–3034.

57. Lin JH, Lu AYH. Role of pharmacokinetics and metabolism in drug discovery and development. *Pharmacol Rev*. 1997;49:403–449.

58. Baumann A. Nonclinical development of biopharmaceuticals. *Drug discov Today*. 2009;14:1112-22.

59. Hintersteiner M, Ambrus G, Bednenko J, Schmied M, Knox AJ, Meisner NC, Gstach H, Seifert JM, Singer EL, Gerace L, Auer M. Identification of a small molecule inhibitor of importin beta mediated nuclear import by confocal on-bead screening of tagged one-bead one-compound libraries. *ACS Chem. Biol*. 2010;5:967–979.

60. Soderholm JF, Bird SL, Kalab P, Sampathkumar Y, Hasegawa K, Uehara-Bingen M, Weis K, Rebecca H. Importazole, a Small Molecule Inhibitor of the Transport Receptor Importin-β. *ACS Chem Biol*. 2011;7:700-708.

61. Moroianu J, Blobel G, Radu A. Nuclear protein import: Ran-GTP dissociates the karyopherin alphabeta heterodimer by displacing alpha from an overlapping binding site on beta. *Proc Natl Acad Sci USA*. 1996;93:7059-7062.

62. van der Watt PJ, Chi A, Stelma T, Stowelll C, Strydom E, Carden S, Angus L, Hadley K, Lang D, Wei W, Birrer J Trent J.O, Leaner V. Targeting the Nuclear Import Receptor KpnB1 as an Anticancer Therapeutic. *Mol Cancer Ther*. 2016;4:560-73.

63. Li Y, You G, Jia B, Si H, Yao X. Prediction on the Inhibition Ratio of Pyrrolidine Derivatives on Matrix Metalloproteinase Based on Gene Expression Programming. *BioMed Res Int*. 2014;2014:210672.

64. Shimada Y, Imamura M, Wagata T, Yamaguchi N, Tobe T. Characterization of 21 newly established esophageal cancer cell lines. *Cancer*. 1992;69:277-284.

65. Beals CR, Clipstone NA, Ho SN, Crabtree GR. Nuclear localization of NF-ATC by calcineurin-dependent, cyclosporine-sensitive intramolecular interaction. *Genes Dev*. 1997; 11: 824-34.

66. Ichida M, Finkel T. Ras regulates NFAT3 activity in cardiac myocytes. *J Biol Chem*. 2001;276:3524-30.

67. Oestreich KJ, Yoon H, Ahmed R, Boss JM. NFATc1 regulates PD-1 expression upon T cell activation. *J Immunol.* 2008;181: 4832-4839.

68. Hill AP, Young RJ. Getting physical in drug discovery: a contemporary perspective on solubility and hydrophobicity. *Drug Discov Today*. 2010;15:648-655.

69. Wohnsland F, Faller B. High-Throughput Permeability pH Profile and High-Throughput Alkane/Water log P with Artificial Membranes. *J Med Chem*. 2001;44:923-930.

70. Alelyunus YW, Pelosi-Killby L, Turcotte P, Kary MB, Spreen RC. A high throughput dried DMSO Log D lipophilicity measured based on 96-well shake-flask and atmospheric pressure photoionization mass spectrometry detection. *J Chromatogr*. 2010;1217:1950-1955.

71. Obach RS. Prediction of human clearance of twenty-nine drugs from hepatic microsomal intrinsic clearance data: an examination of in vitro half-life approach and nonspecific binding microsomes. *Drug Metab Dipos.* 1999;27:1350-1359.

72. Hait WN, Hambley TW. Targeted cancer therapeutics. *Cancer Res*. 2009;69:1263-1267.

73. Neubig RR. International Union of Pharmacology Committee on Receptor Nomenclature and Drug Classification. XXXVIII. Update on terms and symbols in quantitative pharmacology. *Pharmacol Rev*. 2003;55:597-606.

74. Williams GH, Stoeber K. The cell cycle and cancer. *J Pathol.* 2012;226:352-364.

75. Persanidis C, Persanidis B, Wyba F. Evaluation of the Immunohistochemical expression of p53, p21, p27, cyclin D1 and Ki67 in oral and oropharyngeal squamous cell carcinoma. *J Oral Pathol Med*. 2012;41:40-46.

76. Kroemer G, Galluzzi L, Vandenabeele P, Abrams J, Alnemin ES, Baehrecke EH. Classification of cell death: recommendations on the nomenclature committee on cell death 2009. *Cell death Differ*. 2009;16:3-11.

77. Boulares H, Yakovlev A, Ivanova V, Stoica B, Wang G, Iyer S, Smulson M. Role of poly(ADP-ribose) polymerase (PARP) cleavage in apoptosis caspase 3-resistant PARP mutant increases rates of apoptosis in transfected cells. *J Biol Chem.* 1999;274:22932– 40

78. Wana Y, Wang J, Suna F, Chena M, Hoya Y, Fanga H, et al. Design, synthesis and preliminary biological studies of pyrrolidine derivatives as Mcl-1 inhibitors. *Bioorganic Med Chem*. 2015;23:7685–7693.

79. Qu X, Yuan Y, Xu W, Chen M, Cui S, Meng H, Li Y, Makuuchi M, Nakata M, Tang W. Caffeoyl Pyrrolidine Derivative LY52 Inhibits Tumor Invasion and Metastasis via Suppression of Matrix Metalloproteinase Activity. *Anticancer Res*. 2006;26:3573-3578.

80. Newlands ES, Rustin GJ, Brampton MH. Phase I trial of elactocin. *Br J Cancer*. 1996;74:648–9.

81. Turner JG, Sullivan DM. CRM1-mediated nuclear export of proteins and drug resistance in cancer. *Curr Med Chem*. 2008;1526:2648–55.

82. Gravina G, Tortoreto M, Mancini A, Addis A, Di Cesare E, Lenzi A. XPO1/CRM1-selective inhibitors of nuclear export (SINE) reduce tumor spreading and improve overall survival in preclinical models of prostate cancer (PCa). *J Hematol Oncol*. 2014;7:46

83. Sekimoto T, Miyamoto Y, Arai S, Yondeda Y. Impoetin alpha protein acts as a negative regulator for Snail protein nuclear import. *J Biol Chem*. 2011;286:15126-15131.

84. Lam MH, Briggs LJ, Hu W, Martin TJ, Gillespie MT, Jans DA. Importin beta recognizes parathyroid hormone-related protein with high affinity and mediates its nuclear import in the absence of importin alpha. *J Biol Chem*. 1999;11:7391-7398.

85. Moncini M, Toker A. NFAT Protein: Emerging Roles in Cancer Progression. *Nat Rev Cancer.* 2009;11:810-820.

86. Hoesel B, Schmid JA. The complexity of NF-kB signalling in inflammation and cancer. *Mol Cancer*. 2013;12:86.

87. Maguire O, Tornator KM, O'Laughlin K, Venuto RC, Minderman H. Nuclear translocation of Nuclear factor of activated T cells (NFAT) as a quantitative pharmacodynamic Parameter for tacrolimus. *Cytometry A*. 2013;12:1096-1104.

88. Ishiguro K, Ando T, Maeda O, Ohmiya N, Niwa Y, Goto H. Acetate inhibits NFAT activation in T cells via Importin beta 1 interference. *Eur J Immunol.* 2007;37:2309-16.

89. Northrop JP, Ullman KS, Crabtree GR, et al. Characterization of the nuclear and cytoplasmic components of the lymphoid-specific nuclear factor of activated T cells (NF-AT) complex. *J Biol Chem*. 1993;268:2917–23.

90. Gamble C, McIntosh K, Scott R, Ho KH, Plevin R, Paul A. Inhibitory kappa B Kinases as targets for pharmacological regulation. *Br J Pharmacol.* 2012;165:802 –819.

91. Fagerland R, Kinnunen L, Kohler M, Julkunen 1, Melen K. NF-κB is transported into the nucleus by Importin α3 and Importin α4. *J Biol Chem* 2005;280:15942-15951.

92. Stelma T, Leaner VD. KPNB1-mediated nuclear import is required for motility and inflammatory transcription factor activity in cervical cancer cells. *Oncotarget*. 2017;8:32833-32847.

93. Lee SJ, Sekimoto T, Yamashita E, Nagoshi E, Nakagawa A, Imamoto N, Yoshimura M, Sakai H, Chong KT, Tsukihara T. The structure of importin-ß bound to SREBP-2: nuclear import of a transcription factor. *Science*. 2003;302:1571–1575.

94. Kim YH, Ha S, Kim J, Ham SW. Identification of KPNB1 as a cellular target of aminothiazole derivatives with anticancer activity. *ChemMedChem*. 2016;11:1406–1409.

95. Siyoung H, Jiwon O, Yong H, Seung WH, et al. Determination of the binding site of 2-aminothiazole derivative with Importin B1 by UV-crosslinking experiment. *J Chromatogr B Analyt Technol Biomed Life Sci*. 2017;1060:71-75.

96. Zhang D, Luo G, Ding X, Lu C. Preclinical experimental models of drug metabolism and disposition in drug discovery and development. *Acta Pharmaceutica Sinica B*. 2012;6:549-561.

97. Bohnert T, Gan LS. Plasma Protein Binding: From Discovery to Development. *J Pharm Sci*. 2013;102:2953-2994.

98. Arnott JA, Kumar R, Planey SL. Lipophilicity Indices for Drug Development. *J Appl Biopharm Pharmacokinet.* 2013;1:31-36.

99. Arnott JA, Planey SL. The influence of lipophilicity in drug discovery and design. *Expert Opin Drug Discov*. 2012;10:863-75.

100. Khadka P, Ro J, Kim H, Kim I, Tae Kim J, Kim H, Min J, Yun G, Lee J. Pharmaceutical particle technologies: An approach to improve drug solubility, dissolution and bioavailability. *Asian J Pharm Sci*. 2014;9:304-316.

101. Wang N, Dong J, Deng Y, Zhu M, Wen M, Yao Z, Lu A, Wang J, Cao D. ADME Properties Evaluation in Drug Discovery Prediction of Caco-2 cell Permeability Using a Combination of NSGA-II and Boosting. *J Chem Inf Model.* 2016;56:763-773.

102. Masimirembwa CM, Bredberg U, Anderson TB. Metabolic Stability for Drug Discovery and Development. *Clin Pharmacokin*. 2003;42:515-528.

103. Parasurm S. Toxicology Screening. *J Pharmacol Pharmacother*. 2011;2:74-79.

104. Edward KH, Li D, et al. Solubility in Drug Like Properties: Concept, Structure, Design and Methods, from ADME to Toxicity Optimization. *Elsevier*.2008:56.

105. van de Waterbeemd H, Gifford E. ADMET in silico modelling: towards prediction paradise? *Nat Rev Drug Discov*. 2003;2:192-204.

106. Barka T, Popper H. Liver enlargement and drug toxicity. *Medicine (Baltimore).* 1967;46:103-117.

107. Verma P, Thakur AS, Deshmukh K, Jha AK, Verma S. Route of drug administration Int *J Pharm Study Res*. 2010;1:54-59.

108. Coutre P, Kreuzer KA, Pursche S, Bonin Mv, Leopold T, Baskaynak G, Dorken B, Ehninger G, Ottmann O, Jenke A, Barnhauser M, Scheleyer E. Pharmacokinetics and cellular uptake of imatinib and its main metabolite CGP74588. *Cancer Chemother Pharmacol*. 2004;53:313-323.

109. Peters S, Zimmermann S, Adjei AA. Oral epidermal growth factor receptor tyrosine kinase inhibitors for treatment of non-small cell lung cancer: comparative pharmacokinetics and drug-drug interactions. *Cancer Treat Rev.* 2014;40:917-926.

110. Kane RC, Farrell AT, Saber H, Tang S, Williams G, Jee JM, Liang C, Booth B, Chidambaram N, Morse D, Sridhara R, Garvey P, Justice R, Pazdur R. Sorafenib for the treatment of advanced renal cell carcinoma. *Clin Cancer Res.* 2006;12:7212-7278.

111. Dikmanns A, Monecke T, Ficner R. Structural Basis of Targeting the Exportin CRM1 in Cancer. *Cells*. 2015;4:438-568.

APPENDIX I-SOLUTIONS

Cell culture solutions

Trypsin-EDTA
0.5 g Trypsin
1.45 g $Na_2HPO_4.2H_20$
8 g NaCl
0.2 g $KHPO_4$
0.2 g KCL
10 mM EDTA, pH 8
Make up to 1L with PBS

Cell- freezing Media
90 % Complete Media
10 % DMSO

MTT reagent (5 mg/ml)
100 mg MTT
20 ml PBS
Vortex and incubate in water bath at 37˚C for 15 minutes
Filter sterilize through 0.22 µm filter
Store at 4˚C in the dark for a maximum period of a month

Solubilisation Reagent
25 g SLS in 250 mL dH_20
76.6 µl concentrated HCl

Protein solutions

RIPA buffer
150 mM NaCl
1% Triton-X-100
1% Sodium Deoxycholate
0.1% SDS
10 mM Tris-CL pH 7.5
Store in fridge

PBS (10X)
40 g NaCl
1 g KCl
3.82 g $Na_2HPO_4.2H_20$
1 g KH_2PO_4
Make up to 500 ml with dH_20

1M Tris (pH 6.8)
24.23 g Tris
200 ml dH_2O
Adjust pH with concentrated HCl to pH 6.8
Make up to 200 ml with dH_2O

1 M Tris (pH 8.8)
24.23 g Tris
200 ml dH_2O
Adjust pH with concentrated HCl to pH 8.8
Make up to 200 ml with dH_2O

<u>Western blot solutions</u>

4% Stacking Gel
3.65 ml dH_20
0.625 ml Tris (pH 6.8)
50 µl 10% SDS
0.650 ml 30% Acrylamide
60 µl 10% APS
6 µl TEMED

10% Separating Gel
2.75 ml dH_20
3.75 ml 1 M Tris (pH 8.8)
100 µl 10% SDS
3.35 ml 30 % Acrylamide
200 µl 10% APS
20 µl TEMED

15% Separating Gel
3.3 ml dH_20
3.9 ml 1 M Tris (pH 8.8)
150 µl 10% SDS
7.5 ml 30% Acrylamide
150 µl 10% APS
15 µl TEMED

Loading dye (6X)
0.8 ml Glycerol
0.1 ml Bromophenol Blue
0.5 ml Tris pH 6.8
0.6 ml 20 % SDS
10 µl 100% β-mercaptoethanol

10 X Running Buffer
20 g Glycine
31.6 g Tris
50 ml 10% SDS
Up to 500 ml with dH_2O

1 X Running Buffer
100 ml 10 X running buffer
900 ml dH_2O

10 X Transfer Buffer
72 g Glycine
19 g Tris
Up to 500 mL with dH_2O

1 X Transfer Buffer
200 ml Isopropanol
100 ml 10 X Transfer
700 ml dH_20

10 X TBS
24.23 g Tris
80.06 g NaCL
Add 800 ml dH_2O
pH with concentrated HCl to pH 7.6
Volume made up to 1 L dH_2O

1 X TBST
100 ml 10 X TBS
900 ml dH_2O
1 ml Tween-20

5% milk powder
1 g milk
20 ml TBST

<u>Nuclear/ Cytoplasmic fractionation solutions</u>

Harvest Buffer (10 ml)
100 µl 1M HEPES pH 7.9
0.5 ml 1 M NaCl
2 µl 500 mM EDTA
50 µl Triton-X-100
Up to 10 ml with dH_20

Buffer A (10 ml)
100 µl 1 M HEPES pH 7.9
100 µl 1 M KCl
2 µL 500 mM
2 µL 500 mM
Up to 10 ml with dH_20

Buffer C (10 ml)
10 µl 1 M HEPES pH 7.9
0.5 µl 1 M NaCl
1 µl 100 mM EDTA
1 µl 100 mM EGTA
20 µl 5% NP-40
Up to 10 ml with dH_20

Cell cycle solutions

5M NaCl
58.44 g NaCl
200 ml dH_20

0.1M PIPES
3.02 g PIPES
100 ml dH_20
Adjust pH to 6.8

FACS staining solution
5 µl Triton-X-100
10 µl 1M $MgCL_2$
100 µl 5M NaCl
500 µl 0.1 M PIPES (pH 6.8)
5 µL Propodium Iodide (1 mg/mL)
4335 µl dH_20

Immunofluorescence solutions

4% Paraformaldehyde
40 g paraformaldehyde
900 ml PBS
Heat to approximately 60˚C with constant stirring
Raise pH by adding 1 M NaOH, until solution clears
Make to 1 L with PBS
Store at 4˚C

Mowiol Mounting Solution
2.4 g Mowiol-488 6 g Glycerol
6 ml dH_2O
Stir vigorously
12 ml 200 mM Tris-Cl, pH 8.5
Heat to 60˚C with stirring for 10 minutes
Remove undissolved particles by centrifugation for 15 minutes
Store at -20˚C

General

1 M HEPES
238.80 g HEPES
800 ml dH_2O
Adjust to desired pH
Make up to 1 L with dH_2O

0.5 M EDTA
186.12 g Na2EDTA-$2H_2O$
800 ml dH_2O
Adjust to pH 8.0 with NaOH
Up to 1 L with dH_2O

0.5 M EGTA
190.18 g EGTA
800 ml dH_2O
Adjust to pH 8.0 with NaOH
Up to 1 L with dH_2O

APPENDIX II- PROTEIN MARKER

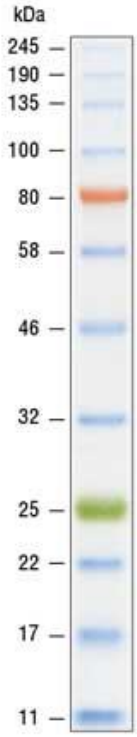

Figure AII. Protein molecular weight marker: Colour Prestained Protein Standard. Ladder used to determine the molecular weight of proteins subjected to polyacrylamide gel electrophoresis on 10-15% SDS-PAGE gels